



AMERICAN UNIVERSITY OF BEIRUT

DESIGN AND ANALYSIS OF A HYBRID SOLAR STIRLING  
ENGINE SYSTEM FOR POWER GENERATION

by  
MARC GILBERT HABER

A Thesis  
submitted in partial fulfillment of the requirements  
for the degree of Master of Science  
to the Department of Chemical and Petroleum Engineering  
of the Maroun Semaan Faculty of Engineering and Architecture  
at the American University of Beirut

Beirut, Lebanon  
April 2019

AMERICAN UNIVERSITY OF BEIRUT

DESIGN AND ANALYSIS OF A HYBRID SOLAR STIRLING  
ENGINE SYSTEM FOR POWER GENERATION

by  
MARC GILBERT HABER

Approved by:

Dr. Joseph Zeaiter, Associate Professor  
Department of Chemical Engineering



---

Advisor

Dr. Fouad Azizi, Associate Professor  
Department of Chemical Engineering



---

Member of Committee

Dr. Sabla Al Nouri, Assistant Professor  
Department of Chemical Engineering



---

Member of Committee

Date of thesis defense: April 25, 2019

AMERICAN UNIVERSITY OF BEIRUT

THESIS, DISSERTATION, PROJECT RELEASE FORM

Student Name: HABER MARC GILBERT  
Last First Middle

Master's Thesis       Master's Project       Doctoral Dissertation

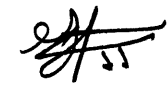
I authorize the American University of Beirut to: (a) reproduce hard or electronic copies of my thesis, dissertation, or project; (b) include such copies in the archives and digital repositories of the University; and (c) make freely available such copies to third parties for research or educational purposes.

I authorize the American University of Beirut, to: (a) reproduce hard or electronic copies of it; (b) include such copies in the archives and digital repositories of the University; and (c) make freely available such copies to third parties for research or educational purposes after:

**One ---- year from the date of submission of my thesis, dissertation, or project.**

**Two ---- years from the date of submission of my thesis, dissertation, or project.**

**Three ---- years from the date of submission of my thesis, dissertation, or project.**



Signature

May, 06, 2019

Date

## ACKNOWLEDGEMENTS

I would like to express my deepest gratitude for Dr. Joseph Zeaiter for his advisory, guidance and for his belief in my potential. This work couldn't be done without his expertise in Solar Energy applications. It should be mentioned that Dr. Zeaiter made it possible for me to be part of an internship program in The Cyprus Institute in the Concentrating Solar Power (CSP) field, and that helped me expand my knowledge in this domain. He also made me take part in a European School Program for Solar Thermal Energy (NESTER school: Networking for Excellence in Solar Thermal Energy Research) as well as an International Conference for CSP technologies in Cyprus.

I would like to thank Dr. Fouad Azizi and Dr. Sabla Al Nouri for being members of my thesis committee.

Special thanks to Mr. Nicolas Abdelkarim Aramouni (PhD. Candidate) for the countless workshops he gave me on operating the facilities at the AUB manufacturing workshop. Mr. Abdelkarim Aramouni also used his expertise in process design to give a hand in the assembly of the Solar Stirling Engine and that includes the water cooling system, the combustion chamber as well as the solar tracker coding.

Deep gratitude also goes to Mr. Waddah Malaeb (M.E.) for using his advanced skills in SolidWorks to help me visualize different parts of the system before the manufacturing steps. Mr. Malaeb never hesitated to advise me whenever something went wrong.

I would also like to thank Mr. Joseph Nassif, Mr. Ramzi Safi, Mr. Bilal Chehabeddin and the AUB manufacturing workshop personnel, for their help and expertise in manufacturing parts for the Stirling Engine Assembly.

Special thanks go to Ms. Rita Khalil for guaranteeing a perfect lab environment and helping me during the stage of buying parts for the system, and to the chemical engineering department for making the lab space available for my work.

Moreover, I would like to thank the Chemical Engineering undergraduate team that had a role to play in each part of the system assembly and testing. The list includes Hussein Issa, Mouhanad AbouDaher, Ali Chaaaban and Riad Halabi.

I would also like to show deep gratitude and appreciation to my family members and my friends for their support throughout the past years.

# AN ABSTRACT OF THE THESIS OF

Marc Gilbert Haber for

Master of Science

Major: Chemical Engineering

Title: Design and Analysis of a Hybrid Solar Stirling Engine System for Power Generation

Since the 1990s, Lebanon has faced shortages in the supply of electricity which accounted for more than 10 hours a day. In fact, these shortages have led to the wide use of back-up diesel generators that are priced at 27 ¢/kWh. Moreover, the greenhouse gas emissions from a diesel engine accounts for around 20 tons of CO<sub>2</sub> yearly per household, which aggravates the problem even more.

This project aims to decrease the Cost of Energy (COE) and achieve a continuous energy generation. In a country where the grid power is weak, the solution envisaged is the implementation of a Microgrid system based on a Hybridized Stirling Engine (HSE). In fact, the HSE runs on solar thermal energy when available, and consumes natural gas during hours of darkness or clouds. Moreover, the system is coupled to a PV plant with Li-ion battery storage.

By using optimization tools such as SAM and HOMER, it appeared that a 3kW HSE coupled with a PV capacity of 4kW and a 5kWh Li-ion battery storage is the most optimal configuration. In a nutshell, the COE was accounted to be 16.3 ¢/kWh and decreased the CO<sub>2</sub> emissions by 52%. These numbers were compared to alternative systems such as PV/Diesel/Batteries configurations and were still found to be the finest.

Because of the economic feasibility of this project, lab scale Stirling Engine prototypes were assembled and tested.

## CONTENTS

ACKNOWLEDGEMENTS .....	v
ABSTRACT .....	vi
LIST OF ILLUSTRATIONS .....	xii
LIST OF TABLES .....	xv
NOMENCLATURE .....	xvii

### Chapter

I. INTRODUCTION .....	1
A. World Wide Energy Status .....	1
B. Lebanon's Energy Status .....	1
C. The need for Microgrid decentralized energy systems .....	4
D. The need for Renewable Energy .....	5
E. Lebanon's Solar Energy .....	5
F. Lebanon's Oil and Gas opportunity .....	9
G. Review of Solar Energy Systems .....	11
H. The Solar Powered Stirling Engine .....	12
I. The Hybridized Stirling Engine (HSE) .....	14
J. Previous work done with the Solar Powered Stirling Engine .....	16
K. Recapitulation and Aims of the Thesis and Thesis Plan .....	17
L. Structure of the Thesis .....	19
II. SIMULATION INPUT AND PROCEDURE .....	20
A. First Simulation Using SAM .....	20
1. Simulation Input on SAM .....	20
2. Results from SAM .....	23
B. Simulation Input on HOMER .....	24
1. Natural Gas Consumption per Stirling Engine .....	24
2. Li-ion Batteries and Charging Methods .....	25
3. Converter .....	26
4. The Load .....	27

5. Simulation Procedure .....	29
6. Optimization Elements .....	31
a. Economics .....	31
i. Inflation Rate .....	31
ii. Nominal and Real Discount Rate.....	31
b. Constraints .....	32
c. Optimization parameters.....	33
7. Cost Factor .....	35
a. Initial Capital Cost of Stirling Engine .....	35
b. O&M cost of Solar Stirling Engine .....	36
c. O&M Cost of Natural Gas Operation Stirling Engine.....	36
d. Cost of Natural Gas.....	37
8. Natural Gas Engine Operating Conditions: Minimum Load Ratio.....	38
9. Lifetime of the system.....	39
a. Lifetime Validation.....	40
C. Area Consideration.....	41
<b>III. OTIMIZATION RESULTS AND DISCUSSION .....</b>	<b>42</b>
A. Standalone PV system .....	42
B. PV/Diesel Engine Simulation.....	44
C. Standalone Hybrid Stirling Engine (HSE).....	47
D. HSE/PV system results and cost comparisons .....	50
1. Economic Evaluation .....	52
a. Link with the Battery Bank Size and the fuel consumption ....	56
2. Best Performing Systems .....	62
3. Sensitivity Analysis on the Capital Price of the Stirling Engine System .....	64
<b>IV. COMPARISON WITH THE BENCHMARK.....</b>	<b>71</b>
A. Payback Period, Internal Rate of Return and Return On Investment.....	71
B. Payback Period, IRR and ROI evaluation .....	73
1. Compare with 4.8kW Diesel, 4.8kW Diesel/12.1kW PV and 4.8kW Diesel/9.6kW PV/3kWh Batteries.....	73



V. PERFORMANCE ANALYSIS OF A 3KW HSE/4KW PV/5KWH BATTERIES.....	76
A. Electrical Performance .....	76
B. Solar Powered Stirling Engine .....	77
C. Natural Gas Powered Stirling Engine.....	78
D. Emissions Evaluation .....	80
E. PV Plant Electricity Production.....	81
F. Li-ion Batteries Performance .....	82
G. Conclusion of the Simulation.....	87
VI. THERMODYNAMIC PRELIMINARY ANALYSIS.....	89
A. Ideal Stirling Process.....	89
B. Different Kinds of Stirling Engines.....	93
1. Alpha ( $\alpha$ ) Stirling Engine .....	93
2. Beta ( $\beta$ ) Stirling Engine.....	94
3. Gamma ( $\gamma$ ) Stirling Engine .....	95
4. Assessment of the three Stirling Engines.....	96
C. Efficiency of the ideal Stirling Cycle .....	97
D. Heat and Work of the ideal Stirling Cycle .....	100
E. Losses in the Stirling Engine .....	101
1. Sinusoidal approximation, Crank Angle and Phase shift angle .....	101
2. Effect of the Regenerator on the performance .....	103
3. Remarks about the stored heat from the regenerator.....	106
4. Remarks on the isothermal changes of state .....	109
5. Dead Volume losses in Power.....	110
6. Leakages and Pressure Losses in the Stirling Engine .....	110
7. Mechanical Friction and Heat Losses inside the Stirling Engine.....	111
8. Real Stirling Engine process .....	112
F. Volume Measurements .....	112
G. Ideal Cycle Analysis: Performance of both the Lab Scale Gamma Stirling Engine and Beta Stirling Engine.....	114
1. Thermal Efficiency.....	115

2. Volume Analysis: Results .....	116
a. Volume Study of the Gamma Stirling Engine .....	117
b. Volume Study of the Beta Stirling Engine .....	119
3. Heat and Work performance of the ideal Stirling Cycle in the given Engine.....	122
4. p-v Diagram of the ideal process.....	124
H. 0 <sup>th</sup> order analysis.....	126
1. Goal of the 0 <sup>th</sup> order analysis .....	126
2. Efficiency Prediction by the Carlquist's Method.....	126
3. Power Estimation by Beale's Method.....	127
4. Power Estimation by West's Method.....	129
5. Conclusion of the 0 <sup>th</sup> order analysis .....	132
<b>VII. TESTING OF A LAB SCALE GAMMA STIRLING ENGINE.....</b>	<b>133</b>
A. Equipment .....	133
B. First Approach using different resistance values and Power Expected from the Generator at different RPMs.....	134
C. Second Approach: Finding the Engine's optimal power.....	137
1. Increasing the load .....	137
2. First run: Varying the field resistance value and the heat input to the engine .....	139
3. Second run: Higher loads .....	141
D. Third approach: Combining the results and calculation of power dissipated by the dynamo.....	144
E. Conclusion and outcomes of these experiments .....	146
<b>VIII. TESTING OF A LAB SCALE BETA STIRLING ENGINE.</b>	<b>149</b>
A. Modifications and Addition to the engine .....	149
B. Addition of a Combustion Chamber.....	150
C. The implementation of a cooling system.....	152
D. Results .....	154
E. Future Works with the beta-Stirling Engine .....	155
1. Dynamo and Gears .....	157

2. Combustion chamber.....	157
3. Battery Storage.....	158
4. Solar Applications.....	158
IX. CONCLUSION.....	159
REFERENCES .....	160
APPENDIX A.....	164
APPENDIX B – 2500 USD/KW .....	168
APPENDIX B – 4000 USD/KW .....	170
APPENDIX B – 5000 USD/KW .....	172
APPENDIX B – 6000 USD/KW .....	174
APPENDIX C .....	176
APPENDIX D.....	177

## LIST OF ILLUSTRATIONS

Figure	Page
1. Forecasting of the electrical power deficit of EDL [5] .....	2
2. DNI World Map © 2017 The World Bank, Solar resource data: Solargis. ....	7
3. DNI Lebanon Map © 2017 The World Bank, Solar resource data: Solargis. ....	8
4. The Duck curve for the California Energy Grid .....	9
5. Parabolic Dish-Stirling system's different components [25] .....	14
6. Yearly DNI values in Lebanon .....	22
7. Yearly GHI values in Lebanon .....	22
8. SAM simulation for a 1kW Solar Powered Stirling Engine under the Lebanese weather	23
9. Daily Load per Household .....	27
10. Monthly Load per Household .....	28
11. Simulation Logic Brief Flowchart .....	29
12. A More Detailed Flowchart about the simulation logic (done using SmartDraw Software) .....	30
13. Focus Factor effect.....	34
14. Average price of Natural Gas form different sources.....	37
15. HOMER simulation set up for a PV Standalone System where 1kWh LI stands for a 1kWh Li-ion Battery .....	42
16. HOMER simulation setup for an HSE standalone system where SP SE stands for Solar Powered Stirling Engine and NGO SE stands for Natural Gas Operation Stirling Engine..	47
17. HOMER simulation setup for a HSE/PV system .....	50
18. NPC comparison of a Stirling Engine with an optimal PV plant .....	50
19. Initial Cost comparison.....	52
20. NPC comparison .....	54
21. Cost of Energy Comparison.....	56
22. Variation in the Size of the batteries with respect to the system configuration.....	57
23. Performance Analysis in the Month of February of a 3kW HSE/3kW PV/9kWh Batteries .....	61
24. NPC of different HSE/PV configurations for different Capital Costs.....	64
25. NPC variation for different Capital Costs of the HSE.....	65
26. Weighted Present Worth Plot .....	68
27. NPC comparison with Diesel/PV configurations .....	69
28. COE comparison with Diesel/PV configuration.....	70
29. Cumulative Discounted Present Cost .....	74
30. Power Output of a 3kW Solar Powered Stirling Engine (Showing on the x-axis: number of days per year, right y-axis: hours a day and left y-axis power output in kW) .....	77
31. Power Output of a 3kW HSE (Natural Gas) (Showing on the x-axis: number of days per year, right y-axis: hours a day and left y-axis power output in kW) .....	79

32. Power Output of a 4kW PV plant (Showing on the x-axis: number of days per year, right y-axis: hours a day and left y-axis power output in kW).....	82
33. Yearly State of Charge of 5kWh Batteries .....	83
34. Monthly Evaluation of the state of charge of 5kWh Batteries .....	83
35. System's performance in January.....	84
36. System's performance in May.....	85
37. System's performance in August .....	85
38. System's performance in November .....	86
39. Solar Data in November 17 .....	87
40. Thermodynamic Scheme of the Stirling Cycle.....	89
41.(right) P-V diagram and (left) T-s diagram of the Stirling Cycle (1-2-3-4) and the Carnot Cycle (1-5-3-6) .....	91
42. Alpha type Stirling Engine [51].....	93
43. Beta Type Stirling Engine.....	94
44. Beta Stirling Engine configuration showing the linkage between the power piston and the displacer .....	94
45. The three kinds of Stirling Engine.....	95
46. Free Piston Stirling Engine Parts [55] .....	96
47. Motion in the Stirling Engine .....	101
48. p-v diagram with continuous motion.....	102
49. Angles and Dimensions in a Beta Stirling Engine.....	103
50. Effect of Regenerator Effectiveness on Efficiency.....	105
51. Regenerator heat and work produced for different working fluids .....	108
52. Effect of the imperfect isothermal processes.....	109
53. Dead Volume effect illustrated in the p-v diagram.....	110
54. Realistic p-v diagram.....	112
55. Expansion, Compression and total volume change with respect to crank angle in the Beta Stirling Engine .....	118
56. Expansion, Compression and total volume change with respect to crank angle in the Beta Stirling Engine .....	121
57. p-v diagram for the ideal process of the BSE .....	125
58. p-v diagram for the ideal process of the GSE.....	125
59. Beale Number variation in function of the hot side temperature (from Wagner).....	129
60. Electrical Circuit of the generator (coupled with the Stirling Engine) in series with the load resistor and Ampere-meter as well as in parallel with the voltmeter (drawn on openModelica) .....	134
61. Electrical Power Delivered by the Engine when coupled to different resistance values .....	134
62. Voltage and Current changes with respect to the field resistance and the RPM .....	135
63. Power of the generator as a function of Rotational Speed for different resistance values .....	136

64. Set up for two 150 Ohm resistances in parallel, equivalent to a 75 Ohm load.....	139
65. Set up for three 150 Ohm resistances in parallel to model the 75 Ohm load: 1 – gamma-Stirling Engine 2 – Gear Ratio of 1 to 4 3 – Dynamo 4 – Breadboard with three 150 Ohm resistors in parallel connected to a voltmeter and an ampere meter. ....	139
66. showing the Power of the engine for different loads in Amps .....	140
67. RPM vs Load in Amps.....	141
68. Variation in the power delivered by the engine with respect to low resistance values	142
69. Effect of the variation in the field resistance on the current and the power of the engine .....	143
70. Variation of the RPM and the voltage with the decrease in the field resistance .....	143
71. Power Delivered by the Stirling Engine for different resistance values.....	144
72. V-I line.....	145
73. Power Delivered, Power Dissipated and total power .....	146
74. Beale factor for the gamma-Stirling Engine .....	147
75. Beta-Stirling Engine from GreenPowerScience with adaptor and gear addition .....	149
76. Stirling Engine Casing .....	150
77. Hot zone on the Expansions Cylinder.....	150
78. Cross section view of the Combustion chamber 1 - hot zone of the engine 2 - Flame side .....	151
79. Combustion chamber parts 1 – cover for the hot zone 2 – chamber casing .....	152
80. Final setup 1 - Flame Torch 2 - combustion chamber with mineral wool insulation 3 - water jacket 4 - overflow tank 5 - Stirling Engine's flywheel 6 - Dynamo 7 – Radiator ...	153
81. Fans attached behind the radiator .....	153
82. Overall Stirling Engine System .....	154
83. Power of the gamma-Stirling Engine.....	155
84. Beale factor for the beta-Stirling Engine .....	156

## LIST OF TABLES

Table	Page
1. Cost of Energy in per Lebanese Household.....	3
2. Techno-economic analysis of Solar Energy Systems .....	11
3. <i>Description of various CSP technologies [23]</i> .....	12
4. SAM input values .....	21
5. Natural Gas Flowrate and Electrical Energy Delivered.....	25
6. Load Summary.....	28
7. Specific Costs of the system .....	35
8. Natural Gas Price .....	38
9. Lifetime of the system .....	40
10. PV Standalone System Optimal Size.....	43
11. PV Standalone System Cost.....	44
12. PV/Diesel Engine's configuration.....	45
13. Diesel/PV/Li-ion optimal configuration .....	46
14. Diesel/PV/Li-ion System's cost .....	46
15. Hybrid Stirling Engine (HSE) Standalone optimal Size.....	47
16. Hybrid Stirling Engine Standalone Cost.....	48
17. Hybrid Stirling Engine Standalone Cost (5kW Stirling Engine).....	48
18. Initial Cost Drop .....	53
19. NPC drop when the 4kW HSE/1kW PV/2kWh Batteries is compared to other configurations .....	55
20. Yearly Battery State of Charge with respect to the system's configuration.....	59
21. Fuel Consumption of three different systems. ....	60
22. Optimal Component sizes of a HSE/PV/Batteries system.....	63
23. HSE/PV/Batteries Hybrid Standalone Cost.....	63
24. Unweighted Present Worth Comparison .....	66
25. Weighted Present Worth Comparison .....	67
26. Economic Evaluation when compared to a 4.8kW Diesel System.....	74
27. Electrical Performance of a 3kW HSE/4kW PV/5kWh Batteries .....	76
28. Natural Gas Stirling Engine Performance.....	79
29. comparing the emissions from a 3kW HSE/4kW PV/5kWh Batteries to the ones of a 4.8kW Diesel Engine.....	80
30. comparing the emissions from a 3kW HSE/4kW PV/5kWh Batteries to the ones of a 3kW HSE/9kWh Batteries .....	81
31. Performance Evaluation of a 4kW PV .....	82
32. Performance of the 5kWh Batteries .....	83
33. Decision Matrix for the Three Types of Stirling Engines.....	96
34. Inputs to the Numerical Run .....	115
35. Thermal Efficiency of the Stirling Cycle without water cooling.....	115

36. Thermal Efficiency of the Stirling Cycle with water cooling.....	116
37. Volume Analysis on the Gamma-Type SE.....	117
38. Volume Analysis on the Beta-Type SE .....	119
39. Volume, Temperature and Pressure for different points in the ideal process for the GSE...	124
40. Volume, Temperature and Pressure for different points in the ideal process for the BSE ...	124
41. 0 <sup>th</sup> order analysis of the GSE .....	130
42. 0 <sup>th</sup> order analysis of the BSE.....	131
43. Comparison of ideal process values and 0 <sup>th</sup> order analysis values .....	132
44. Experimental Results at resistances from 300 to 37.5 Ohm. ....	140
45. Experimental results at resistance values from 43.2 to 3.6 Ohm.....	142
46. 0 <sup>th</sup> Order results compared to the experimental result .....	146
47. Results obtained from the beta-Stirling Engine .....	154



## NOMENCLATURE

SAM	System Advisory Model
HOMER	Hybrid Optimization of Multiple Electric Renewables
EDL	Electricité du Liban or Electricity of Lebanon
USD	United States Dollar
¢	United States Cents
COE	Cost of Energy
GHI	Global Horizontal Irradiance
DNI	Direct Normal Irradiance
DHI	Diffuse Horizontal Irradiance
IRENA	International Renewable Energy Agency
PV	Photovoltaic
PT	Parabolic Trough
ST	Solar Tower
LF	Linear Fresnel
PD	Parabolic Dish
HTF	Heat Transfer Fluid
CSP	Concentrating Solar Power
SE	Stirling Engine
HSE	Hybrid Stirling Engine
GSE	Gamma Stirling Engine
BSE	Beta Stirling Engine
$A_p$	Projected Area
$\psi_{rim}$	Rim Angle
$A_t$	Total Area
Li-ion	Lithium Ion
LF	Load Following
CC	Cycle Charging
NPC	Net Present Cost
$i_r$	Real Discounted Rate
$i_n$	Nominal Discount Rate
$j$	Inflation Rate
IRR	Internal Rate of Return
ROI	Return on Investment
CRF	Capital Recovery Factor
P-V	Pressure-Volume
T-s	Temperature-Specific Entropy
$Q_C$ or $Q_{1-2}$	Heat During Isothermal Compression
$Q_E$ or $Q_{3-4}$	Heat During Isothermal Expansion
W	Work
$\eta_{thermal}$	Thermal Efficiency
P	Pressure
V	Volume
n	Number of Moles
m	Mass

R	Gas Constant
T	Temperature
J	Joules
$\alpha$	Crank Angle
$\varphi$	Phase Shift Angle
$T_L$	Temperature Leaving the Regenerator
$T_C$ or $T_{\min}$	Temperature at the Cooler
$T_H$ or $T_{\max}$	Temperature at the Heater
$C_v$	Specific Heat at Constant Volume
$C_p$	Specific Heat at Constant Pressure
$V_1$	Expansion Volume
$V_2$	Compression Volume
$V_{SE}$	Swept Volume at the Expansion
$V_{SC}$	Swept Volume at the Compression
$V_D$	Dead Volume of the engine
$V_{DE}$	Dead Volume at the Expansion
$V_{DC}$	Dead Volume at the Compression
$V_E$	Volume at the Expansion
$V_C$	Volume at the Compression
$d_d$	Displacer Piston Diameter
$d_w$	Working (or Power) Piston Diameter
h	Length of the Stroke
$V_{SCp}$	Swept Volume At The Compression With Respect To The Power Piston
$\varepsilon$	Compression Ratio

# CHAPTER I

## INTRODUCTION

### **A. World Wide Energy Status**

The demand for energy increased dramatically since the industrial revolution. Through the 17<sup>th</sup> and 18<sup>th</sup> century, the evolution of the steam turbine “significantly ramped up” and opened up an entire new world of consumption of energy [1]. The first approaches to the generation of energy relied on burning coal and fossil fuels. However, the advancements in science lead to the acknowledgement of the fact that fossil fuel burning resulted in the emergence of economic and environmental problems [2].

The price of fossil fuels, being geopolitically dependent, is never stable [3]. In fact, not only the world’s population is increasing but also the standard of livings, in terms of material goods, are getting higher. Additionally, power generation from fossil fuels is always associated with environmental and health concerns [4]. Last but not least, the fear of depletion of this energy source in the following centuries stimulated engineers to seek a renewable, inexhaustible and free of harmful pollutant sources of energy.

### **B. Lebanon’s Energy Status**

Lebanon faces greater problems concerning the energy generation. Since the end of the Civil war in the 1990s, Lebanon was never able to provide a 24/7 energy supply. This is due to the demolition and damage of the electricity infrastructure as well as the weak technical and financial capacities of EDL (Electricité Du Liban or Electricity of Lebanon)

[5]. Since then, the electricity consumption per capita increased and the electricity generation was never able to serve the load. This shortage in the supply of electricity caused regular power cuts in all areas of the country. This problem got aggravated even more by the uncontrolled influx of the Syrian refugees to Lebanon, “leading to a wider electricity capacity shortage” [6]. The electricity production capacity was 1,505 megawatts (MW) in 2013 [6] and estimated to decrease to 1,350 MW most recently [7], while the demand was 2,000 to 2,100 MW, increasing to 2,450 megawatts (MW) in 2009 [6, 7] and estimated to reach a maximum of 3,280 MW in 2016.

In order to compensate the shortage of electricity, some private back-up diesel generators “started spreading across the country” selling their electricity locally to the neighborhood during the EDL rationing hours.

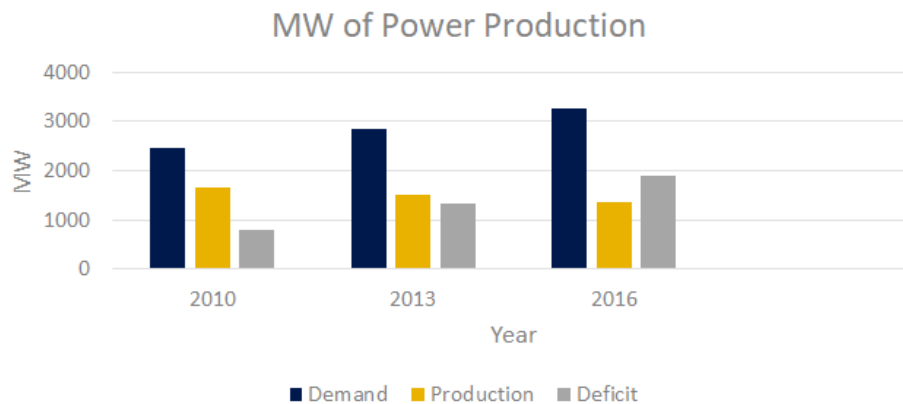


Figure 1. Forecasting of the electrical power deficit of EDL [5]

However, the cost of energy from those private generators, which is sold at a largely higher cost compared to EDL, is a major contributor to increase in the household budgets. Actually, EDL sells its electricity at 13.33 US cents per kWh (¢/kWh), where 8.26 ¢ (62%) goes to the fuel costs and “the generation, transmission and distribution constitute the remaining costs” (38%) [6, 8]. This price is also accompanied by a fixed monthly

rehabilitation tax of 6.66 USD. While this might seem reasonable, another bill is commonly added to the household containing the backup generator’s cost of energy. In fact, in the last 6 months the average cost of energy from the diesel generators was around 400 L.L. per kWh which is equivalent to 27 ¢/kWh [9]. This amounts to an average of 19.03 ¢/kWh, if we assume that each household receives in average 14 hours a day of electricity from EDL and the remaining time from the private generators [9].

$$13.33 * \left(\frac{14 \text{ hours}}{24 \text{ hours}}\right) + 27 * \left(\frac{10 \text{ hours}}{24 \text{ hours}}\right) = 19.03 \text{ US cents per kWh}$$

Moreover, a membership fee is paid monthly in the generators’ bill, along with the 27 ¢/kWh. That extra number accounts for an average of 15 USD. Adding the fixed costs to the total would result then in a total cost of energy of 20.25 ¢/kWh. This causes a constraint both to the personal consumption of the household and to the economic growth of the country.

*Table 1. Cost of Energy in per Lebanese Household*

<b>Source of Electricity</b>	<b>EDL</b>	<b>Back-up generators</b>
<b>Price (¢/kWh)</b>	17.14	27
<b>Average Cost of</b>		
<b>Energy per</b>		~20.25 ¢/kWh
<b>Lebanese Household</b>		

EDL has been depending on the Lebanese Government money. In fact, subsidies to the electricity production have been increasing in the last three decades from 62 million USD in 1998 to 2,026 million USD in 2013. Having a yearly compounded growth rate of 26.17%,

the electricity subsidies reached 14.85% of the government budget, contributing to 3.2% of the national debt [6].

In order to overcome the energy issue, the Ministry of Energy and Water in Lebanon planned for a strategy to reach an installed capacity of 5,000MW after the year 2015. This required importing electricity from Turkey via floating generators to act as a stop-gap solution in the short term of the strategy. Meanwhile, the rehabilitation of the actual EDL electricity reactors would have resulted in an increase in the produced electricity by 245 MW, filling part of the gap in the deficit. The next steps of the plan outline an increase of the installed capacity to 2,500 MW via the introduction of renewable energies and the rehabilitation of existing hydro plants. Thus, around 1,000 million USD was needed from the Lebanese Government, around 2,700 million USD from the private sector and finally 880 million USD were estimated to be added to the international loans, excluding the cost of the imported floating generators.

Anyhow, the plan is still stalled by the Government due to political reasons and this delay intensified the economical load of EDL, knowing that the subsidies, estimated lately to be around 2 billion USD, are added to the countries' loan yearly [6].

### **C. The need for Microgrid decentralized energy systems**

The capacity of the centralized energy generation in Lebanon is getting lower while the need is getting higher. Solutions provided by the country are costly and barely taking steps further. In order to overcome this issue, Microgrid systems are envisaged to solve the problem.

By definition, a Microgrid is a decentralized energy generation system. In fact, it consists of a load and distributed energy sources that “act as a single controllable energy entity” [10]. Microgrids are recognized to operate independently from the grid, in an “islanded mode”. Another important characteristic of the Microgrid is that it increases the renewable energy share, increases the energy efficiency and lower the Cost of Energy (COE). Knowing that the grid is weak, implementing Microgrid systems seems to be one of the solutions to the crisis.

#### **D. The need for Renewable Energy**

The last two decades faced a boom of ideas for renewable energy. That boom was divided into two main categories: Solar and Wind power. Each of these energy sources has some disadvantages like not being efficient enough, being highly fluctuating and not working in some weather conditions like windless weather for wind power, or hours of darkness or clouds for solar power. For this reason, their implementation within an interconnected energy system is envisaged to fit well. Actually, Lebanon has some benefits in increasing the penetration of Solar energy in its power generation system.

#### **E. Lebanon’s Solar Energy**

Classified as the most abundant energy resource on earth, the solar radiation reached the earth’s surface at about 1.3 kilowatts per square meter ( $\text{kW/m}^2$ ) “under clear condition and when the sun is near the zenith” (the zenith is the "highest" point on the celestial sphere). This radiation, known as the Global Horizontal Irradiance (GHI), is the sum of both the Direct Normal Irradiance (DNI) and the Diffuse Horizontal Irradiance (DHI). In fact, the

DNI is the “density of the available solar resource per unit area on the surfaces perpendicular to the direct sunbeam”, and the DHI, is the density of solar resource per unit area that reached the earth after being spread in all directions by the atmosphere [11].

Lebanon has an exceptional geographic position that advantages the use of Solar Energy. A good DNI value “is found in hot and dry regions with reliably clear skies and low aerosol optical depths” [11].

Aerosols, as clarified by NASA, are the solid and liquid particles suspended in the atmosphere [12]. The optical thickness of the aerosol is the degree to which the aerosols prevent the transmission of light by absorption or spreading of light. According to the aerosol thickness map presented by NASA, subtropical latitudes, from a latitude of 15° to 40° north or south, has the lowest aerosol level, nearly zero [11]. Thus those are the favorable areas for solar energy applications. It comprises Northern Africa, extreme south of Europe, south western United States and specifically the Middle East. Actually, Lebanon has a latitude of 33.8 ° North and a longitude of 35.5 ° East, an advantageous geographical position for solar applications.



Thus, the use of solar energy in Lebanon has a promising future. Moreover, the sun is proven to shine around 300 days per year, 8 to 9 hours a day [13]. The driving force to the use of solar energy in Lebanon is also be accentuated by the results obtained from the Ministry of Energy and Water, claiming that around 76% of the total area of Lebanon is eligible for Solar application as it can reach a DNI value above 2000 kWh/(m<sup>2</sup>.year) [14], which is shown in the DNI maps below.

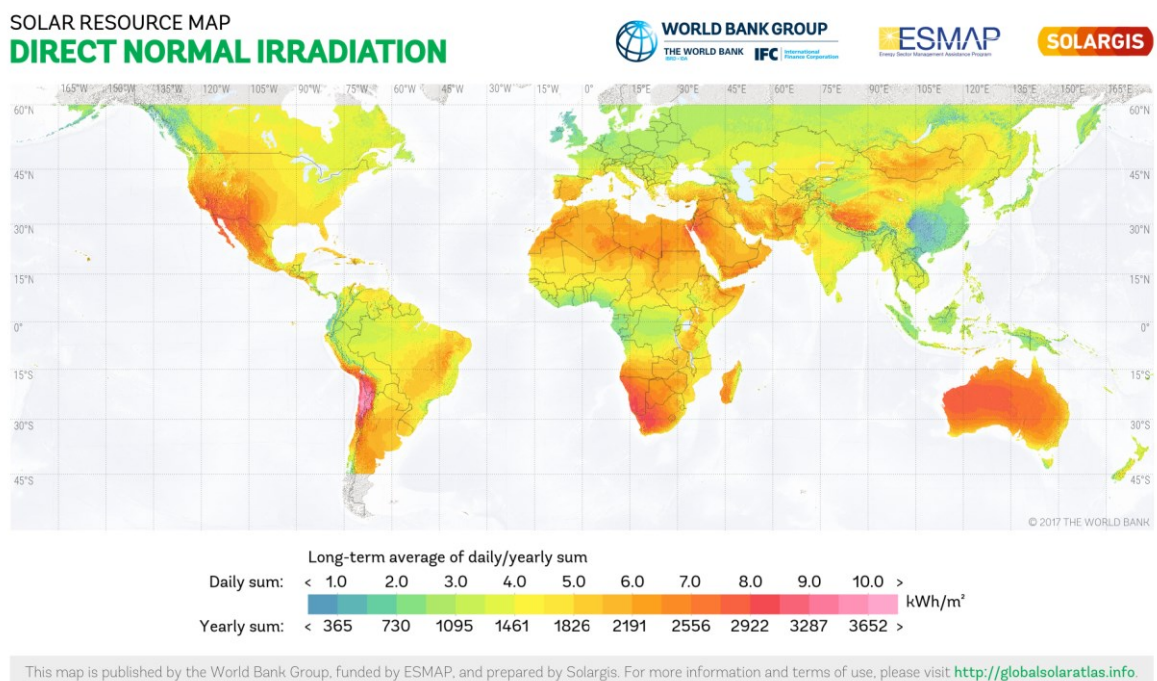
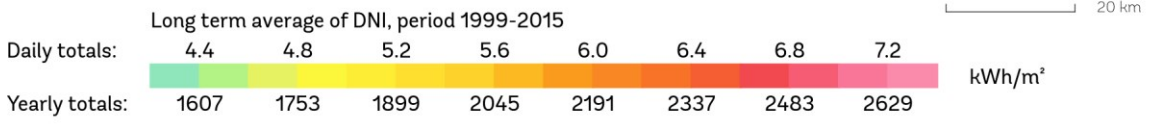
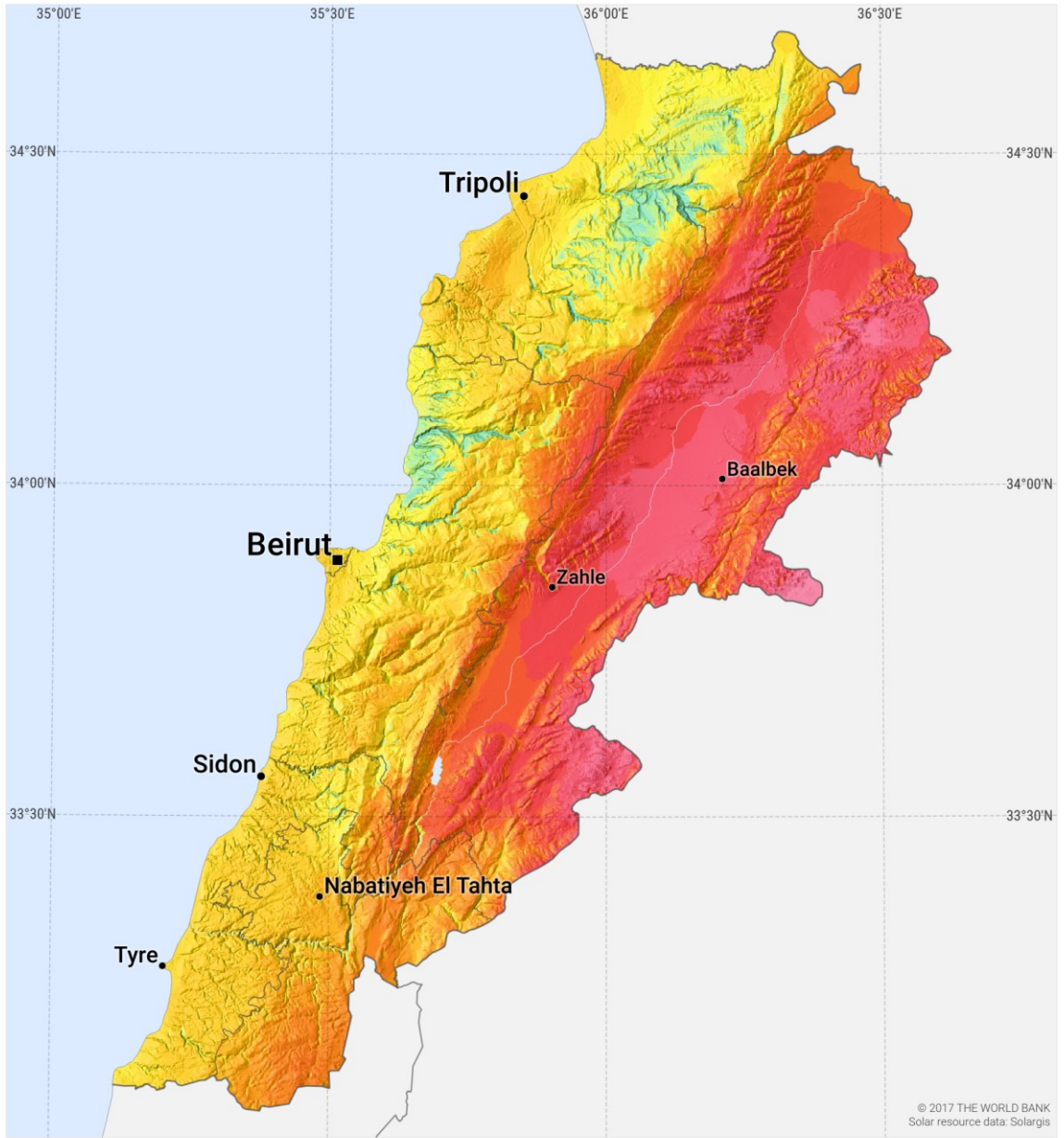


Figure 2. DNI World Map © 2017 The World Bank, Solar resource data: Solargis.

# DIRECT NORMAL IRRADIATION LEBANON



This map is published by the World Bank Group, funded by ESMAP, and prepared by Solargis. For more information and terms of use, please visit <http://globalsolaratlas.info>.

Figure 3. DNI Lebanon Map © 2017 The World Bank, Solar resource data: Solargis.

However, the drawback of implementing solar energy systems is the transient nature of the sun as explained earlier. In fact, the peak demands of electricity are in the mornings and nights as people leave and come home from work. In these times of the day the solar resources decreases. In fact, DNI and GHI are at their maximum in the middle of the day. The problem can be visualized in the following “duck” curve [15].

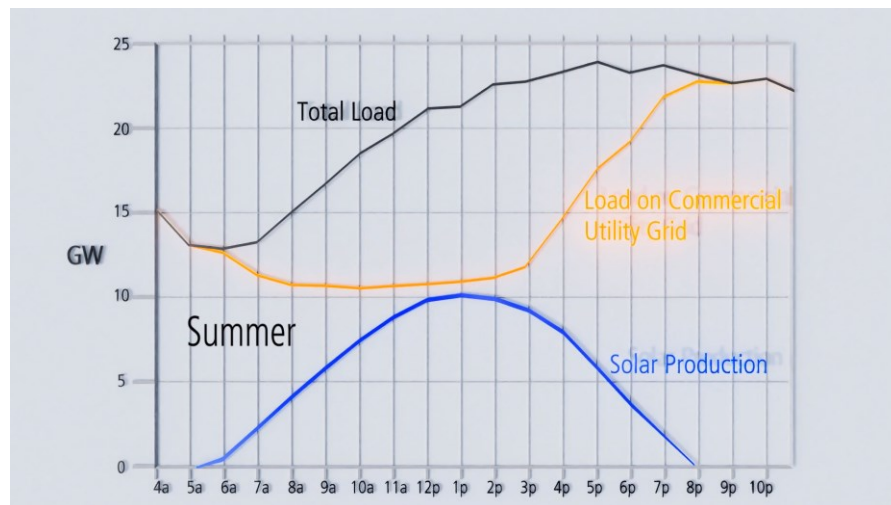


Figure 4. The Duck curve for the California Energy Grid

In this last figure, the x-axis represents the hours of the day while the y-axis represents the electricity load demand for the black and yellow curve and the energy generated from solar energy for the blue curve.

For this reason, dispatching a solar energy system from the grid can't be done without its coupling with hybridization and/or storage.

## F. Lebanon's Oil and Gas opportunity

On the other side of the coin, Noble Energy discovered in December 2009 that Lebanon's sea, in the Levant Basin region, contains Natural Gas resources. According to LOGI and Credit Libanais Economic Research Unit, Lebanon is estimated to produce 1

trillion cubic feet of natural gas production in the following 20 years. That position Lebanon the 30<sup>th</sup> worldwide in terms of Natural Gas Production, and the 8<sup>th</sup> in the region [16].

Thus Lebanon should benefit from both its geographical position and the recent Natural Gas findings offshore, and adopt solar hybrid systems for efficient 24/7 electricity delivery. This will not only reduce the fossil fuel environmental impacts and provide a continuous energy generation, but also increase the lifetime of the Natural Gas reserves underground.

## G. Review of Solar Energy Systems

Having a latitude of 33.8°, Lebanon is in a region with clear skies and a low aerosol level, perfect for Solar Energy application. The price and performance of the solar energy solutions are summarized in the table below, according to the International Renewable Energy Agency (IRENA) [17].

Table 2. Techno-economic analysis of Solar Energy Systems

Solar Energy Application	Photovoltaic (PV)	Parabolic Trough (PT) [18, 19]	Solar Tower (ST) Molten Salt [18, 19]	Solar Tower (ST) Direct Steam Generation (DSG)	Linear Fresnel (LF) (DSG)	Linear Fresnel (LF) Molten Salt	Parabolic Dish (PD) Stirling Engine [20]
Specs	PV Cell	Molten Salt as HTF and storage	Molten Salt as HTF and storage	Water as HTF	Water as HTF	Molten Salt as HTF	Stirling Engine
Installation cost (\$/kW)	1,000-1,300	4,300-5,550 [21]	5,700	4,170	3,725	5,470	2,000-4,000
Efficiency (%)	15	18	15-18	~20	11~13		25-32
Operation and Maintenance Cost (USD/kWh)	0.01-0.02	0.02-0.03		0.03-0.04		0.02-0.03	0.01-0.02
Direct Land Used (acres/MW) [22]	2	6.2		8.9		2.0	2.8
Capacity Factor (%)	16-18				30-50%		
Microgrid Application	Possible	Impossible		Impossible		Partially Possible	Possible

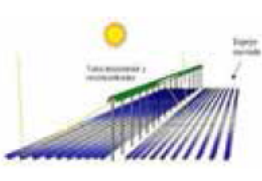
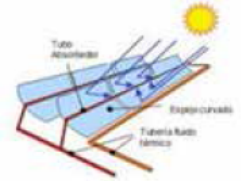
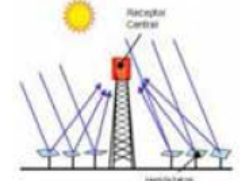
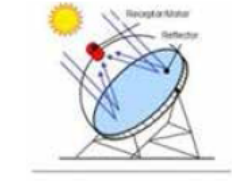
Although mature and cheap, Photovoltaic (PV) systems faces many drawbacks such as a low efficiency (15%), a low capacity factor (an average of 17%) and finally a dramatically elevated cost when coupled with Li-ion batteries (priced at an average of 600

USD/kWh). Concerning other Concentrating Solar Power (CSP) solutions such as the PT, ST and LF, they suffer from an elevated initial capital cost. Moreover, a huge land is required for installation. Therefore, their implementation in a Microgrid system is inappropriate. On the other hand, the Solar Stirling Engine merges high efficiency, high capacity factor and a small land use. In fact, it has been proven in November 2012 that it can reach an efficiency of 32% [20]. For this reason, the following section is investigating more this technology.

## H. The Solar Powered Stirling Engine

The solar powered Stirling Engine belongs to the Concentrating Solar Power (CSP) family, explained briefly in the table 3.

Table 3. Description of various CSP technologies [23]

LINEAR CONCENTRATION SYSTEMS		POINT FOCUS CONCENTRATION SYSTEMS	
LINEAR FRESNEL REFLECTOR	PARABOLIC TROUGH	POWER TOWER SYSTEM	PARABOLIC DISH OR ENGINE (STIRLING)
			
<ul style="list-style-type: none"> <li>LF reflector concentrating systems use flat or slightly curved mirrors to focus solar radiation onto a linear receiver.</li> </ul>	<ul style="list-style-type: none"> <li>PT systems concentrate the solar radiation with a parabola-shaped mirror onto a linear receiver located at its focal length.</li> <li>The PT system is the predominant linear system and is the most developed and commercially tested CSP technology.</li> </ul>	<ul style="list-style-type: none"> <li>A Central Receiver system uses mirrors called heliostats with two-axis sun-tracking to focus concentrated solar radiation on a receiver at the top of a tower.</li> <li>Two main technical designs can be distinguished depending on the working fluid used: water/steam and molten salts.</li> </ul>	<ul style="list-style-type: none"> <li>PD systems consist of a mirrored dish that collect and concentrate sunlight onto a receiver mounted at the focal point of the dish.</li> <li>The receiver is integrated into a high-efficiency engine (the Stirling engine is the most common type of heat engine used).</li> </ul>

Characterized as a unit of a wide class of heat engines, the Stirling engine is a device with a main objective to “convert thermal energy into mechanical motion by cyclic compression and expansion” of a working gas (air, hydrogen or helium) through external heating. The cyclic motion is the origin of a back and forth movement of a piston, also called displacer, between the hot and the cold heat exchanger inside the “pressure chamber” [11]. The piston is directly connected to a rotating wheel that is responsible of providing mechanical power that will then be transformed into electrical energy by a generator (AC current) or a DC motor (DC current).

This closed thermodynamic cycle is a key feature for a net conversion of heat energy to mechanical work. In fact, very similar to the Carnot cycle, the temperature difference between the hot and cold ends is a major factor for the efficiency of the Stirling Engine.

The addition of fins or application of water cooling might be sufficient for the cold end part. However, the main issue is the energy source responsible for the heat at the hot end of the engine. This heat might be originated from burning fossil fuels, burning biomass or from concentrated solar thermal energy, which is obviously the cleanest and most sustainable among the two other options. This emphasizes the multi-fuel characteristic obtained because of the external-heating nature of the Stirling Engine. The Stirling Engine is also known for the “direct conversion of solar power into mechanical power” which reduces the cost and complexity of the system [11], as it is known to be “perhaps the simplest form of engines” [24]. For these reasons, the Stirling engine has been admired since its creation by Rev. Robert Stirling in 1816. However, due to the transient nature of the solar energy, hybridization and



storage are crucial for any renewable energy system. The following section will discuss the proposed configuration.

## I. The Hybridized Stirling Engine (HSE)



Figure 5. Parabolic Dish-Stirling system's different components [25]

As seen in the picture above, the Stirling Engine is integrated into a system that includes a parabolic dish, a support structure, a 2 axis tracking system, foundations as well as a receiver. It might also include a storage system such as Li-ion batteries [26].

Characterized as being an attractive configuration in the solar thermal field, the Stirling engine was initially found to have a high power conversion efficiency of 30 to 45% and a peak solar-to-electric efficiency of 32% [20, 26]. Recently, the Stirling engine has regained interest by researchers because of its “multi-fuel capability”, simplicity and “reasonable size for small scale stationary power” [27]. Hybrid solar/natural gas systems are being tested and were found to increase the capacity factor and provide a better performance during solar transient durations [26, 28].



As previously mentioned, the Stirling Engine is an external combustion engine. Thus it needs a specific temperature value on the hot side of the engine and keeping this temperature at a constant value is crucial for a continuous run. In a HSE system, this temperature value can be generated by concentrating the solar rays on the hot side of the engine. As soon as the temperature gets lowered due to the transient nature of the sun, the Natural Gas burning will take over to supply this deficit in energy.

Not only capable of being an energy dispatchable system that can operate as a standalone with no interruptions, but the Hybridized Stirling Engine can be installed as an independent unit separated or integrated with other renewable energy systems. Furthermore, when land space becomes a major limitation (Table 2), the hybrid Stirling Engine can provide a superior solution in comparison to Solar Towers, Parabolic Troughs and Linear Fresnel which are not suitable for Microgrid applications.

In conclusion, the proposed HSE produces high efficiency with relatively low cost. In November 2012, Ripasso AB, a manufacturer of the solar power Stirling Engine, proved that the efficiency of this system reached 32% [20] with an O&M cost of 0.01 USD/kWh. For this reason, the Stirling technology has always been described as “The World’s most efficient solar electricity system” [29]. Moreover, Stirling Engine is known for its “high efficiency compared to steam engines, quiet operation and the ease with which it can use almost any heat source” [24].

## **J. Previous work done with the Solar Powered Stirling Engine**

Initially tested by McDonnell Douglas in 1985, a 25 kW Stirling Engine was mounted on a parabolic mirror with a 11 m diameter and a focal point temperature of 1430 °C. The efficiency calculated was about 31%. Moreover, the Sandia National Laboratories and Stirling Engine Systems (SES) proved that the Solar Stirling Engine can reach an efficiency of 31.25% in 2008. In addition, McDonnell Douglas Corp., Aerospace Division, of Huntington Beach, California (MDAC) concluded their analysis with a 30% efficiency [26]. Most recently, the efficiency of the HSE technology has reached 32% with Ripasso AB, which makes this solar system the world-leading efficiency among the other solar systems such as PV that can hardly reach a laboratory efficiency of 20% [1, 20].

Hybrid systems were also implemented by Monné et al. and Bravo et al. who proved that hybridization is feasible and advantageous [28, 30]. Another research group developed and examined a hybrid heat pipe receiver for the HSE and were able to implement it successfully. In order to fluctuate between solar and Natural Gas, they developed an automatic control system for the setup [31].

Ripasso AB is a Swedish company that focuses on HSE system. Actually, the Stirling Engine heat is received by the solar power when available. In the hours of darkness or clouds heat is received by Natural Gas burning. A Li-ion battery bank is coupled to the system and its discharged energy is used to deliver DC current for the 2-axis tracker of the system [20]. Ripasso AB's product is a 33kW Stirling Engine mounted on a 14m diameter parabolic dish. In fact, the product is actually priced at 4,000 USD/kW with an operation and maintenance (O&M) cost of 0.01 USD/kWh. They actually aim to reach an installation cost

of 2,000 USD/kW. They also claim that the HSE doesn't require huge areas like other solar systems [20]. However, it can be broken up into units, which makes this technology attractive to Microgrid applications.

United Sun System (USS), based on the fact that the efficiency of this system previously reached 32%, are implementing the same product. However, the only difference is that the system is coupled to a thermal battery rather than a Li-ion one. Actually, this system is in the production stage and its pricing remains unclear [32].

BioStirling (B4S) uses the solar thermal energy as well as biomass to deliver continuous heat to the HSE, however, Li-ion batteries are used as a storage mean to deliver the load. The system advantages discharging Li-ion rather than consuming Biomass when the solar power is unavailable [33]. Actually, the choice of opting for Li-ion battery storage is proven by the price projections. In fact, the price of the Lithium-ion battery is set to decrease from between USD 200 and 1260/kWh in 2016 to between USD 77 and 574/kWh by 2030 [34].

## **K. Recapitulation and Aims of the Thesis and Thesis Plan**

As a recapitulation:

- Lebanon is actually in an energy crisis that should be solved in the most efficient and economical way

- The need is clear: an efficient electricity production with 24/7 and 365 days of generation with no capacity shortages. Implementing the Microgrid ideology is a favorable candidate to help solving the crisis.
- Lebanon benefits from both an elevated DNI and the presence of Natural Gas in its sea, thus hybridization should be taken into consideration
- CSP systems have the highest efficiency and capacity factors when compared to PV systems, however most of the CSP systems suffer from unavoidable centralization and high costs
- The Solar Stirling Engine system has the possibility of being hybridized with other heat sources (burning Natural Gas or Biomass) and thus can deliver 24/7 energy generation, this is also suitable for a country where the grid power is weak and sometimes unreachable in rural areas.
- Hybridized Stirling Engine (HSE) combines low costs, the highest efficiency (proven and not only on paper [20]), as well as the capability of decentralization, which is suitable for a country like Lebanon where huge flat lands are hard to find

The aim of this thesis is to simulate the combination between a HSE system (Solar Thermal Energy and Natural Gas), a PV system and Li-ion batteries within a Microgrid design. Briefly, the priority will be given to Solar operations. When the DNI and GHI are not enough to supply the load, the Natural Gas operations and discharged energy from batteries will complement the deficit. After simulating this system, lab scales Stirling Engine will be tested with a challenge to understand the practical limitations of the Stirling Engine.

## **L. Structure of the Thesis**

The first part of this thesis (Chapter II-III-IV-V) focuses on simulation and optimization to determine the configuration required for a load of one household. The mentioned analysis also includes cost and emission assessment with comparison to other Microgrid alternative such as Diese/PV/Li-ion configurations. This also comprises a sensitivity analysis made for the capital cost of the Stirling Engine. The System Advisory Model (SAM) and the Hybrid Optimization Model for Multiple Energy Resources (HOMER) are the softwares used to achieve this analysis.

The second part of the thesis (Chapter VI-VII-VII) focuses on testing lab scale Stirling Engines: A Gamma Stirling Engine (GSE) and a Beta Stirling Engine (BSE). Firstly, a preliminary thermodynamic analysis is done for two engines. A second step combines experiments done on the GSE in order to determine its power output. Finally, the BSE's is implemented in a prototype assembly with a combustion chamber and a water cooling system, before testing its performance.

## CHAPTER II.

### SIMULATION INPUT AND PROCEDURE

As previously mentioned, the following chapters discuss the simulation done to come up with the designs of the Microgrid proposed. Chapter II focuses first on the simulation done using SAM to obtain the hourly power output of a Solar Powered Stirling Engine. In fact, SAM has the capability of simulating a solar system's data for specific weather conditions, and that includes solar Stirling Engine. However, this lacks hybridization or storage. Therefore, the hourly power output of a Solar Stirling Engine will be simulated in SAM and the result will then be implemented in HOMER to model hybridization and storage. The subsection B. emphasizes on the simulation procedure as well as on HOMER's input.

#### **A. First Simulation Using SAM**

##### ***1. Simulation Input on SAM***

Lebanon's weather data has been added to SAM in order to obtain accurate values in kW representing the hourly system's power generated. Moreover, a Stirling Engine's single unit capacity has the value of 1kW. The inputs to SAM's simulation are represented in the table that follows while the rest of the inputs are taken from the SES manufacturing company [35].

Table 4. SAM input values

Specification	Value
Mirror Diameter (m)	5
Focal Length (m)	1
Rim Angle (degrees)	77.31
Projected Mirror Area (m <sup>2</sup> )	19.63
Total Mirror Area (m <sup>2</sup> )	25.71
Stirling Engine Capacity (kW)	1

In order to produce a nominal power of 1kW with the weather data implemented, the diameter of the mirror is set to be 5m while the focal length will take the value of 1m. In order to obtain the projected area of the mirror, the following formula is used:

$$A_p = \pi * \frac{d^2}{4}$$

However, in order to calculate the total area of the mirror, one must first calculate the rim angle ( $\psi_{rim}$ ) using the following equations [36]:

$$\psi_{rim} = \tan^{-1}\left(\frac{f/d}{2 * ((f/d)^2 - 1/8)}\right)$$

$$A_t = 4 * \pi * f^2 * \frac{\sin^2(\psi_{rim})}{[1 + \cos(\psi_{rim})]^2}$$

where  $f$  is the focal length of the collector and  $d$  is its diameter.

The Lebanese weather data constitutes another input to SAM. In fact, the Solar resource values are obtained in the city of Aabdeh, having a Latitude of 34.51°N and a

Longitude of 35.977°E, in 2005. Ideally, weather data from different years and different areas of the country should be used to obtain multi-year average values. However, due to the lack of resources, the data from one year (2005) and one area (Aabdeh) are being implemented.

The DNI values can be illustrated as follows.

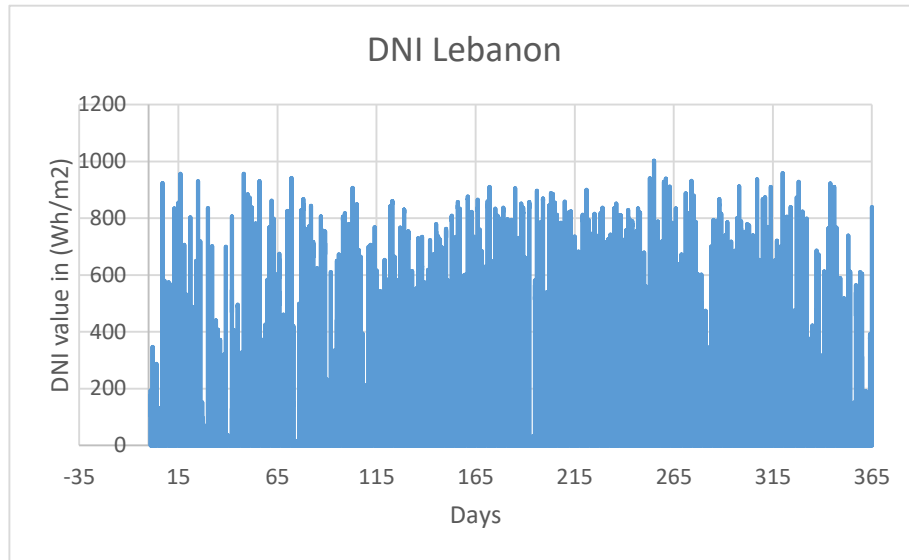


Figure 6. Yearly DNI values in Lebanon

The GHI values can be illustrated as follows.

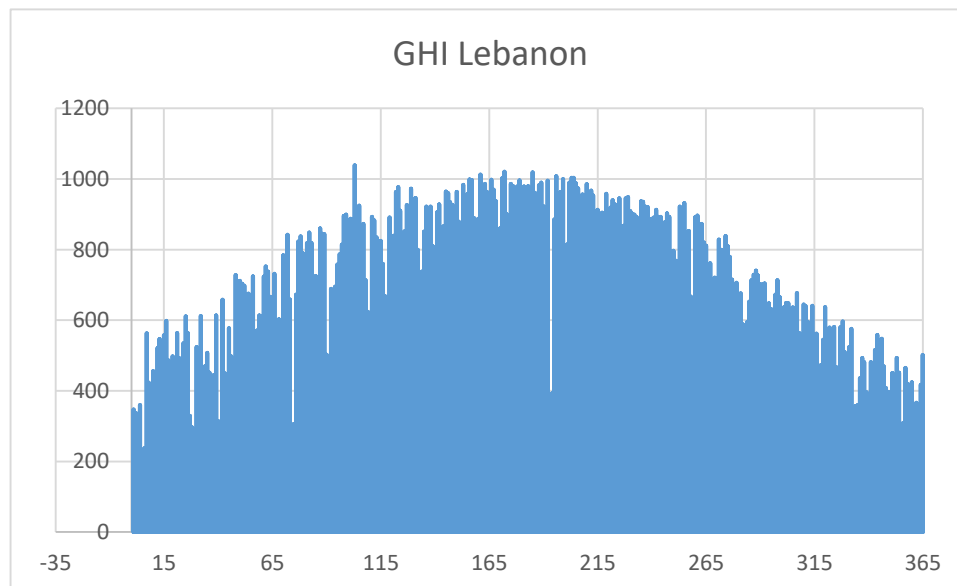


Figure 7. Yearly GHI values in Lebanon



## 2. Results from SAM

After entering the input values in SAM, the result of the simulation of a Stirling Engine system with the Lebanese weather is as follows. These graphs represent the average power output of a Solar Stirling Engine given the mirror dimensions and the Lebanese Solar DNI.

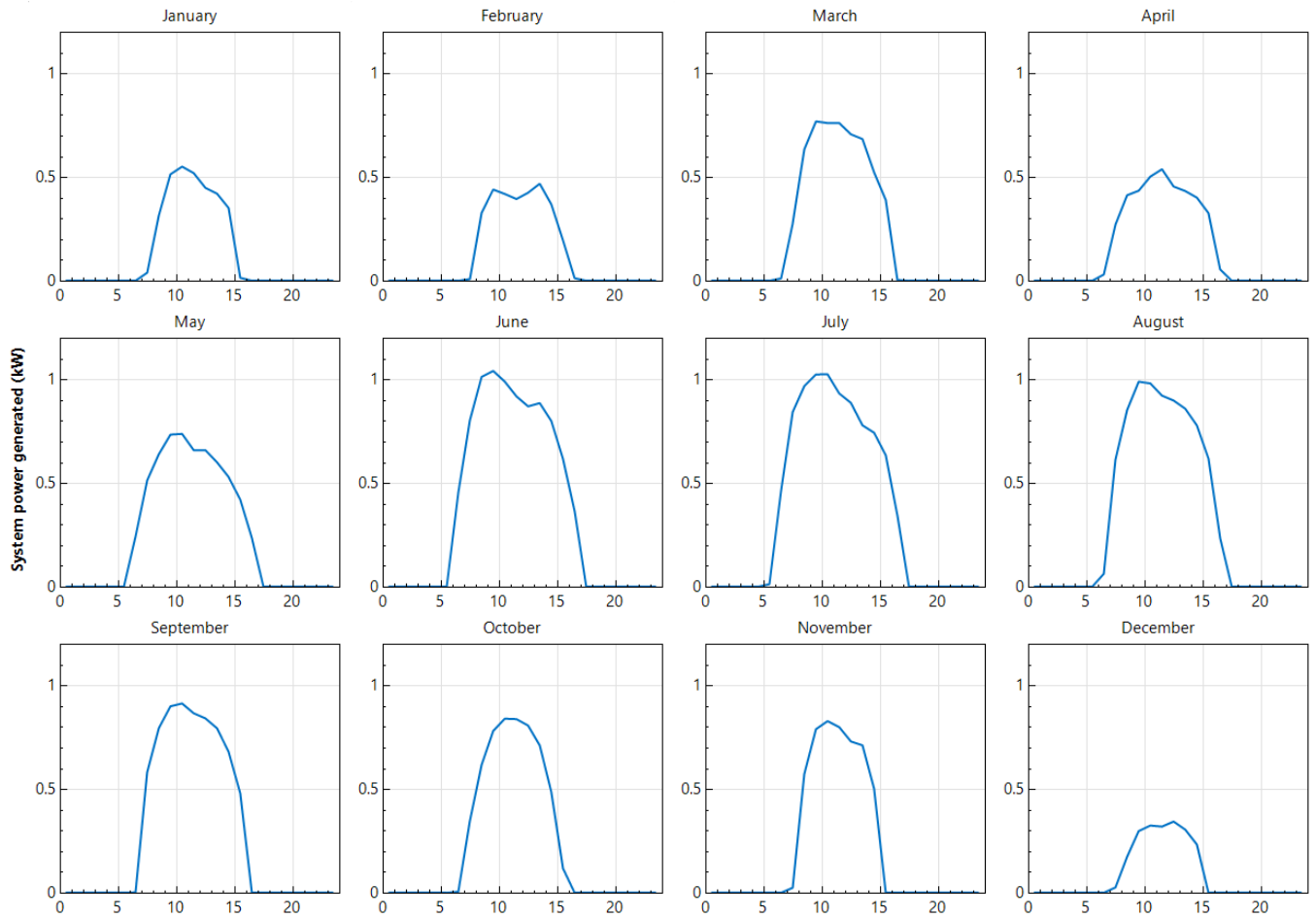


Figure 8. SAM simulation for a 1kW Solar Powered Stirling Engine under the Lebanese weather

## **B. Simulation Input on HOMER**

Characterized as an optimization software, HOMER consists of a simulation, an optimization and a sensitivity analysis algorithm that makes it feasible to evaluate the many possible energy systems configurations, both off-grid and grid-connected. HOMER evaluates the inputs (like technology options, component costs and resource availability) in order to give a list of feasible configurations sorted by net present cost. It also displays simulation results in a form of tables and graphs and compare configurations by evaluating them economically [37, 38].

Actually, HOMER doesn't have the ability of simulating a Solar Thermal Energy system. However, a novel way of expanding the softwares capabilities is used in this project. In fact, the results from a Solar Powered Stirling Engine simulated on SAM are exported to HOMER. Then, the solar power output data is implemented within a Hybridized system that comprises Natural Gas operation, Li-ion storage, converters, PV systems and finally a household's load.

### ***1. Natural Gas Consumption per Stirling Engine***

In order to model a Natural Gas powered Stirling Engine, a custom engine is created in HOMER with a specific fuel curve obtained from the following source [39].

Table 5. Natural Gas Flowrate and Electrical Energy Delivered

Electrical Energy (kW)	Inlet Natural Gas Flowrate (m <sup>3</sup> /h)
4	1.31
4.84	1.58
5.99	1.87

## 2. Li-ion Batteries and Charging Methods

Generic Li-ion battery banks of 1kWh capacity is added from HOMER's database to the overall process.

Concerning the charging and discharging processes of the battery banks, HOMER is capable of running the simulation in two ways: Load Following (LF) and Cycle Charging (CC). LF systems will run in a way that whenever the DNI or GHI are not enough to supply the HSE and the PV, respectively, Natural Gas flow is consumed to meet the load. In some cases, where the load will be higher than the installed capacity, batteries will be used to supplement the excess load. This strategy is also known as 'peak shaving'. When the sun power is enough for the Stirling Engine and the PVs, electrical energy will then be provided to the load. In cases where the sun DNI provides excess power, this excess of electrical energy will be used to charge the batteries.

On another hand, the CC strategy states that whenever the Natural Gas power Stirling Engines are needed, they operate at full power and the excess energy goes toward charging the battery banks [38].

The LF strategy is suitable for a system with high renewable energy sources, such as our case. Thus, the values obtained from a LF simulation will be recorded and analyzed.

### ***3. Converter***

As previously mentioned, the Stirling Engine, whether Natural Gas powered or Solar powered, converts mechanical rotational energy to electrical energy with the help of a generator. Thus, electricity will be provided in an AC current. In this way, the electricity from the Stirling Engine can directly supply the load. However, in order to charge the Li-ion batteries, DC current is needed, and that's the reason why a converter is crucial between the Stirling Engines and the batteries. Obviously when electricity is needed from the batteries in order to supply the load, the same converter will be used to retransform the DC current to AC current.

Moreover, the PV system delivers electrical energy as a DC current. Thus in case PV energy will be needed to deliver the load the converter will play its role of transforming the current from DC to AC.

#### 4. The Load

In a country where all the load, including heating and cooling, is served by the grid, the daily load of any household is estimated to be in average 2.46 kW and has a peak of 4.30 kW, consuming daily an energy of 58.98 kWh/d. The peak time is at 6 o'clock afternoon or 18<sup>th</sup> hour of the day, as shown in the following histogram, and the peak month is estimated to be in January.

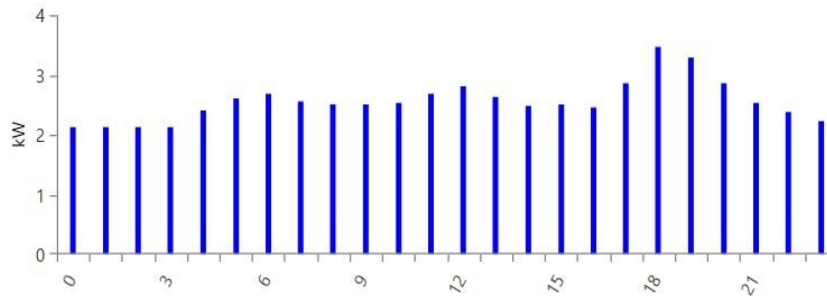


Figure 9. Daily Load per Household

In order to get the closest possible to a real case scenario, the load has a day to day variability factor that is set in the simulation to be 2% (Appendix A). This means that HOMER changes each day's load profile by a random amount ( $\pm 2\%$ ) [38]. The load factor is another characteristic of the load demand distribution and it is the average load divided by the peak load.

Moreover, the Stirling Engine system is equipped with a 2axis tracker system. Recent 2axis tracker systems consumes around 100 kWh/year of energy, which is equivalent to 0.27kWh/day [40]. Adding this constant value to the load demand, the overall consumption of energy is summarized in the following table.

Table 6. Load Summary

	<b>Value</b>
<b>Daily Average (kWh/day)</b>	59.25
<b>Average Load (kW)</b>	2.47
<b>Peak Load (kW)</b>	4.32
<b>Load Factor</b>	0.57

The final schematic of the system implemented in HOMER as shown in *Figure 8* and *9* for a Load of one household.

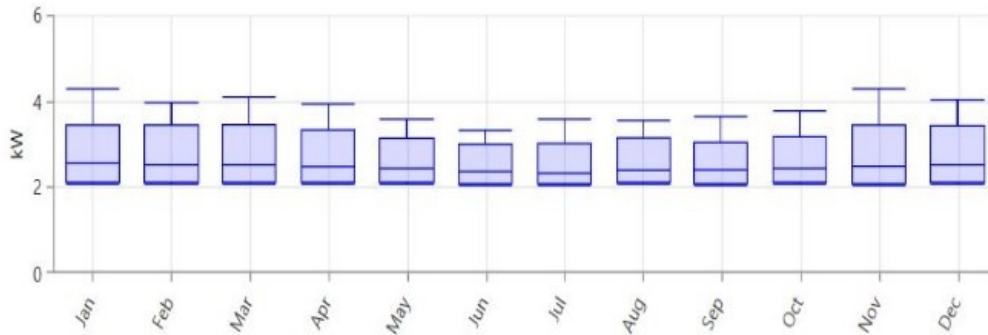


Figure 10. Monthly Load per Household

In the monthly load profile, the top line is the month's overall maximum load. The bottom line, barely visualized in this case, is the overall minimum of the month. In the blue box between those two lines, the top of the box defines the average of the daily maximums while the bottom of the box defines the average daily minimum. Finally, the blue middle line corresponds to the overall average of the month [38].

## 5. Simulation Procedure

The simulation follows the procedure below. This first flowchart presents a simplified simulation procedure while the second displays a more detailed process.

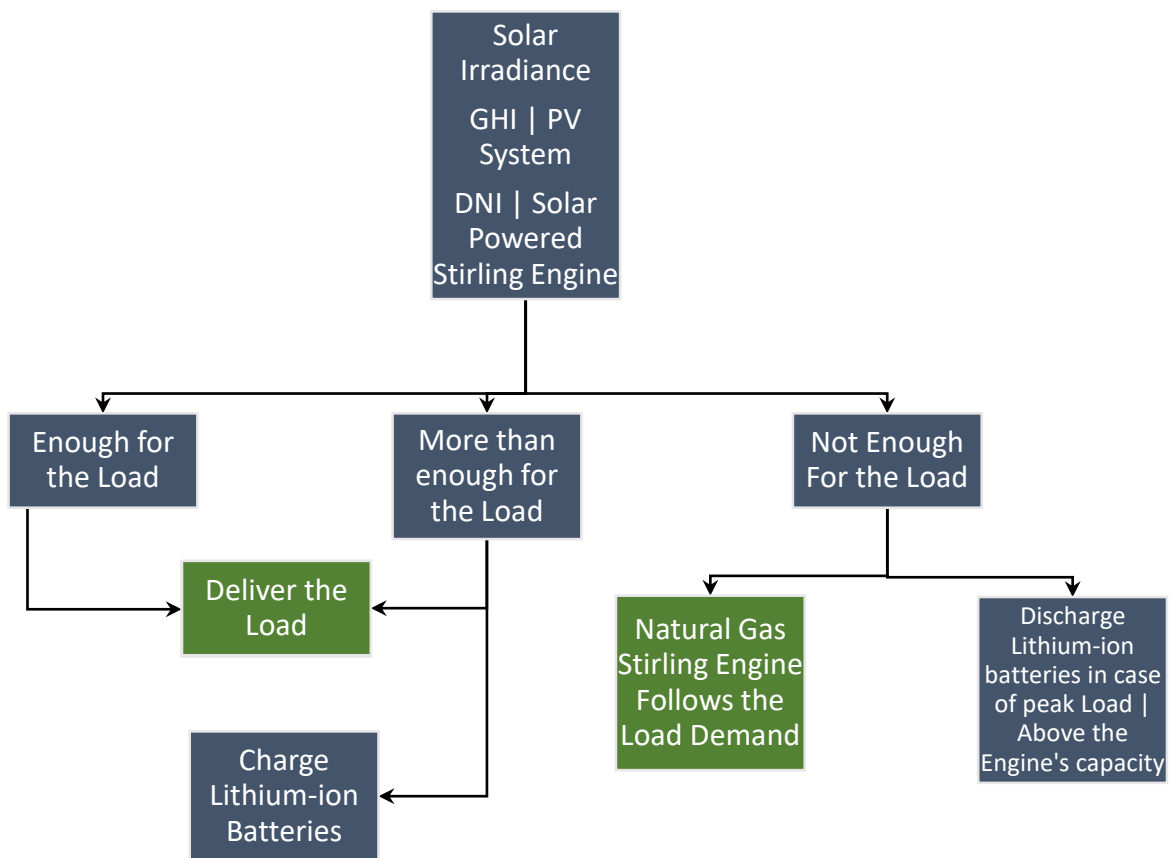


Figure 11. Simulation Logic Brief Flowchart

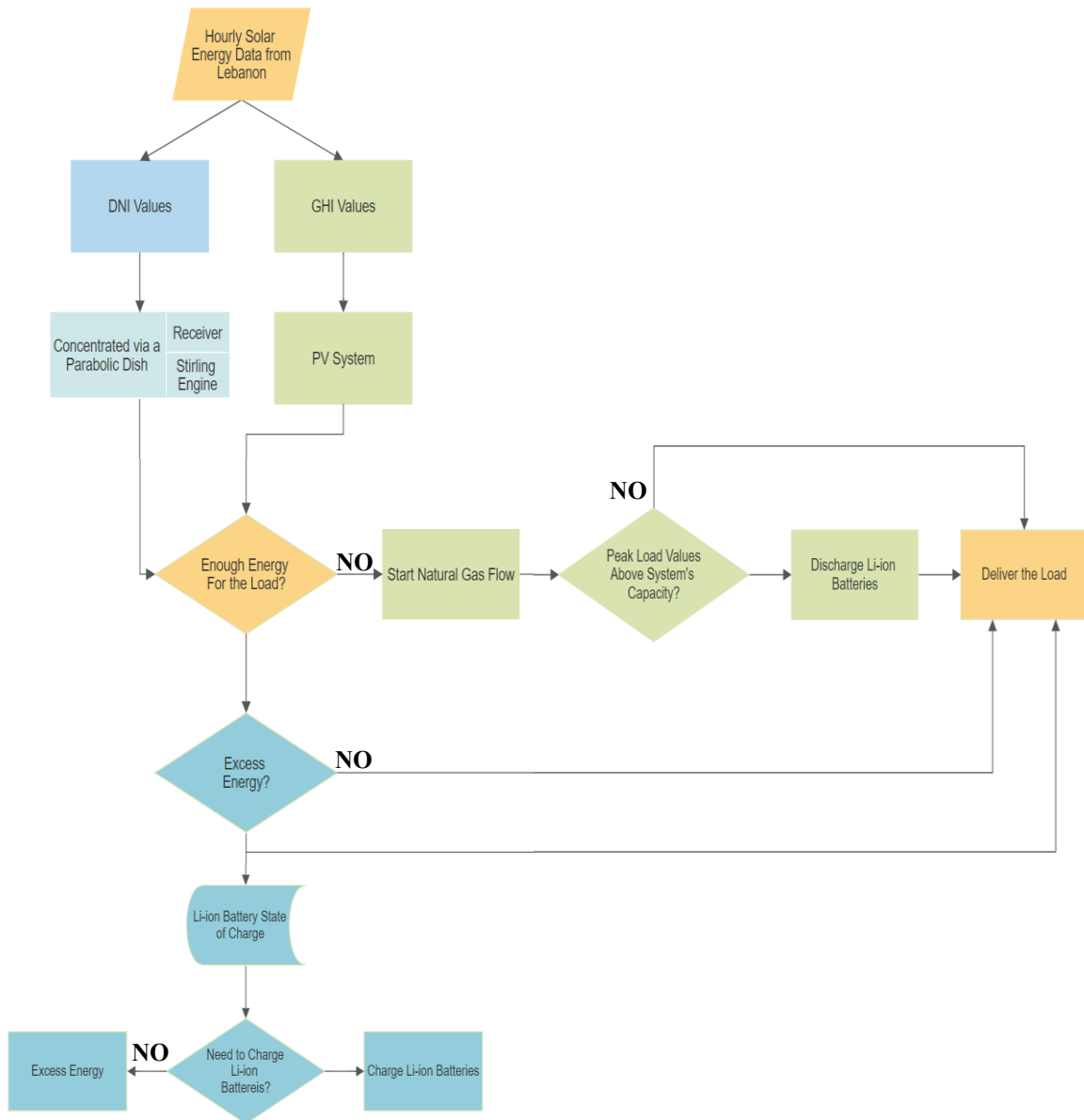


Figure 12. A More Detailed Flowchart about the simulation logic (done using SmartDraw Software)



## **6. Optimization Elements**

Optimization conditions are explained in the following section and more detailed constraints are shown in Appendix A.

### **a. Economics**

#### **i. Inflation Rate**

In the economics analysis, the project lifetime is 25 years. Thus, the Net Present Cost (NPC) of the project will be calculated for 25 years. Money is known to “lose value over the course of time” [41]. This process is known as inflation and the rate at which this process can take place is nothing but the inflation rate. By definition, the inflation rate is defined as the increase in the weighted average price of services and goods over the period of one year. Most central banks aim to keep the value of the inflation rate close to 2% per year, and this value is considered as a benchmark. For this reason, the inflation rate considered in this study is 2%.

#### **ii. Nominal and Real Discount Rate**

The nominal interest rate, by definition, is the rate charged by the bank for the loan. As the inflation rate, it is also expressed in percentage per year and includes inflation.

The real interest rate is the rate added to the inflation rate to yield the nominal discount rate. A simple estimation of the real interest rate is to subtract the inflation rate from the nominal discount rate

$$i_r = i_n - j$$

where  $i_n$  is the Nominal Interest Rate,  $i_r$  is the Real Interest Rate and  $j$  is the Inflation Rate.

According to [41], the rule of thumb for energy sectors the real interest rate varies between “3 to 4 percentage points on top of the inflation”. The inflation rate being 2%, thus the real interest rate can be considered to be 6% for such a project. Thus the Nominal Interest Rate is 8%.

However, in terms of financial mathematics, this method proposed by the last equation is incorrect as it is a basic estimation. The exact way of calculating the Real Interest Rate knowing the value of the Nominal Interest Rate is as follows.

$$i_r = \frac{1 + i_n}{1 + j} - 1 = 5.88\%$$

#### b.Constraints

The initial goal of this study is to calculate the optimal standalone system while taking into consideration that electricity should be delivered to the load 24/7. Thus, a first constraint should be set for the system and it is nothing but a nil capacity shortage.

Another important aspect for a standalone system is the load in current time step. This value specifies how much spare capacity the system should keep operating to serve an unexpected increase in the load. Usually, this value is calculated with respect to the load. Thus, a value of 10% means that the system must keep a spare capacity of 10% of the load

ready for a sudden increase in the load demand [38]. This is important to guarantee a continuous electricity deliverability.

The annual peak load, set at 0% of the load, is a constant amount of the operating reserve that should be kept in case one needs to ensure a minimum load demand. For example, if a system needs to guarantee a minimum amount of power to start up an engine, this should be specified.

The “solar power output as a percentage of renewable output” indicates that the system should keep an extra operational capacity, in each time step, in case the PV output power suddenly decreases by 25%. In other words, if the renewable output is delivering an average 1kW, the energy system should be designed in a way to always deliver 0.25kW more than the actual renewable power delivered to prevent a shortage when the solar resources decrease suddenly.

#### c. Optimization parameters

The optimization on HOMER can be manipulated in this section. The “minutes per time step” input indicates the duration desired minutes simulated per time step. In this case the weather data are presented hourly and therefore the value chosen is 60 minutes. Obviously, this would lead to 8,760 time steps per year.

An important parameter in this list is the focus factor. Imagine that every configuration of systems is a point drawn on a graph with the axis determining the size of every component in the system. The focus factor parameter indicates how the optimizer will evenly “cover the optimization space with points” [38]. “A low focus factor will cover the

space more evenly”, however a high focus factor will fix the points near points with a low net present cost. Obviously, a high focus factor simulation will converge more rapidly as a



Figure 13. Focus Factor effect

smaller number of optimizations is needed. However, in this case one risks to fall into a local optimum. The best way to proceed is to iterate different configurations before finalizing the design on a focus factor with the value of 50 as this will be less time consuming and still give accurate results. When the final design will be set, a last simulation will be done with a lower focus factor of 5 in order to make sure that “the solution reported is the global optimum” [38]. However, during the process, it was found that a capacity factor of 5 kept on converging into local optimum values and to guarantee an accurate simulation, choosing a focus factor of 1 was the best way to proceed.

## 7. Cost Factor

Table 7. Specific Costs of the system

Component	Initial Capital Cost (USD)	O&M Cost
Solar Stirling Engine Setup (1 kW)	2,500	28.65 USD/year
Natural Gas Operation	-	0.0188 USD/h + 0.202 USD/m <sup>3</sup>
PV [17]	1,000	10 USD/year
Lithium-ion Batteries (1 kWh) [34]	600	10 USD/year
Converter (1 kW)	300	-

### a. Initial Capital Cost of Stirling Engine

Concerning the initial capital cost of the system, Ripasso AB estimates that it can sell the entire system at 4,000 USD/kW if it is lower than 30MW and 2,000 USD/kW otherwise, with a goal to stabilize it at 2,000 USD/kW. However, that includes a battery system as well as the inverters, therefore the price of the Stirling Engine and the Parabolic Mirror can be estimated to be somewhere in the 2,000 USD/kW region. In another research papers, the cost of the entire system including direct costs (Collector, the Receiver and the Stirling Engine) and indirect costs (Engineering Procurement and Construction, other costs) is estimated to be around 2,425 USD/kW [42]. On the other hand, an initial capital cost is estimated to be 2 USD/W, or 2,000 USD/kW by other researchers [43].

Thus, for any simulation that takes into consideration the worst case scenario, it is safe to consider the initial cost of a Solar Stirling Engine to be around 2,500 USD/kW, excluding the inverter cost as well as the storage (Li-ion batteries) cost.

However, it was recently found that the only company that is able to mass produce Stirling Engine set the price at 6,000 USD/kW. Thus, the price of the Stirling Engine is not yet fixed and for this reason, the simulation also aims to achieve a sensitivity analysis on the price of the Stirling Engine. The different prices accounted for are 2,500 USD/kW, 4,000 USD/kW, 5,000 USD/kW and finally 6,000 USD/kW.

b.O&M cost of Solar Stirling Engine

According to Ripasso AB [20], the O&M cost of the Stirling Engine is 10 USD/MWh, compared to other CSP technologies with 50 USD/MWh. Thus, the O&M cost of 1kW Stirling Engines are calculated as follows, after obtaining a capacity factor of 32.7% in SAM.

$$1kW * 8,760 \frac{h}{year} = 8,760 kWh = 8.760 \frac{MWh}{year}$$

$$8.760 \frac{MWh}{year} * 32.70\% = 2.865 \frac{MWh}{year} \text{ of energy delivered}$$

$$O\&M = 10 \frac{USD}{MWh} * 2.865 \frac{MWh}{year} = 28.65 \frac{USD}{year}$$

c.O&M Cost of Natural Gas Operation Stirling Engine

The O&M cost of the Stirling Engine is considered to be around 1 ¢/kWh [44]. According to the average energy produced by the Natural Gas Operation Stirling Engine

obtained on HOMER, which is 16,500 kWh/year, the hourly O&M cost can be obtained and implemented for further optimization.

$$0.01 \frac{USD}{kWh} * 16,500 \frac{kWh}{year} = 165 \frac{USD}{year} * \frac{1 year}{8,760 hours} = 0.0188 \frac{USD}{hour} = 1.88 \text{ ¢/hour}$$

#### d. Cost of Natural Gas

The cost of Natural Gas is estimated using the average price of different Natural Gas sources including the average German import, Canada, Japan, the Organization for Economic Cooperation and Development (OECD), the United Kingdom and the United States [45]. The prices of Natural Gas are plotted as follows using the data retrieved from “OurWorldInData.org”.

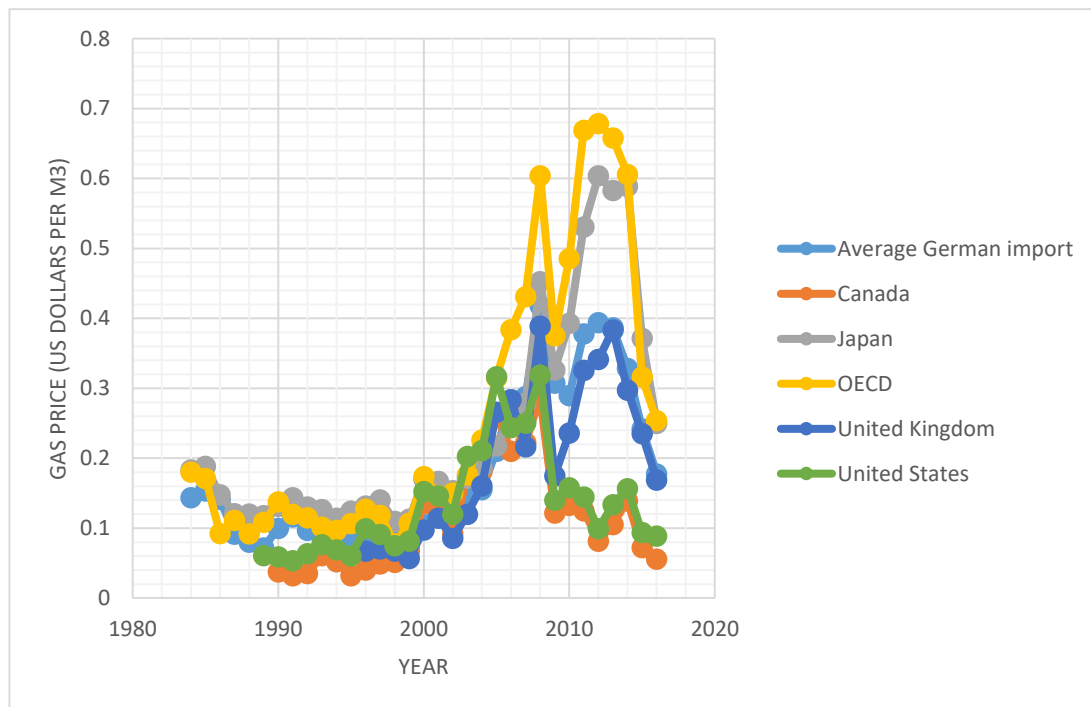


Figure 14. Average price of Natural Gas form different sources

It can be concluded that in the three years presented in the graph, the average price of Natural Gas was 0.202 USD/m<sup>3</sup>.

Table 8. Natural Gas Price

<b>Year</b>	<b>Average Price ( USD/m<sup>3</sup>)</b>
<b>2014</b>	0.222
<b>2015</b>	0.221
<b>2016</b>	0.165
<b>Average Price for the last three years</b>	0.202

### ***8. Natural Gas Engine Operating Conditions: Minimum Load Ratio***

Engines are commonly characterized by their minimum load ratio. This ratio defines the minimum load required by the engines to operate. In other words, this ratio prevents the engine from operating at a too low load [38]. Diesel engines usually are known to have a minimum load ratio of 40%. The Stirling Engine, on the other hand, characterized by being an external combustion engine, do not really depend on a minimum load ratio in this case.

In fact, the engine operates without an internal combustion unit and only depends on an external heat source, which makes it “ideal for use as a converter of thermal energy into mechanical energy” [20]. Keeping the temperature on the hot side of the engine at a constant temperature is the need to continuously transform heat into useful mechanical work and eventually electricity. This high temperature can be generated by concentrating the solar rays on the hot side of the engine.



However, the solar energy is a transient source of heat. The temperature needed on the hot side of the engine can be generated by the sun only in the sun's peak times. In fact, outside the peak sun times, the temperature on the hot side of the engine will not reach its required values and the power will obviously get lower, hence will not be able to deliver the load successfully. However, this is not the case when the system is equipped with a hybridization function. As soon as the temperature on the hot side of the engine gets lower, thus leading to a lower energy delivered, the Natural Gas burning will take over to supply this deficit in energy.

Thus, for any deficit in energy delivered by the sun, the Natural Gas flow burning will compensate the unmet energy. For this reason, the minimum load ratio of the Natural Gas Operation Stirling Engine is set to be 0%. In this way, HOMER operates the two energy components as one component but with different sources.

### ***9. Lifetime of the system***

The simulation studies the system performance and cost for 25 years. However, the lifetime of each component is set as follows.

Table 9. Lifetime of the system

Component	Lifetime (years)
Solar Stirling Engine Setup (1kW)	10
PV	20
Batteries	7
Converter	20

a. Lifetime Validation

The lifetime of the PV was chosen to be 20 years. As a rule of thumb, the PV module's performance degrades in general by 1% per year and a PV module is considered to be unreliable when its rated capacity decreases less than 80% of its nominal power. Even if the 1% rule is considered pessimistic by the National Renewable Energy Laboratory (NREL), this degradation rate is chosen in this simulation as it is considering the worst case scenarios [46].

The lifetime of a Stirling Engine is still unknown. Thus it is considered to be 10 years in this case.

Concerning the batteries, their aging is based on two different degradation processes: cycle aging and calendar aging. Although the warranty given by the batteries' supplier is around 10 to 15 years, it is proven by [47] that the lifetime of a battery in a PV system is around 7 years. The simulation in the paper referenced is based on empirical and

semi empirical data from Tesla's powerwall batteries [47]. For this reason, the lifetime of the battery in this system is considered to be 7 years.

The converter's lifetime is proved by an estimation done in [48]. Based on empirical data, it has been concluded that the lifetime of an electrical converter reaches 20 years.

### C. Area Consideration

The idea behind the area restriction is applied for a system for one household, knowing that the it is preferable not to have a huge place occupied by the PV plant. The area obtained at each run will be used to analyze the feasibility of the system.

In fact, the rated power of a PV system is commonly the value obtained at Standard Test Conditions (STC). This is obtained by measuring the DC output of a PV cell at  $1\text{kW}/\text{m}^2$  of insolation, also known as 1-sun. Thus, in order to find the area of a PV array knowing its rated output, which is the value obtained in the simulation, the following formula should be applied.

$$P_{dc,STC} = 1 \text{ kW}/\text{m}^2 \text{ insolation} \times A (\text{m}^2) \times \eta$$

Assuming an efficiency of 15%, the area of a 1kW PV array is

$$A (\text{m}^2) = \frac{P_{dc,STC}}{1 \frac{\text{kW}}{\text{m}^2} * \eta} = \frac{1 \text{ kW}}{1 \frac{\text{kW}}{\text{m}^2} * 0.15} = 6.67 \text{ m}^2$$

## CHAPTER III

### OPTIMIZATION RESULTS AND DISCUSSION

After implementing the information stated in the previous chapter in HOMER, the following chapter discusses the optimization results obtained. Subsection A shows the simulation of a PV standalone system, whereas the subsection B shows the simulation of different Diesel/PV/Batteries configuration. In addition, subsection C displays the results for a standalone HSE system and finally subsection D illustrates the results obtained for the proposed Microgrid (HSE/PV/Batteries).

#### A. Standalone PV system

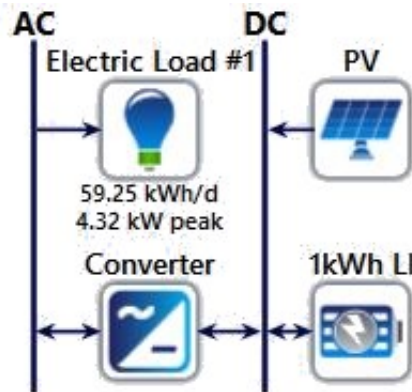


Figure 15. HOMER simulation set up for a PV Standalone System where 1kWh LI stands for a 1kWh Li-ion Battery

Before tackling the simulation of the hybrid system, an optimization for a standalone PV/batteries system is done. Knowing that the simulation considers a decentralized energy source, the capacity shortage is accounted for all the simulation to be 0% leading to a nil unmet load yearly.

A PV plant, delivering electricity as a direct current (DC), is connected to the load via a converter as the load type is AC (Alternative Current). Li-ion Batteries are coupled to the system for storage purposes. In fact, electrical energy in and out of the battery is a DC load. For this reason, the energy discharged from the battery also needs to pass by a converter to be transferred to an AC. The result of the simulation is shown in the table below.

*Table 10. PV Standalone System Optimal Size*

System Component	Size
PV (kW)	72.2
PV area (m <sup>2</sup> )	481
Batteries (kWh)	60
Cost	Value
Initial Capital Cost (USD)	109,783
Net Present Cost (USD)	184,582
Cost of Energy (USD/kWh)	0.660
Renewable Factor (%)	100

*Table 11. PV Standalone System Cost*

The area needed for a standalone PV system is huge, with the value of 481m<sup>2</sup>. Moreover, the initial capital cost and NPC are relatively high when compared to other alternatives.

Obviously, a PV standalone system combined with batteries is an unfeasible solution. However, PV systems are usually combined with a Diesel Engine with the option of combining the system with Li-ion batteries. The simulation for this system is done in the section bellow.

## **B. PV/Diesel Engine Simulation**

In this section the simulation is done considering a PV/Diesel configuration. Knowing that the initial price of a Diesel engine (500 USD/kW [49]) is much lower than the one of the Stirling Engine (2,500 – 6,000USD/kW), it might be interesting to simulate this system and compare it to the one we are focusing on.

The diesel engine configuration for the simulation can be seen in the table below.

Table 12. PV/Diesel Engine's configuration

Component	Initial Capital Cost (USD)	O&M Cost (USD)
Diesel Engine (1 kW)	500 [49]	0.03 USD/hour+ 0.61 USD/liter of diesel [50]
PV (1 kW)	1,000	10 USD/year
Batteries (1kWh)	600	10 USD/year
Converter (1 kW)	300	-

The detailed result of a simulation of a Diesel, PV/Diesel and PV/Diesel/Li-ion batteries can be seen in Appendix C, and an overall comparison will be elaborated in the next section.

Table 13. Diesel/PV/Li-ion optimal configuration

System Design	Size
Diesel (kW)	4.8
Diesel (kW) – PV (kW)	4.8 – 12.1
Diesel (kW) – PV (kW) – Li-ion (kWh)	4.8 – 9.6 – 3

Table 14. Diesel/PV/Li-ion System's cost

System Configuration	Initial Capital Cost (USD)	NPC (USD)	Annualized NPC (USD)	COE (USD/kWh)	Renewable Factor (%)
Diesel (4.8kW)	2,400	97,394.00	7,532.16	0.348	0
Diesel (4.8kW) – PV (12.1kW)	15,488	84,310.00	6,520.28	0.302	35
Diesel (4.8kW) – PV (12.8kW) – Li-ion (5kWh)	14,838	79,855.00	6,175.74	0.286	39

The addition of a PV system obviously increases the initial cost of the system but also decreases its cost along the projects lifetime. The addition of batteries affects the NPC the same way as they reduce the consumption of Diesel. These configurations will later be used as a benchmark for the assessment of the studied configuration.



### C. Standalone Hybrid Stirling Engine (HSE)

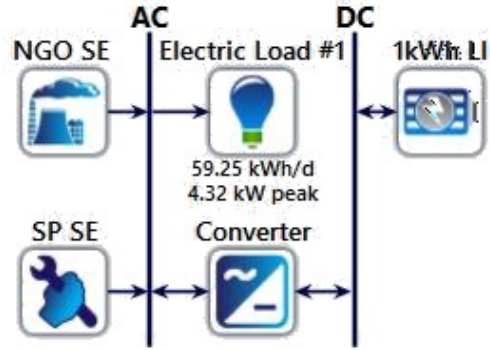


Figure 16. HOMER simulation setup for an HSE standalone system where SP SE stands for Solar Powered Stirling Engine and NGO SE stands for Natural Gas Operation Stirling Engine

Another simulation is done to optimize for a system that consists of a standalone hybrid Stirling Engine system, and the results are as follows. As mentioned earlier, a sensitivity analysis is done on the price of the Stirling Engine and the results are shown below for different prices of the system including 2,500, 4,000, 5,000 and 6,000 USD/kW.

Table 15. Hybrid Stirling Engine (HSE) Standalone optimal Size

System Component	Size
Stirling Engine (kW)	3
Batteries (kWh)	9
Converter (kW)	2.19

Table 16. Hybrid Stirling Engine Standalone Cost

Cost	Installation Price of Stirling Engine			
	2,500 USD/kW	4,000 USD/kW	5,000 USD/kW	6,000 USD/kW
Initial Capital Cost (USD)	13,557	18,031	21,057	24,057
Net Present Cost (USD)	48,553	56,461	61,781	67,072
Cost of Energy (USD/kWh)	0.174	0.202	0.221	0.240
Renewable Factor (%)	24			

This system is much cheaper than a PV standalone system. However, another solution was suggested by HOMER and it is to install a 5kW Stirling Engine with no batteries. The values are shown below.

Table 17. Hybrid Stirling Engine Standalone Cost (5kW Stirling Engine)

Cost	Installation Price of Stirling Engine			
	2,500 USD/kW	4,000 USD/kW	5,000 USD/kW	6,000 USD/kW
Initial Capital Cost (USD)	12,500	20,000	25,000	30,000
Net Present Cost (USD)	47,410	60,630	69,456	78,274
Cost of Energy (USD/kWh)	0.170	0.217	0.248	0.280
Renewable Factor (%)	25			

The initial cost was then 12,500 USD and the cost of energy 0.170 USD/kWh for an installation cost of 2,500 USD/kW. Although this system might seem to be the most optimal for this initial capital cost, in real applications a 5kW system would require much more space than a 3kW engine. In addition, for an installation cost above 2,500 USD/kW, this system is not considered to be optimal to any further extent. Moreover, the market has approved the application of 1kW, 2kW and 3kW for small load application and a 5kW Stirling Engine was never mentioned. For these reasons, this system is considered to be out of the equation.

### D. HSE/PV system results and cost comparisons

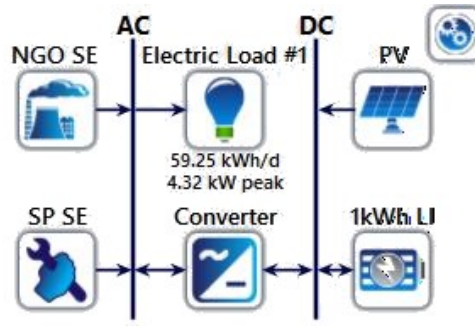


Figure 17. HOMER simulation setup for a HSE/PV system

In order to find out whether adding PV units will lower or increase the cost of a Stirling Engine, and knowing that the load has a mean value of 2.47 kW and an average of 4.32 kW, a first step would be to variate the size of the Stirling System (1kW, 2kW, 3kW,4kW) and find the optimal PV size for each of the systems. The specific results of each

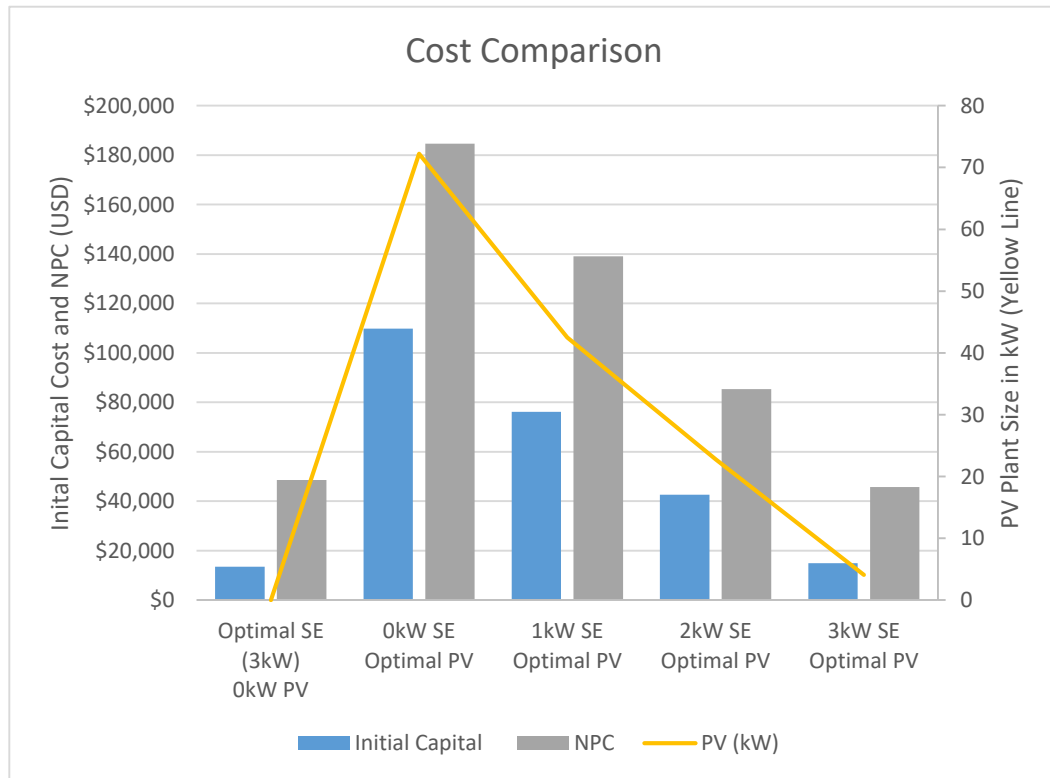


Figure 18. NPC comparison of a Stirling Engine with an optimal PV plant

simulation are found in Appendix B. However, the last figure summarizes the results for a 2,500 USD/kW Stirling Engine system.

The first conclusion that can be drawn from this last figure is that the addition of a Stirling Engine system can lower the price of a PV Standalone system. Moreover, the NPC of the Stirling Engine system will get slightly lowered with the addition of a PV system. This is a first indication that the combination PV/Stirling Engine system works for the advantage of both.

The last figure (*Figure 18*) gives us an idea about the region where the best performing system would be and this is around the 3kW Stirling Engine Area. However, interesting conclusions might be drawn from this graph:

- Adding a 1kW HSE system to a PV plant will reduce the NPC of the system by 45,509 USD.
- Adding a 2kW HSE system to a PV plant will reduce the NPC of the system by 99,204 USD, which sums up to a reduction of 53.7%.
- Adding a 3kW HSE system to a PV plant will reduce the NPC of the system by 138,798 USD, which sums up to a reduction of 75.2%.
- Combining a 4kW PV system with a 3kW HSE will reduce the NPC of a HSE Standalone by 2,769 USD, which sums up to a reduction of 5.7%.

Thus, combining PV/Stirling Engine systems works for the advantage of both systems by reducing the NPC.

To make sure that the experiment did not fall into a local or false optimum, a more specific study was done. In this study, the PV size was fixed (for 1kW, 2kW, 3kW and 4kW) and the size of the Hybrid Stirling system was varying (taking the values of 1kW, 2kW, 3kW and 4kW). Thus, the simulation would then require to optimize between all the different combinations. The specific results of the entire simulation can be found in Appendix B.

### 1.Economic Evaluation

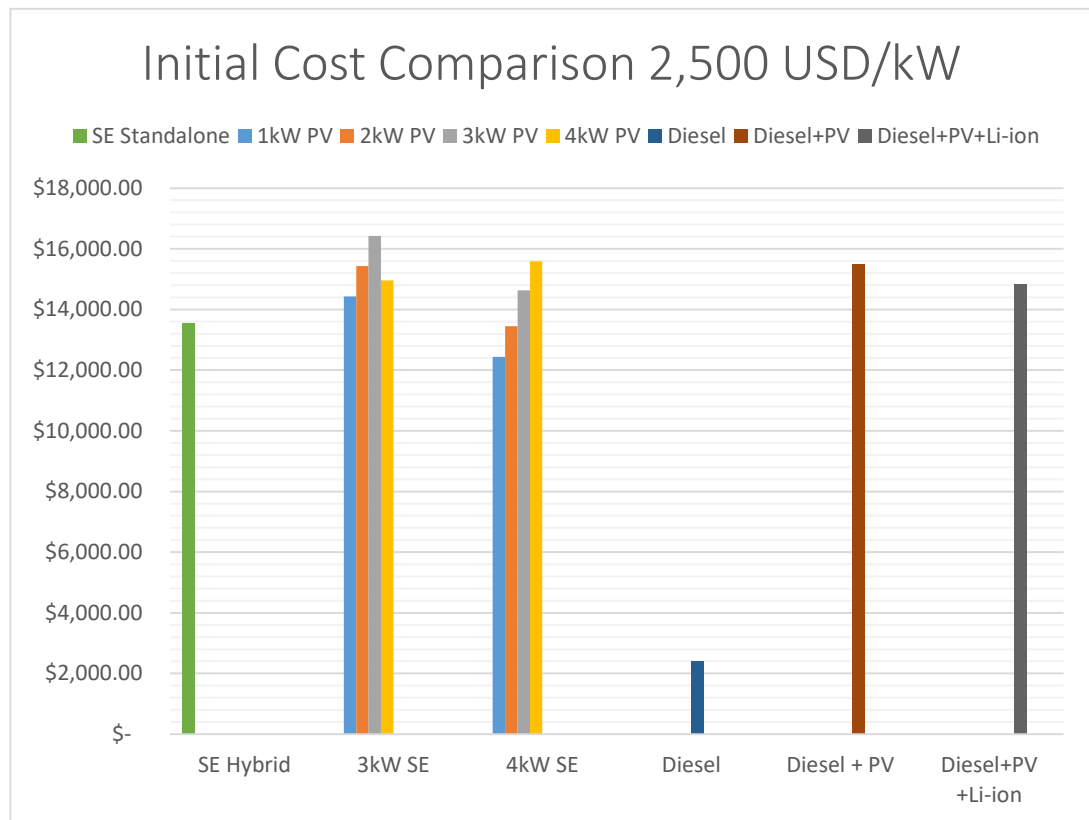


Figure 19. Initial Cost comparison

The last figure shows the initial cost of those different systems. It should be noted that for 1kW and 2kW HSE sizes configurations, the results were either economically unfeasible or even impossible to supply the load. Figure 18 also shows the effect of adding a

PV system so the Stirling Hybrid system. As seen, the initial cost of the system is increasing with the increase of the PV plant until it reached the value of 4kW. In fact, at 4kW PV, the initial cost of the system decreased for a 3kW HSE. The reason for this is linked with the distribution of the batteries, explained later on.

In fact:

- The addition of a PV system to the HSE system reduces the initial cost of a HSE by 8%.
- The coupling of a HSE to a PV/Batteries system reduces the size of the PV plant needed and thus decreases the price by 89%.
- The 4kW HSE/1kW PV/2kWh Batteries is 20% cheaper than a 4.8kW Diesel/12.1kW PV system and 16% cheaper than a 4.8kW Diesel/9.6kW PV/3kWh Batteries system.

*Table 18. Initial Cost Drop*

<b>System Being Compared to</b>	<b>Initial Cost Drop (%)</b>
<b>3kW HSE/9kWh Batteries</b>	8
<b>PV System</b>	89
<b>4.8kW Diesel/12.1kW PV</b>	20
<b>4.8kW Diesel/9.6kW PV/3kWh Batteries</b>	16

Thus, the combination with a PV system is considered to be an added value to the HSE. But the advantages can be mostly observed in the Net Present Cost analysis.

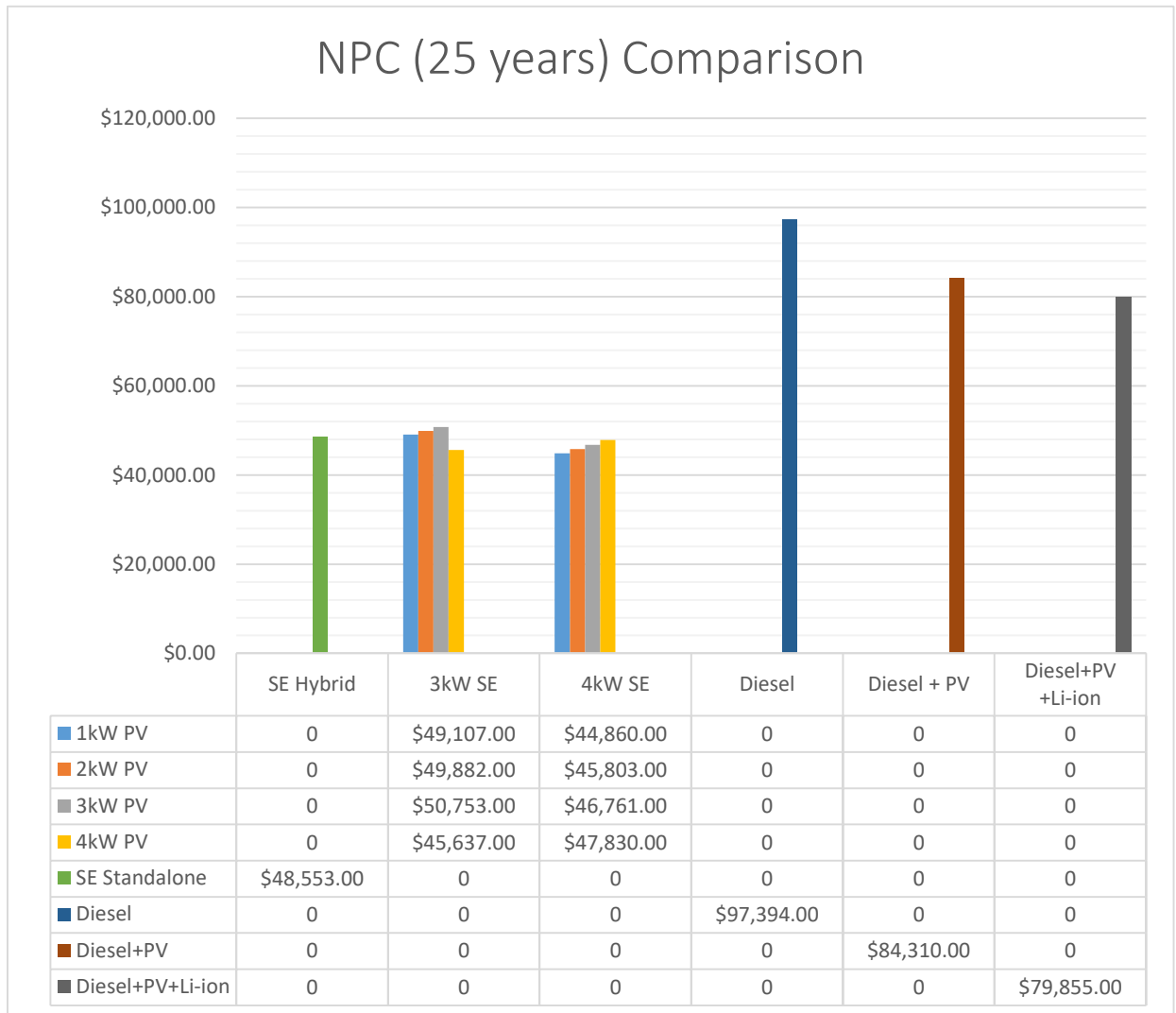


Figure 20. NPC comparison

The best performing system in terms of lowest NPC is obtained at a 4kW HSE/1kW PV/2kWh Batteries for a value of 44,860 USD. Another very close value is obtained for a 3kW HSE/4kW PV/5kWh Batteries for a value of 45,637 USD. In Fact:

- The 4kW HSE/1kW PV/2kWh Batteries is 8% cheaper than a 3kW HSE/9kWh Batteries system over the lifetime of the project (25 years), while the 3kW HSE/4kW PV/5kWh Batteries is 6% cheaper than the 3kW HSE/9kWh Batteries.



- When compared to a 4.8 kW Diesel system, which seems to be very cheap in the beginning with an initial cost of 2,400 USD, the 4kW HSE/1kW PV/2kWh Batteries system is 54% cheaper over 25 years of consumption while the 3kW HSE/4kW PV/5kWh Batteries is 53% cheaper
- The 4kW HSE/1kW PV/2kWh Batteries system is also 47% and 44% cheaper than a 4.8kW Diesel/12.1kW PV and a 4.8kW Diesel/9.6kW PV/3kWh Batteries system.
- The coupling of a HSE to a PV/Batteries system reduces the NPC of the PV system by 76%.

*Table 19. NPC drop when the 4kW HSE/1kW PV/2kWh Batteries is compared to other configurations*

<b>System Being Compared to</b>	<b>Initial Cost Drop (%)</b>
<b>3kW HSE/9kWh Batteries</b>	8
<b>PV System</b>	76
<b>4.8kW Diesel</b>	54
<b>4.8kW Diesel/12.1kW PV</b>	47
<b>4.8kW Diesel/9.6kW PV/3kWh Batteries</b>	44

The cost of energy in USD/kWh is also distributed for the different systems.

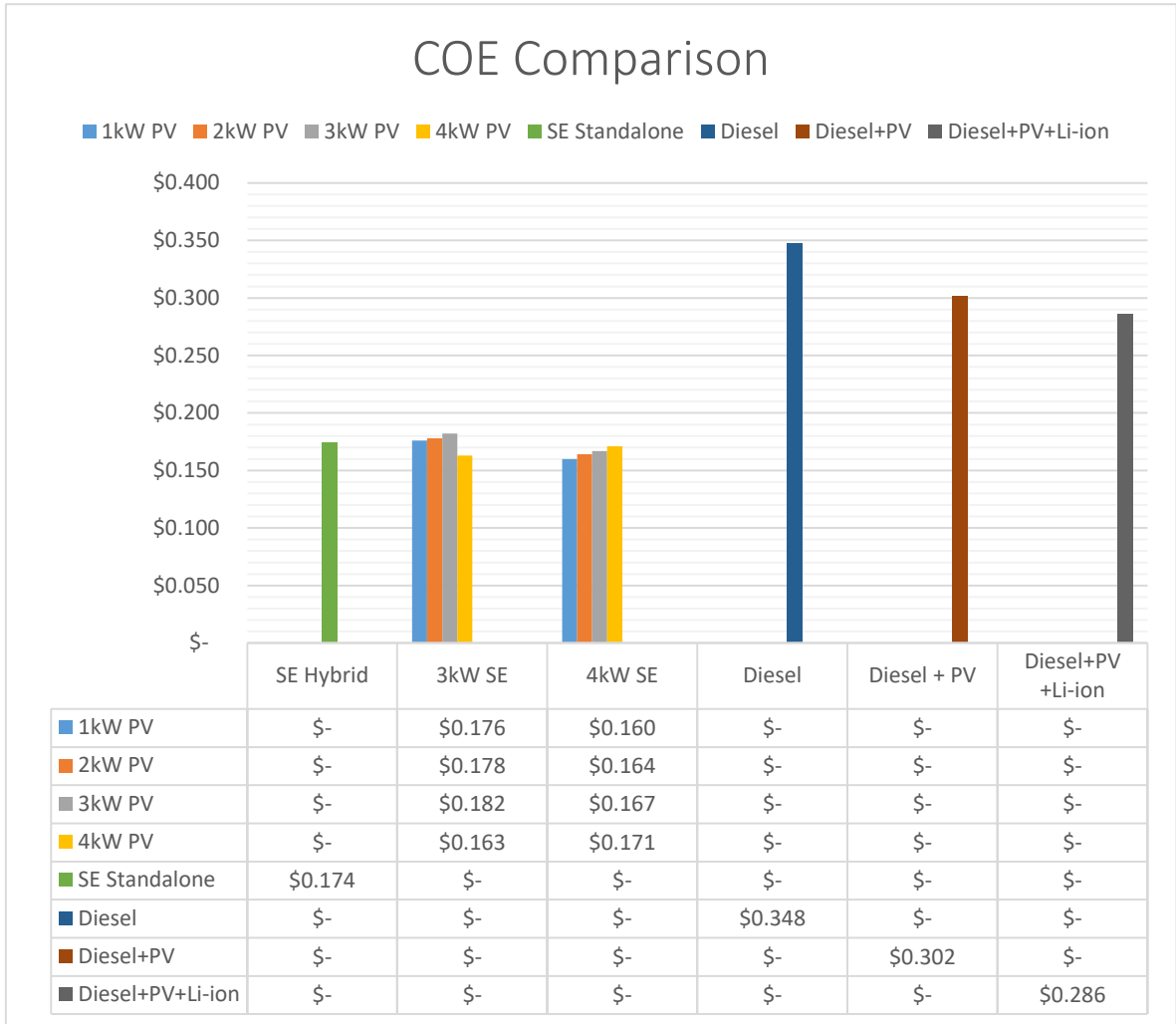


Figure 21. Cost of Energy Comparison

According to the last figure, the best performing system is the 4kW HSE/1kW PV/2kWh Batteries with 16 ¢/kWh. The second best performing one is the 3kW HSE/4kW PV/5kWh Batteries with a very close value of 16.3 ¢/kWh.

a. Link with the Battery Bank Size and the fuel consumption

Appendix B shows the variation in the size of the batteries with respect to the variation in the system's configuration.

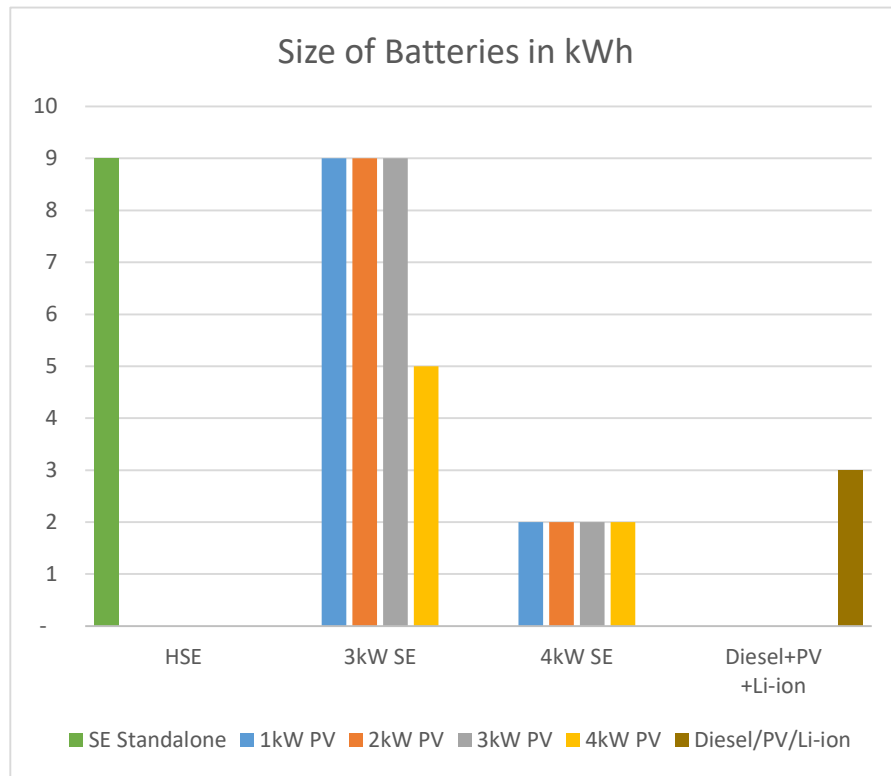


Figure 22. Variation in the Size of the batteries with respect to the system configuration

This shows that the more the capacity of the system is increased, the less batteries are needed. This can be explained by the fact that the smaller the Stirling Engine size is, the more it needs batteries to supply the load. A 1 or 2kW Stirling Engine combined with PV plant, will need a huge size of batteries to supply the peak loads that usually varies from 3.6 kW to 4.32 kW. For this reason, as it can be seen in the Appendix B, a 2kW Stirling Engine combined with a 2kW PV system would require 533 kWh of batteries and an initial capital cost of 329,131 USD. During sun hours, a 2kW HSE/2kW PV system is more than enough to supply the load. However, during the nights or cloudy days, when the HSE operates under using Natural Gas, a huge amount of batteries needs to be coupled with a 2kW Stirling Engine to supply the load.

Thus, for a 2kW Stirling Engine, the optimum size of the PV plant needed is, as shown in the previous analysis (*Figure 18*), is 22.8 kW with a battery bank of 22 kWh. However, a 22.8 kW PV plant is equivalent to a land area of 150 m<sup>2</sup>, which is physically inappropriate when the land is not available or costly. A 4kW PV plant needs around 27 m<sup>2</sup> of space, which is relatively feasible.

The size of the battery bank is constant for the HSE system as well for the 3kW HSE/1-2-3kW PV as it is equal to 9kWh.

In the “3kW SE” section of *Figure 22*, a 3kW HSE/4kW PV requires a smaller amount of batteries. Actually, the smaller the PV plant is, the smaller the excess energy produced is, and the smaller the rate of charge of the batteries is. Therefore, a bigger size of batteries is needed to supply the excess loads for a longer duration of time. The bigger the size of the PV plant is, the faster batteries can charge and serve the excessive loads the second day.

In order to prove this, the yearly battery state of charge of 3kW HSE/9kWh Batteries, 3kW HSE/3kW PV/9kWh Batteries and 3kW HSE/4kW PV/5kWh Batteries can be shown in *Table 15*.

*Table 20. Yearly Battery State of Charge with respect to the system's configuration*

System	Yearly Battery State of Charge	Capacity Shortage (%)	Unmet Load (kWh/year)
3kW HSE/9kWh Batteries		0.00476	0.259
3kW HSE/3kW PV/9kWh Batteries		0	0
3kW HSE/4kW PV/5kWh Batteries		0	0

Actually, a HSE systems coupled with Batteries would not be able to continuously deliver the load without shortages, unless a bigger amount of batteries is added hence elevating the cost of energy and making the project unfeasible. In fact, blue areas can be

found in the state of charge graph and this indicates that the battery bank reached a low state of charge and was not able to deliver the load during peak times leading to an unmet load of 0.259kWh per year. With a 3kW PV installation, the excess energy will increase and thus the batteries will be charged faster and as seen in the state of charge graph in the table below, the state of charge of the battery is most of the time above 50% and always ready to serve the load.

The last case, 3kW HSE/4kW PV/5kWh Batteries, proves what has been analyzed earlier. In fact, the size of the PV plant increased and the size of the battery bank decreased. The excess energy produced by the system also increased leading to a faster charging rate of the batteries. Therefore, a smaller battery bank can be used as it is charged faster than a bigger battery bank.

A question however might be raised from the battery distribution and it is that for a 3kW HSE, a 3kW HSE/1-2-3kW PV, the amount of batteries is constant at 9kWh. Thus, the issue of rate of charging the battery is not anymore an issue. While increasing the capacity of the PV system is not reducing the capacity of the battery bank, then the role of the PV plant should be investigated.

In fact, what is changing in this case is the fuel (Natural Gas) consumption. The table below shows the consumption of fuel for 3 different systems.

*Table 21. Fuel Consumption of three different systems.*

<b>Fuel Consumption</b>	<b>m3</b>	<b>USD</b>
<b>3kW HSE</b>	5,624.00	1,136.00
<b>3kW HSE/3kW PV</b>	5,135.00	1,037.00
<b>3kW HSE/4kW PV</b>	5,054.00	1,021.00

Adding a PV system able to reduce the yearly fuel consumption of the Stirling Engine in times where the GHI of is enough for the PV plant and the DNI is not enough for the Solar Stirling Engine. In order to prove this, an example in the month of February will be taken for a 3kW HSE/3kW PV/9kWh batteries will be illustrated.

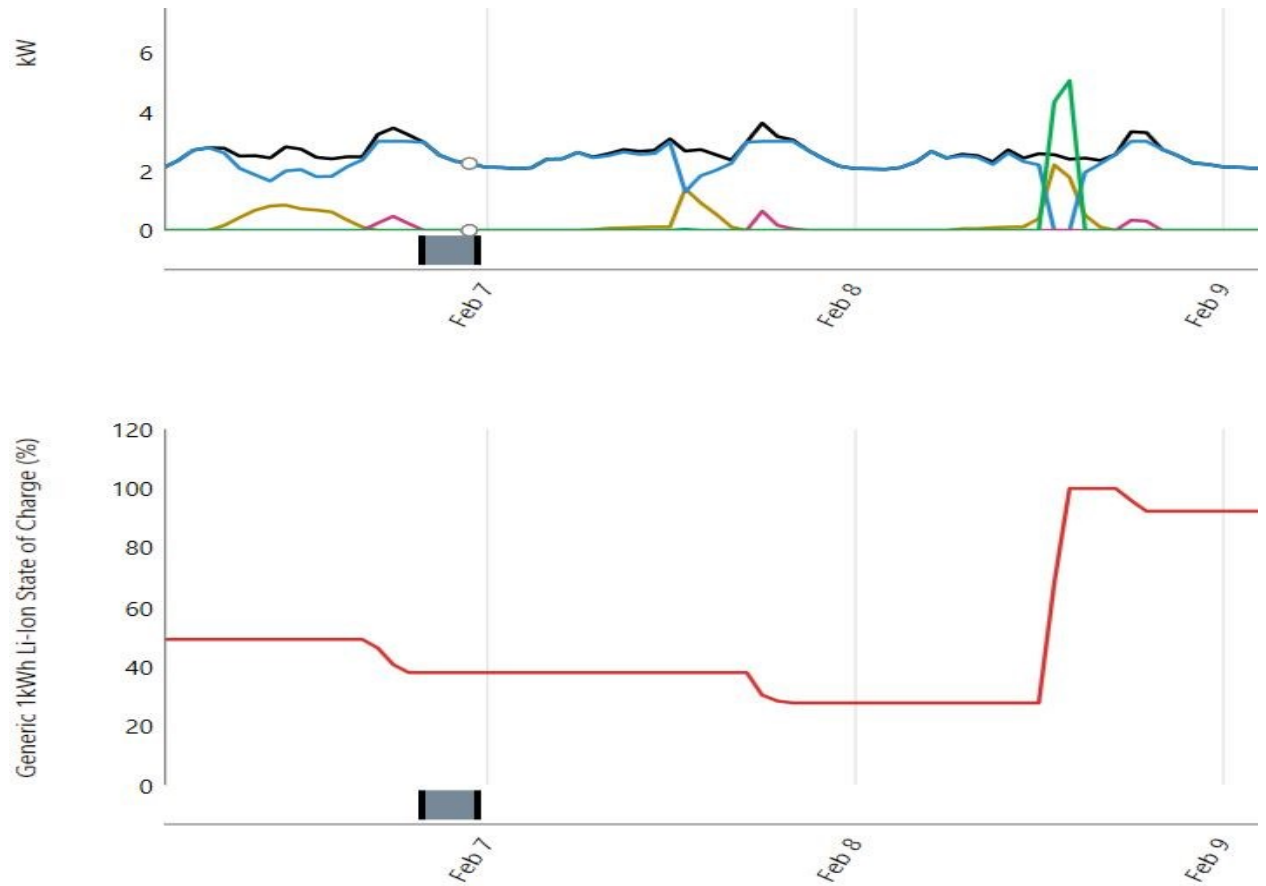


Figure 23. Performance Analysis in the Month of February of a 3kW HSE/3kW PV/9kWh Batteries

The black curve represents the load demand while the yellowish curve represents the power output of the PV plant in kW. The blue and green curves represent the HSE power output operated by Natural Gas and the DNI respectively. The purple one represents the battery discharge power while the red curve in the lower graph represents in the state of charge of the 1kWh battery in %.

This figure proves the idea stated earlier. It can be seen on February 7 that the DNI is not enough to run the HSE as its power output is nil. In fact, the GHI is enough to let the PV deliver electricity. For this reason, the Natural Gas flow gets reduced and the energy delivered is from both the PV and the HSE operated by Natural Gas in parallel. In this instance, the price of fuel will get lowered. In the case where the HSE is not equipped with a PV system, the operation will entirely be done using Natural Gas and thus consuming more fuel, thus elevating the cost of energy of the system.

For these reasons, the size of the battery bank doesn't need to vary in these cases because optimizing the fuel consumption seems to have a higher weight.

## ***2. Best Performing Systems***

The result obtained validated that the 4kW Stirling System combined with a 1kW PV system with 2kWh of Lithium-ion batteries and a 0.78kW converter is the best configuration with a NPC (25 years) of 44,860 USD that sums up to a yearly payment of 3,469 USD, an initial capital cost of 12,343 USD as well as a cost of energy value of 0.160 USD/kWh. A very close system also encountered in the simulation is a 3kW HSE/ 4kW PV/5kWh Batteries. This system has a NPC of 45,637 USD with a yearly payment of 3,529 USD, an initial cost of 14,956 USD and finally a cost of energy of 0.163 USD/kWh.



Table 22. Optimal Component sizes of a HSE/PV/Batteries system

Performance	System Component	Size
Best Performing System	Stirling Engine (kW)	4
	PV (kW)	1
	PV Area (m <sup>2</sup> )	7
	Batteries (kWh)	2
Second Best Performing System	Stirling Engine (kW)	3
	PV (kW)	4
	PV Area (m <sup>2</sup> )	27
	Batteries	5

Table 23. HSE/PV/Batteries Hybrid Standalone Cost

System	Cost	Value
4kW HSE/1kW PV/2kWh Batteries	Initial Capital Cost (USD)	12,434
	Net Present Cost (USD)	44,860
	Cost of Energy (USD/kWh)	0.160
	Renewable Factor (%)	26
3kW HSE/4kW PV/5kWh Batteries	Initial Capital Cost (USD)	14,956
	Net Present Cost (USD)	45,637
	Cost of Energy (USD/kWh)	0.163
	Renewable Factor (%)	32

### 3.Sensitivity Analysis on the Capital Price of the Stirling Engine System

In fact, it has been shown that the most optimal system, having a capital cost of 2,500 USD/kW for a Stirling Engine system, that the 4kW HSE/1kW PV/2kWh Batteries, and the second best performing is the 3kW HSE/4kW PV/5kWh Batteries.

As it has been explained earlier, the price of the Stirling Engine is variable and can eventually take the value of:

- 2,000 USD/kW, considering a perfect scenario from Ripasso AB
- 2,500 USD/kW, taking into consideration the works already been done on a simulation level
- 4,000 USD/kW, considering the actual scenario from Ripasso AB
- Between 5,000 and 6,000 USD/kW considering the price given from the only available mass production manufacturer, MicroGen

The simulations are done for 2,500 USD/kW, 4,000 USD/kW, 5,000 USD/kW and 6,000 USD/kW, and the NPC results are displayed in the following figure.

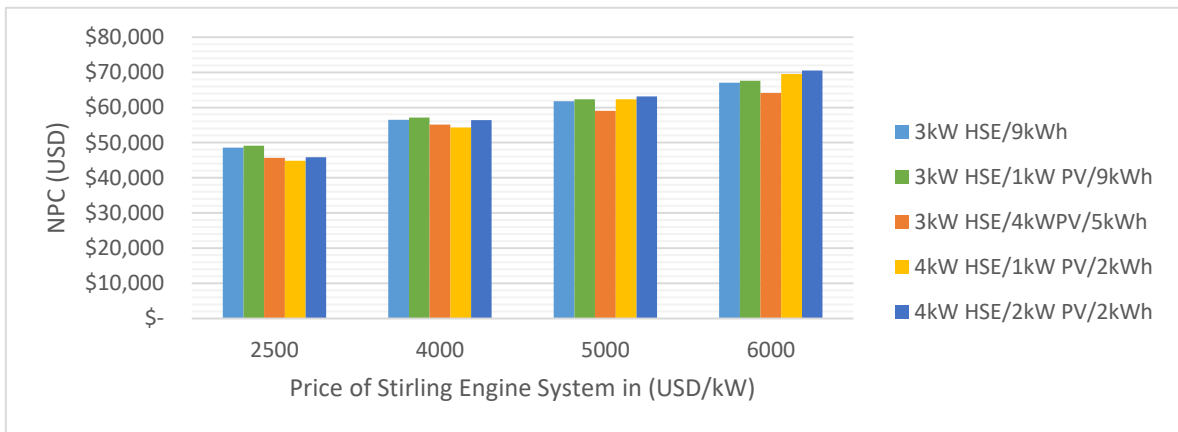


Figure 24. NPC of different HSE/PV configurations for different Capital Costs

In fact, for a capital cost of 2,500 USD/kW, the optimal design is at 4kW HSE/1kW PV/2kWh Batteries. However, it is not for a 5,000 USD/kW Stirling. In order to visualize the variation in a better way, the following figure shows the variation of each configuration with respect to the initial cost of a HSE system. Moreover, an estimation is done for 2,000 USD/kW and 7,000 USD/kW by fitting a polynomial to each configuration.

The yellow line, representing the NPC of a 4kW HSE/1kW PV/2kWh Batteries. In low initial cost systems, it is considered to be the most optimal configuration. However, as the initial price of the HSE increases, the NPC of this system becomes by far one of the least optimal configurations. On the other hand, the 3kW HSE/4kW PV/5kWh Batteries,

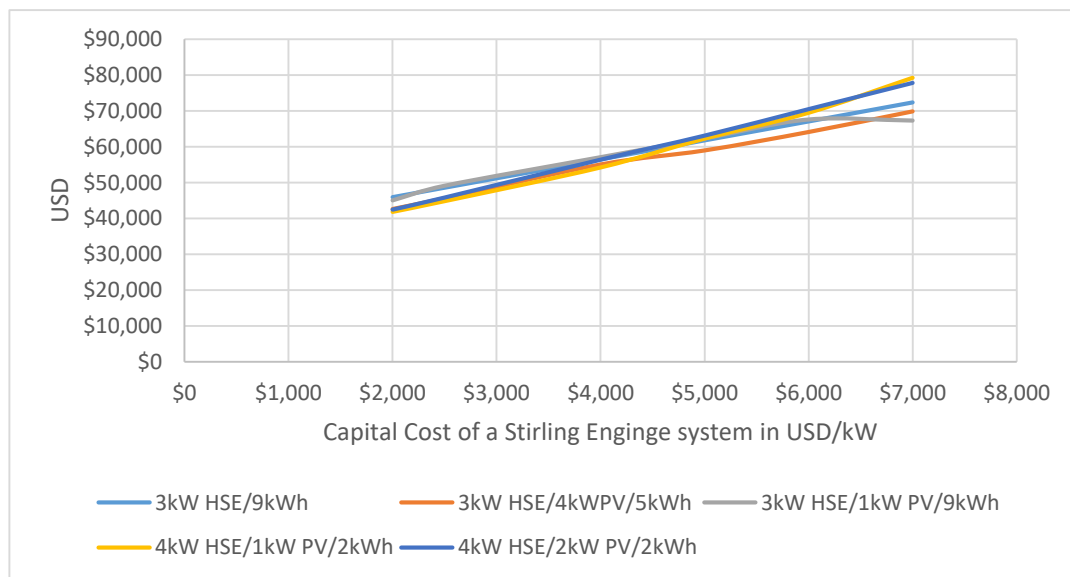


Figure 25. NPC variation for different Capital Costs of the HSE

represented by the orange line and considered as the second optimal configuration for low initial capital costs, turned out to be the most optimal design for higher capital costs. For an extremely high initial cost of the HSE system, the 3kW HSE/1kW PV/9kWh Batteries is the most optimal.

Thus, the optimal design for a Hybrid Stirling Engine (HSE) coupled with a PV system might vary if we consider different scenarios on a capital cost level. For this reason, a sensitivity analysis is made on the initial price of the Stirling Engine system for the following values: 2,000 USD/kW, 2,500 USD/kW, 4,000 USD/kW, 5,000 USD/kW, 6,000 USD/kW and finally 7,000 USD/kW.

Table 24. Unweighted Present Worth Comparison

Capital Cost of the HSE (USD/kW)	Present Worth of 3kW HSE/4kW PV/5kwh Batteries vs 3kW HSE/9kWh Batteries (USD)	Present Worth of 4kW HSE/1kW PV/2kwh Batteries vs 3kW HSE/9kWh Batteries (USD)	Present Worth of 3kW HSE/1kW PV/9kwh Batteries vs 3kW HSE/9kWh Batteries (USD)	Present Worth of 4kW HSE/2kW PV/2kwh Batteries vs 3kW HSE/9kWh Batteries (USD)
2,000	3,266.6	4,049.2	895.6	3,485.8
2,500	2,916	3,693	-554	2,750
4,000	1,369	2,187	-5,223	76
5,000	2,769	-554	-554	-1,328
6,000	2,916	-2,479	-554	-3,422
7,000	2,473.1	-6,930.3	5,064.6	-5,437.2
<b>SUM</b>	15,709.7	-34.1	3,670.2	-3,875.4

The present worth is actually the difference between the NPC of the studied system and a benchmark (in this case the 3kW HSE/9kWh Batteries). In other words, it is the savings one can make by choosing a system over a base system. Thus, the more it is positive, the bigger the savings are.

Thus, the 3kW HSE/4kW PV/5kWh Batteries is by far the most optimal design for any initial cost. However, the distribution of the different initial costs of the Stirling Engine is not equally weighed. Actually, capital costs around 4,000 USD/kW and 6,000 USD/kW are validated by the market. In fact, it is confirmed by a MicroGen that the price will vary between 5,000 USD/kW and 6,000 USD/kW so these two values will be assigned a weight

of 20% each. Moreover, Ripasso AB has set its price for this system at 4,000 USD/kW, thus this value will be assigned the weight of 30%. In addition, the 2,500 USD/kW will be assigned a weight of 20%. And the two extreme values, 2,000 USD/kW and 7,000 USD/kW will be assigned each a weight of 5%.

Table 25. Weighted Present Worth Comparison

Capital Cost of the HSE (USD/kW)	Weights	Present Worth of 3kW HSE/4kW PV/5kwh Batteries vs 3kW HSE/9kWh Batteries (USD)	Present Worth of 4kW HSE/1kW PV/2kwh Batteries vs 3kW HSE/9kWh Batteries (USD)	Present Worth of 3kW HSE/1kW PV/9kwh Batteries vs 3kW HSE/9kWh Batteries (USD)	Present Worth of 4kW HSE/2kW PV/2kwh Batteries vs 3kW HSE/9kWh Batteries (USD)
		<b>2,000</b>	<b>0.05</b>	163.33	202.46
<b>2,500</b>	<b>0.2</b>	583.2	738.6	-110.8	550
<b>4,000</b>	<b>0.3</b>	410.7	656.1	-1,566.9	22.8
<b>5,000</b>	<b>0.2</b>	830.7	-166.2	-166.2	-398.4
<b>6,000</b>	<b>0.2</b>	291.6	-247.9	-55.4	-342.2
<b>7,000</b>	<b>0.05</b>	123.655	-346.515	253.23	-271.86
<b>SUM</b>	<b>1</b>	2,403.185	836.545	-222.79	-265.37

In fact, with the weighted Present Cost Comparison, the 3kW HSE/4kW PV/5kWh Batteries remains by far the most optimal design with the most positive value. Moreover, for each initial capital cost, the present worth is positive, thus savings will always be made when

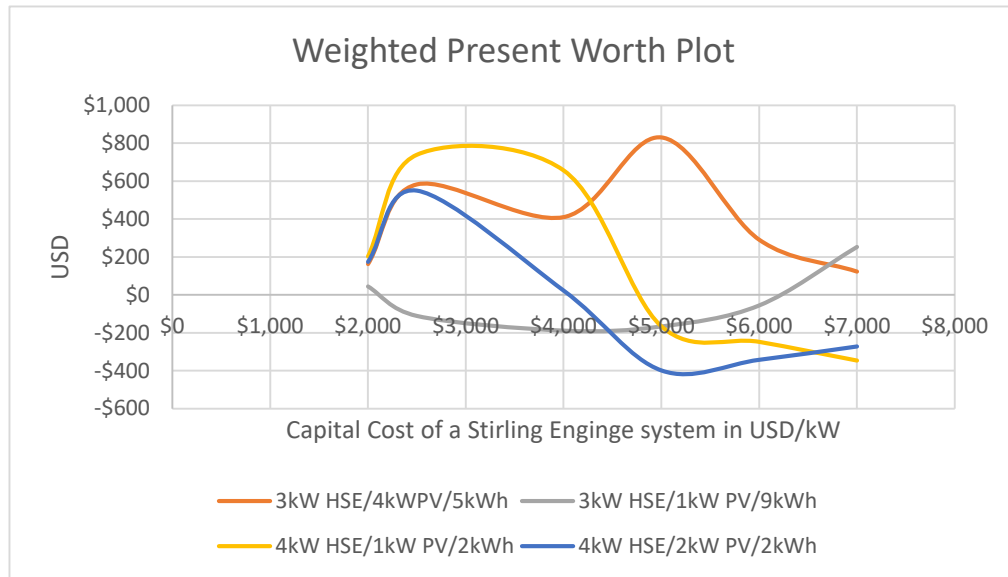


Figure 26. Weighted Present Worth Plot

choosing to add a 4kW PV system to a 3kW HSE system for any initial cost of the system. In order to prove this, the present worth of each system are plotted in function of the initial cost of the HSE.

This plot comes as a proof to what has been said earlier. In fact, the only curve holding a positive value for all the initial costs of the systems is the orange curve that represents the 3kW SE/4kW PV/5kWh Batteries.

However, for any initial price configuration, the NPC over 25 years will always remain lower than the diesel/PV configurations.

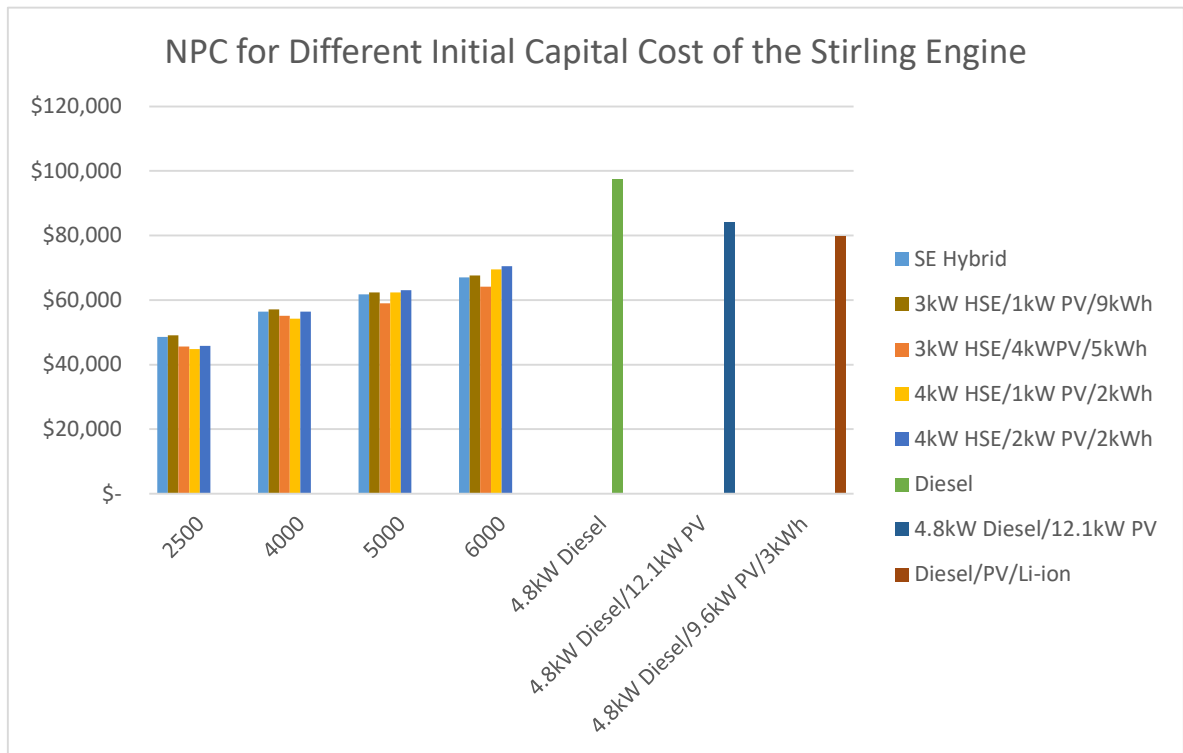


Figure 27. NPC comparison with Diesel/PV configurations

The COE plot is illustrated in *Figure 28*. The conclusion drawn from this plot is that for the scenario where the cost of the Stirling Engine is 2,500 USD/kW and 4,000 USD/kW, the COE is less than the one paid by the Lebanese population (20.25 ¢/kWh). Whereas for the other scenarios, the COE is reach higher values. However, for any scenario, the COE remains less than the Diesel/PV/Batteries configurations.

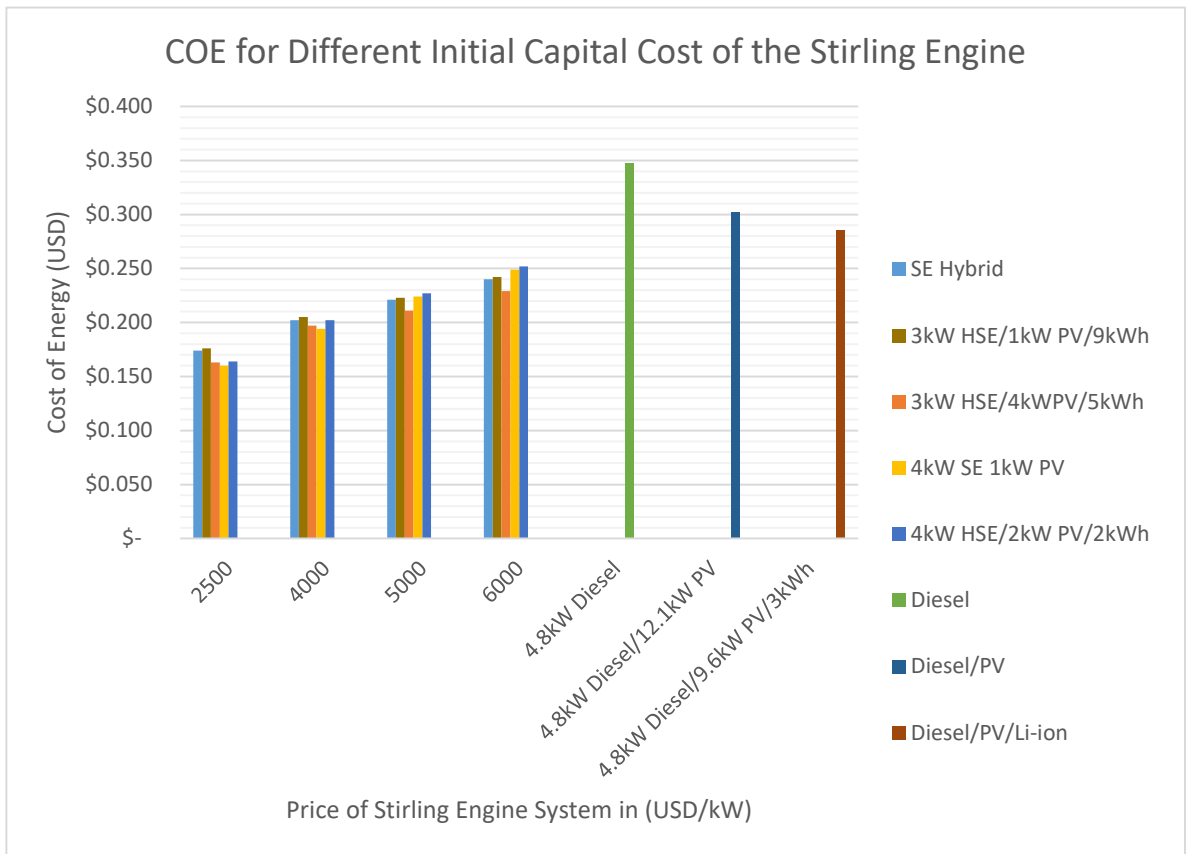


Figure 28. COE comparison with Diesel/PV configuration



## CHAPTER IV

### COMPARISON WITH THE BENCHMARK

Chapter IV elaborates the economic comparison made between the proposed Microgrid system and Diesel/PV/Batteries after explaining different economic factors such as the Payback Period, the Internal Rate of Return as well as the Return on Investment.

#### **A. Payback Period, Internal Rate of Return and Return On Investment**

A very known way of evaluating the economic results of a project is using a payback period analysis [51]. The payback period of an energy system is the ratio of the extra first cost to the annual saving, with respect to another energy system. In a nutshell, it is the amount of “years it takes to recover an investment” [38].

$$\text{Payback Period (years)} = \frac{\text{Extra First Cost (USD)}}{\text{Annual Savings } \left(\frac{\text{USD}}{\text{year}}\right)}$$

According to [51], “surveys consistently show that individuals, and corporations alike, demand very short payback periods—on the order of only a few years—before they are willing to consider an energy investment”. According to [bpie.eu](http://bpie.eu), 77% of European companies accept a payback period of 5 years and more for energy projects, and this is due to the fact that Europeans are seeking to meet their 2020 renewable energy target which is a 20% renewable energy penetration to the gross final consumption [52]. However, 90% of

American companies accept a payback value smaller or equal to 5 years [53]. Moreover, a payback period for an energy system should not increase 3 years [54].

On the other hand, the Internal Rate of Return (IRR) is nothing but the inverse of the payback period. Thus, “it is the ratio of the annual savings to the extra initial investment”.

$$IRR = \frac{\text{Annual Savings } (\frac{USD}{\text{year}})}{\text{Extra First Cost (USD)}}$$

In other terms, in the discount rate at which the case being compared to and the actual system have the same NPC [38].

The Return on Investment (ROI) is the yearly cost savings with respect to the investment of the project. It is commonly expressed in percentage of the initial investment [38]. In other words, it the ratio of the “average yearly difference in nominal cash flows over the project lifetime” to the difference in capital cost.

$$ROI = \frac{\sum_{i=0}^n (C_{i,ref} - C_i)}{n * (C_{cap} - C_{cap,ref})}$$

where  $C_{i,ref}$  is the annual cash flow of the reference system,  $C_i$  is the annual cash flow for the concerned system,  $n$  is the project lifetime,  $C_{cap}$  is the capital cost of the system in question and finally  $C_{cap,ref}$  is the capital cost of the reference system.

## B. Payback Period, IRR and ROI evaluation

The following analysis is based on comparing the 4kW HSE/1kW PV/2kWh Batteries as well as the second optimal solution, the 3kW HSE/4kW PV/5kWh Batteries with the 4.8kW Diesel, 4.8kW Diesel/12.1kW PV and 4.8kW Diesel/9.6kW PV/3kWh Batteries.

### *1. Compare with 4.8kW Diesel, 4.8kW Diesel/12.1kW PV and 4.8kW Diesel/9.6kW PV/3kWh Batteries*

The following table summarizes the ROI, IRR and Simple Payback Period. Moreover, the present worth is nothing but the difference between the NPC of the base case (here the 4.8kW Diesel Engine, 4.8kW Diesel/12.1kW PV and 4.8kW Diesel/9.6kW PV/3kWh Batteries) and the most optimal system (3kW HSE/4kW PV/5kWh Batteries). The annual worth is the present worth multiplied by the Capital Recovery Factor (CRF) which is illustrated in the formula below. Finally, the difference between the discounted payback and the simple payback period is that the discounted one takes into consideration the time value of money [38].

$$CRF = \frac{i(1+i)^n}{(1+i)^n - 1}$$

where  $i$  is the real discount rate and  $n$  is the lifetime of the project expressed in number of years.

Table 26. Economic Evaluation when compared to a 4.8kW Diesel System

<b>3kW HSE/4kW PV/5kWh Batteries</b>	<b>Compared with 4.8kW Diesel</b>	<b>Compare with 4.8kW Diesel/12.1kW PV</b>	<b>Compare with 4.8kW Diesel/9.6kW PV/3kWh Batteries</b>
<b>Present Worth (USD)</b>	\$51,756	\$38,662	\$34,207
<b>Annual Worth (USD/year)</b>	\$4,003	\$2,990	\$2,647
<b>ROI (%)</b>	39.4%	-	-
<b>IRR (%)</b>	42%	-	-
<b>Simple Payback (year)</b>	2.29	-	-
<b>Discounted Payback (year)</b>	2.59	-	-

Thus, one needs 2.6 years to recover the extra payment invested in a 3kW HSE/4kW

PV/5kWh Batteries system when compared to a 4.8kW Diesel system. Moreover, there are no extra costs paid for the other two configurations.

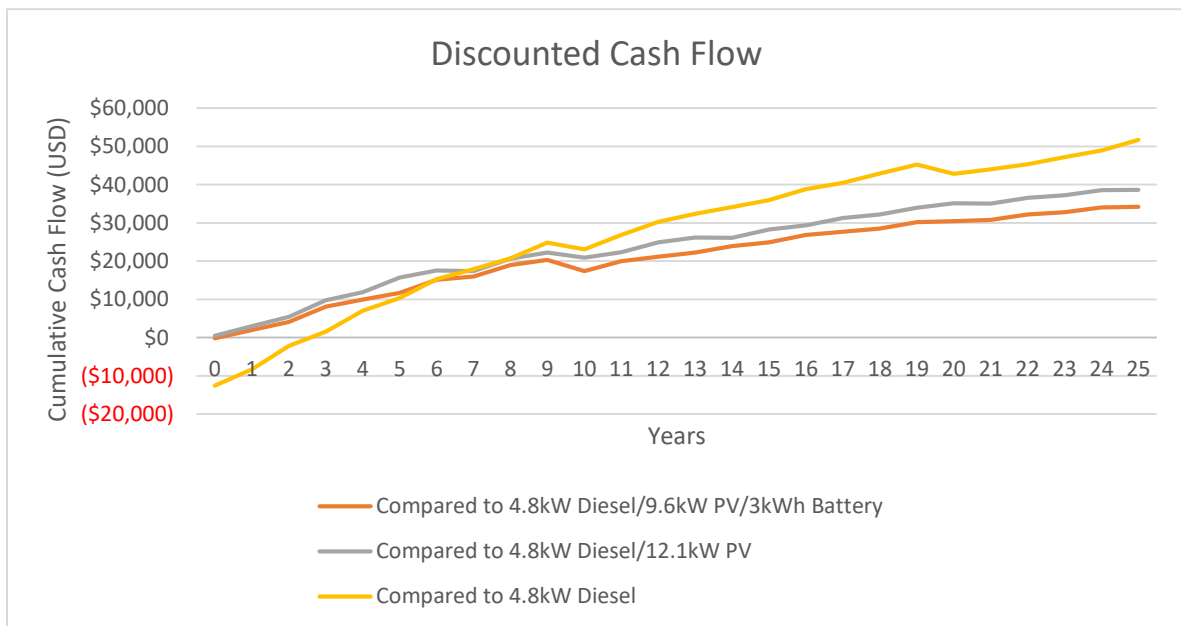


Figure 29. Cumulative Discounted Present Cost

Actually, a second definition of the discounted payback period is “where the discounted cash flow difference crosses zero” [38]. In fact, at year number 2.6, the curve crosses the 0\$ line in *Figure 29*.

In fact, the Present and Annual worth, giving positive values, are indicators that the system being studied presents a high advantage when compared to a Diesel/PV configuration.

This last plot illustrates the savings made when the investment is done on a 3kW HSE/kW PV/5kWh Batteries rather than a Diesel/PV configuration.

## CHAPTER V

# PERFORMANCE ANALYSIS OF A 3KW HSE/4KW PV/5KWH BATTERIES

Knowing that the best configuration turned out to be 3kW HSE/4kW PV/5kWh Batteries, this section studies and analyses the result of the simulation done on HOMER for this configuration. The analysis will cover the electrical performance of the system, the Stirling Engine power delivered by the sun and the Natural Gas, the Natural Gas consumption, the PV plant electricity production, the Li-ion batteries energy throughput, as well as the emissions of the system compared to the emissions out of a Diesel Engine.

### A. Electrical Performance

The electrical performance of the system describes the yearly production of electrical energy delivered to the load.

*Table 27. Electrical Performance of a 3kW HSE/4kW PV/5kWh Batteries*

<b>System Component</b>	<b>Yearly Production (kWh/year)</b>	<b>Percentage of the total production (%)</b>
<b>4kW PV Plant</b>	6,275	20.90
<b>3kW HSE/Solar Powered</b>	9,032	30.08
<b>3kW HSE/Natural Gas Powered</b>	14,718	49.02
<b>Total</b>	30.025	100

The overall consumption of this energy has the value of 21,625 kWh/year, which leads to an excess of 8,280.3 kWh/year of electrical energy from which batteries are charged. The renewable fraction of this configuration is 31.9%.

## B. Solar Powered Stirling Engine

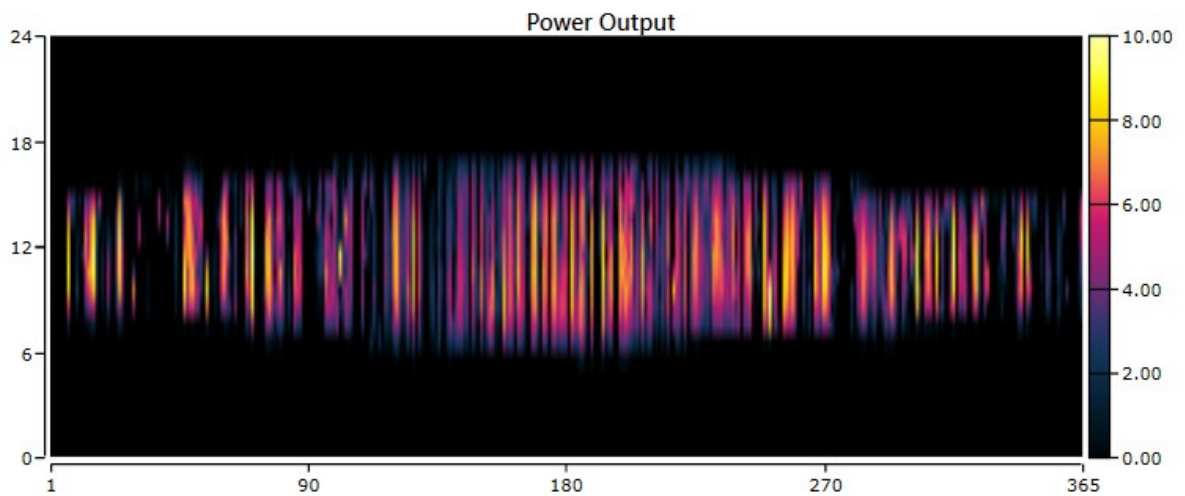


Figure 30. Power Output of a 3kW Solar Powered Stirling Engine (Showing on the x-axis: number of days per year, right y-axis: hours a day and left y-axis power output in kW)

In fact, while the rated capacity of the engine is 3kW, its mean output is 1.03kW, leading to a total production of 9,032.11kWh/year and a capacity factor of 34.4%. In order to find the capacity factor of the Solar Powered Stirling Engine, the actual power output of the system should be divided by the rated power output, also known as the power output of this component at full capacity. The solar powered Stirling Engine delivers the load for 2,431 hours/year, or 27.8% of the time. Finally, the LCOE of this component is 0.123 USD/kWh.

### C. Natural Gas Powered Stirling Engine

When the power obtained from the sun is not enough to deliver the load, the Natural Gas will be burned to supply the Stirling Engine. According to the simulation, the Natural Gas Powered Stirling Engine operates for 6,774 hours a year, thus 78.1% of the time, with 322 number of starts. Knowing that its nominal electrical output is 3kW and its yearly electrical output is 14,700 kWh/year, its capacity factor is 56%. It actually has a minimum electrical output of 0.00803kW, which confirm the choice we made for a minimum load ratio of 0%.

The fixed cost of generation is at 0.0674 USD/hour, while its marginal cost of at 0.0641 USD/kWh. In fact, the fixed cost is nothing but the running cost of the generation whatever is the electrical output. It is obtained by adding the O&M cost of the engine (0.019 USD/hour) to the specific fuel consumption cost hourly,  $0.240 \frac{m^3}{h} * 0.202 \frac{USD}{m^3} = 0.048 \frac{USD}{h}$ , which is equal to 0.0674 USD/hour.

The power Output of the Natural Gas Stirling Engine can be visualized in the following graph.



Table 28. Natural Gas Stirling Engine Performance

	Values	Comparison to 4kW HSE/1kW PV/2kWh Batteries
<b>Yearly Hours of Operation</b>	6,774	<6,828
<b>Number of Starts</b>	322	>312
<b>Capacity Factor *(%)</b>	56	>45.66
<b>Fixed Generation Cost (USD/hour)</b>	0.0674	<0.090
<b>Marginal Generation Cost (USD/kWh)</b>	0.0641	=0.0641
<b>Mean Electrical Efficiency (%)</b>	29.6	=29.6
<b>Electrical Production (kWh/year)</b>	14,700	<16,000

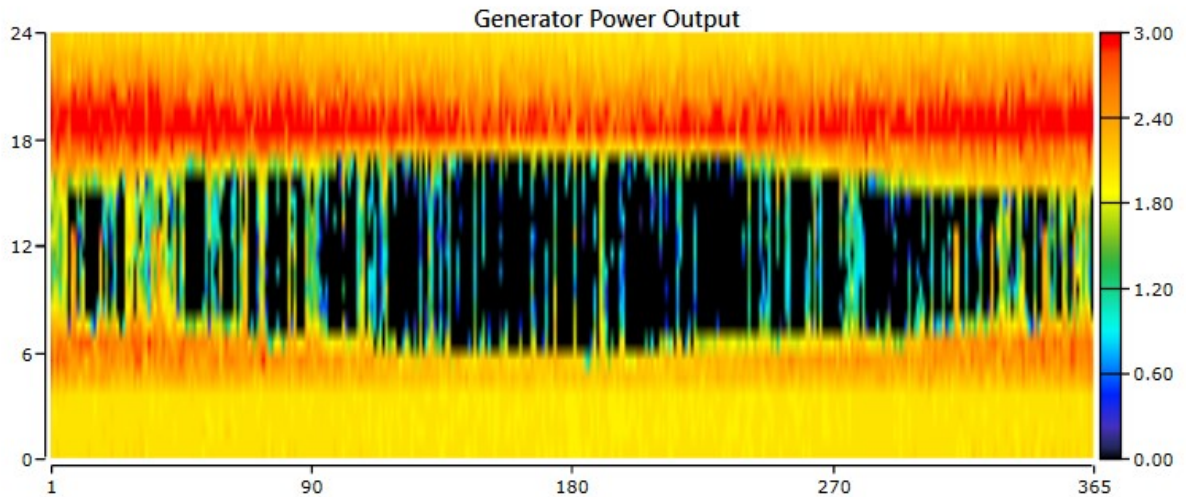


Figure 31. Power Output of a 3kW HSE (Natural Gas) (Showing on the x-axis: number of days per year, right y-axis: hours a day and left y-axis power output in kW)

As is can be realized, the power delivered by the Natural Gas Powered Stirling engine in the middle of the day is commonly nil because the solar power is enough to deliver the load. However, at around 6 o'clock and in winter times, the power output of the Stirling Engine is at its maximum and that's because the load is set to peak at that time of the day and those times of the year. Although the peak load value is more than 3kW (between 3 and 4.32kW), the batteries will act as a peak shaving factor.

## D. Emissions Evaluation

This section benefits from HOMER's capabilities of evaluating the fuel consumption of an energy system. This study disregards the life cycle assessment of energy components and focuses on the emissions during the project's lifetime.

Table 29. Table comparing the emissions from a 3kW HSE/4kW PV/5kWh Batteries to the ones of a 4.8kW Diesel Engine

Emission type	Value for 3kW	Value for a 4.8kW	Drop of Emissions (%)
	HSE/4kW PV/5kWh Batteries	Diesel Engine	
CO <sub>2</sub> (kg/year)	9,734.60	20,416.09	52%
CO (kg/year)	32.37	128.69	75%
<b>Unburned</b>			
Hydrocarbons (kg/year)	0	5.62	100%
SO <sub>2</sub> (kg/year)	0	49.99	100%
NO <sub>x</sub> (kg/year)	67.92	120.89	44%

Obviously, there's a great reduction of emissions out of the system when compared to a diesel engine system. This proves that this system is not only able to overcome the price issue of the diesel engine but also the emissions problems.

However, it might also be interesting to compare the role of the introduction of the PV system with the emissions.

Table 30. Table comparing the emissions from a 3kW HSE/4kW PV/5kWh Batteries to the ones of a 3kW HSE/9kWh Batteries

Emission type	Value for 3kW	Value for a 3kW	Drop of Emissions (%)
	HSE/4kW PV/5kWh Batteries	HSE/9kWh Batteries Engine	
CO <sub>2</sub> (kg/year)	9,734.60	10,857.37	10%
CO (kg/year)	32.37	36.1	10%
<b>Unburned</b>			
Hydrocarbons (kg/year)	0	0	-
SO <sub>2</sub> (kg/year)	0	0	-
NO <sub>x</sub> (kg/year)	67.92	75.75	10%

Thus, the introduction of the PV plant to the simulation didn't only reduce the initial and Net Present costs, but also reduced the amount of emissions by roughly 10%.

### E. PV Plant Electricity Production

The rated capacity of the PV system is 4kW and its mean output is around 0.72kW, leaving the system with a capacity factor of 17.91%. The Levelized cost of the PV is 0.0625 USD/kWh. The following graph illustrated the daily and hourly power output of the PV system, that sums up to 6,274.59 kWh/year.

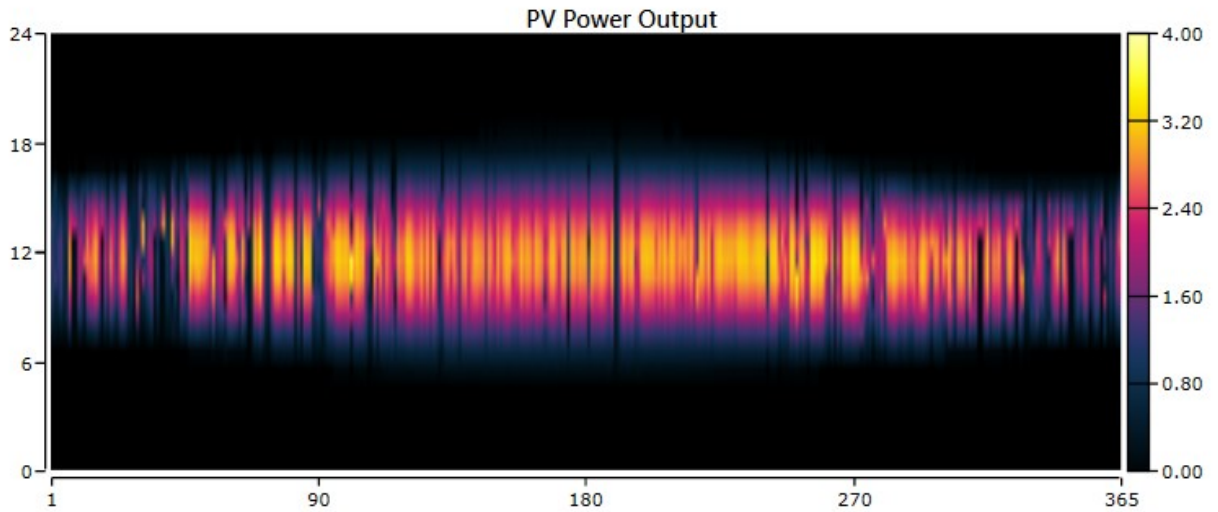


Figure 32. Power Output of a 4kW PV plant (Showing on the x-axis: number of days per year, right y-axis: hours a day and left y-axis power output in kW)

Table 31. Performance Evaluation of a 4kW PV

	Value
<b>Mean Output (kW)</b>	0.72
<b>Capacity Factor (%)</b>	17.91
<b>Total Production (kWh/year)</b>	6,274.59
<b>LCOE (USD/kWh)</b>	0.0625

## F. Li-ion Batteries Performance

The size of the battery bank is 5kWh. Over its lifetime, 7 years, the battery has a throughput of 1,106.91 kWh and an annual throughput of 158.13 kWh/year.

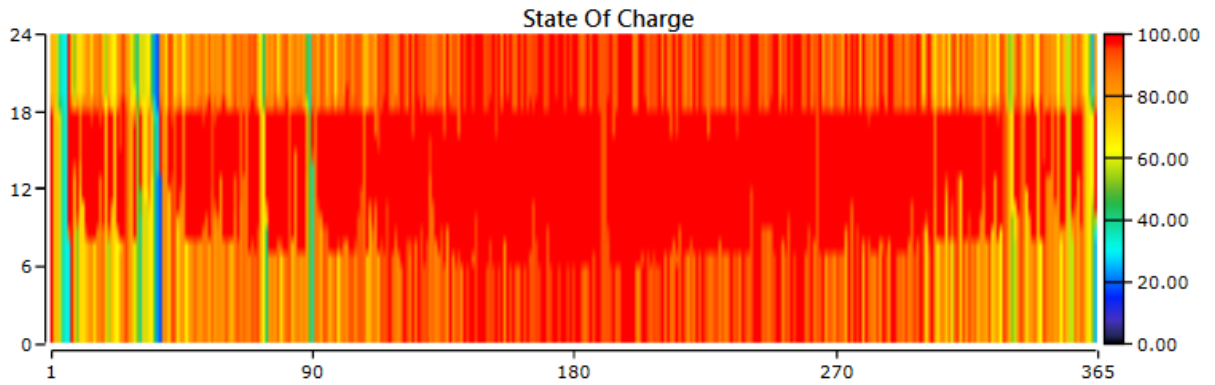


Figure 33. Yearly State of Charge of 5kWh Batteries

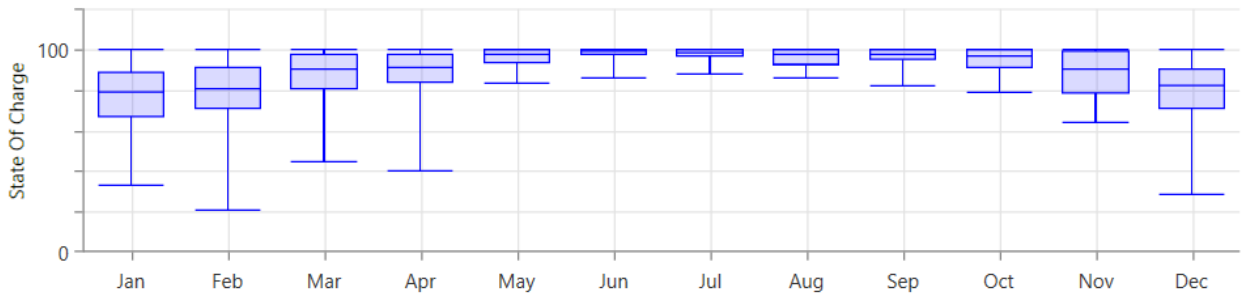


Figure 34. Monthly Evaluation of the state of charge of 5kWh Batteries

Table 32. Performance of the 5kWh Batteries

	Values
<b>Annual Throughput (kWh/year)</b>	158.13
<b>Lifetime Throughput (kWh)</b>	1,106.91
<b>Energy In (kWh/year)</b>	165.77
<b>Energy Out (kWh/year)</b>	150.02

At the peak months, the state of charge of the battery varies much more than in summer. This is due to the fact that winter months were assigned to be the peak months. Moreover, the state of charge of the batteries is most of the time at maximal values in the middle of the day and that is because of the excess energy produced by the sun. The discharge happens mostly at peak hours. In order to investigate more the behavior of the batteries. Different plots will be drawn in the months of January, May, August and November.



Figure 35. System's performance in January

This plot shows three instances of peak shaving. On January 14 at around 6 o'clock, the Stirling Engine having a nominal power output of 3kW can't deliver the load that happens to be 3.53kW in January 14. Thus the batteries supply the system with 0.56kW in order to continuously deliver the load. And the following day, the batteries are charged again to reach a state of charge of 100%. Thus, this plot also clarifies how the excess in solar power is used to charge the batteries and to deliver the load.

The battery bank used as peak shaving are important not only to ensure a nil capacity shortage but also to prevent the installation of a 4kW Stirling Engine just to deliver this hour or two per day.



Figure 36. System's performance in May

May 15 turned out to be a great example showing how the energy from the Stirling Engine and the PV can be summed up to deliver the load and charge the batteries. Moreover,

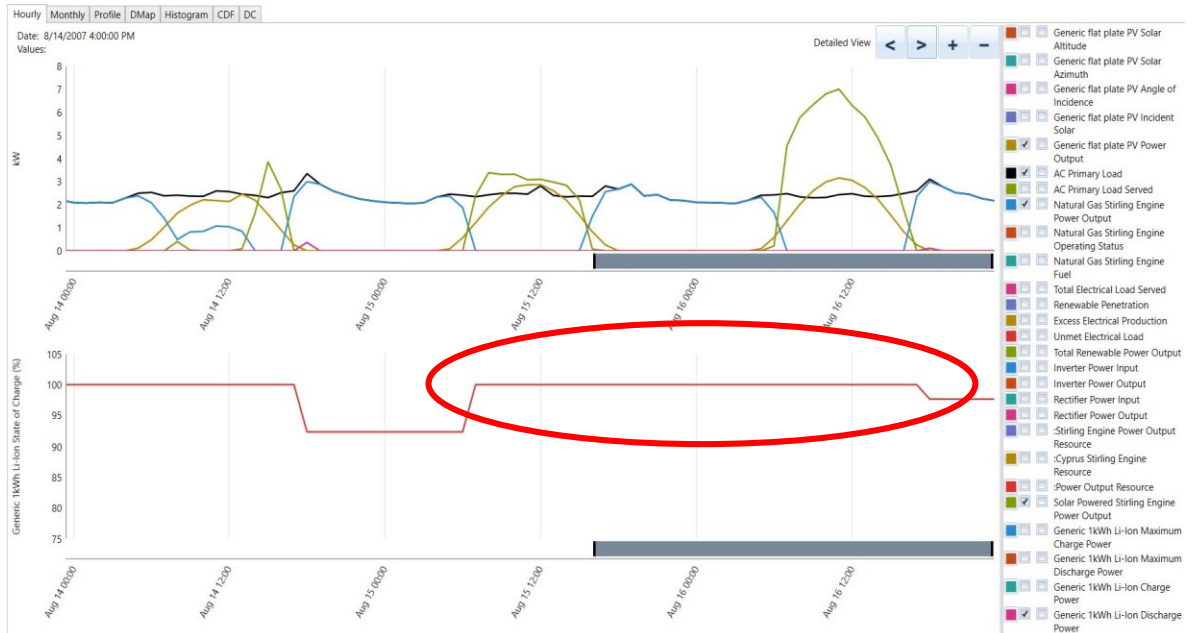


Figure 37. System's performance in August

in the same day at 6 o'clock, charged batteries can now discharge and act as a peak shaving factor.

In the month of August, considered as being a month with a small electrical load demand, the batteries are mostly kept at a high state of charge and are barely used. Moreover, in August 14 at around 10 o'clock seems to be a good example to highlight the minimum load demand of the Natural gas Stirling Engine that was set to be 0%. As soon as the solar energy power (either from the Stirling Engine or from the PV) reaches a value less than the load, the Natural Gas burning take over and complement the shortage of energy.



Figure 38. System's performance in November



On the other hand, November 17 at noon illustrates a phenomena explained earlier.

It seems that this day was a cloudy day with a nil DNI value and an elevated GHI value.

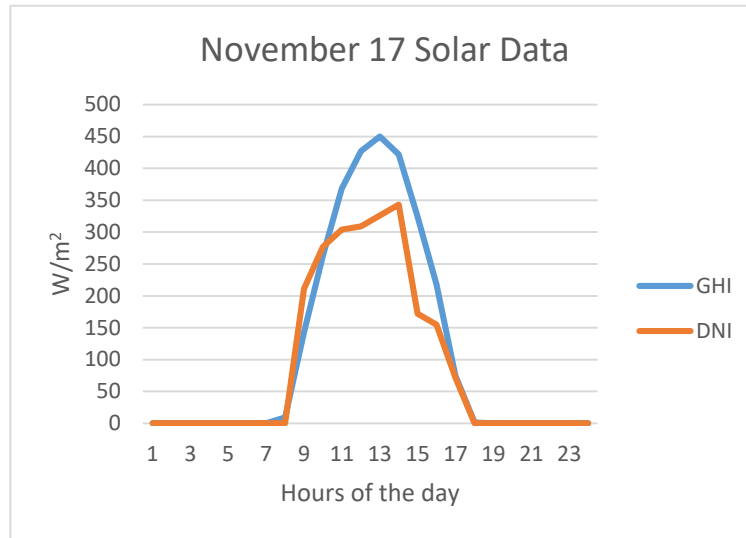


Figure 39. Solar Data in November 17

In fact, knowing that the PV power output is able to reach a value close to 2kW, the Natural Gas Flow rate will get lower to reach an electrical power of 1kW. Thus, the load demanding a value close to 3kW is successfully supplied, while saving fuel, lowering the emissions, and lowering the cost of production.

## G. Conclusion of the Simulation

In the section above, a techno-economic analysis of the Microgrid system was done. The results showed that a 3kW HSE/4kW PV/5kWh Batteries is the best configuration for any Initial Capital Cost of the Stirling Engine. In fact, the COE will vary from 16.3 ¢/kWh to 22.9 ¢/kWh.

The performance analysis of this system showed that the Microgrid in question was able to accomplish different goals:

- A continuous energy generation by achieving a nil capacity shortage
- A reduction in the COE when compared to Diesel/PV/Batteries configurations
- A reduction in the COE actually paid by the Lebanese population for the first two scenarios
- A reduction in greenhouse gas emissions
- An increase in the renewable penetration and a decrease in the fossil fuel share

Knowing that this system turned out to be economically feasible, the next chapters will assess its technical feasibility by testing different lab scales Stirling Engines.

## CHAPTER VI

### THERMODYNAMIC PRELIMINARY ANALYSIS

Two documents were mainly used to come up with a preliminary analysis for the Stirling Engine: the first being “Stirling Engine Design Manual” by William R. Martini [27] and the second is a Doctoral Thesis entitled “Calculations and Experiments on  $\gamma$ -type Stirling Engines” by Andreas Wagner from the University of Wales [55]. According to these two sources, an ideal thermodynamic analysis is crucial before getting a hands on the Stirling Engine.

The first step of the chapter explains the ideal Stirling Process before tackling the ideal analysis on the two Engines as well as a 0<sup>th</sup> cycle analysis. Microsoft Excel was used to do the following analysis. Note that at a first step, the analysis was done on a lab scale Gamma Stirling Engine prepared by Mechanical Engineering Students at the AUB and then it was repeated for the Beta Stirling Engine bought from GreenPowerScience.

#### A. Ideal Stirling Process

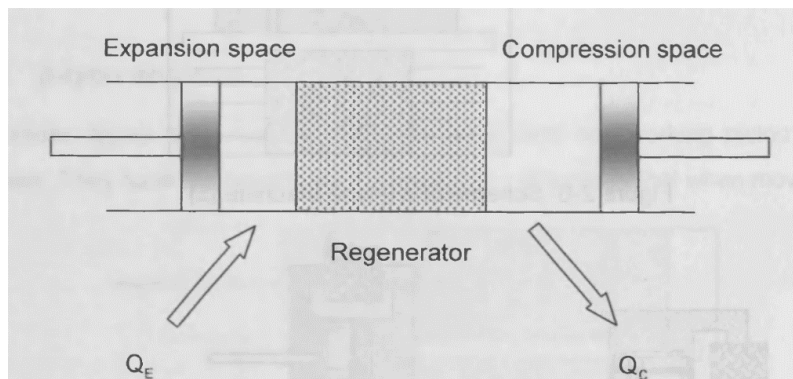
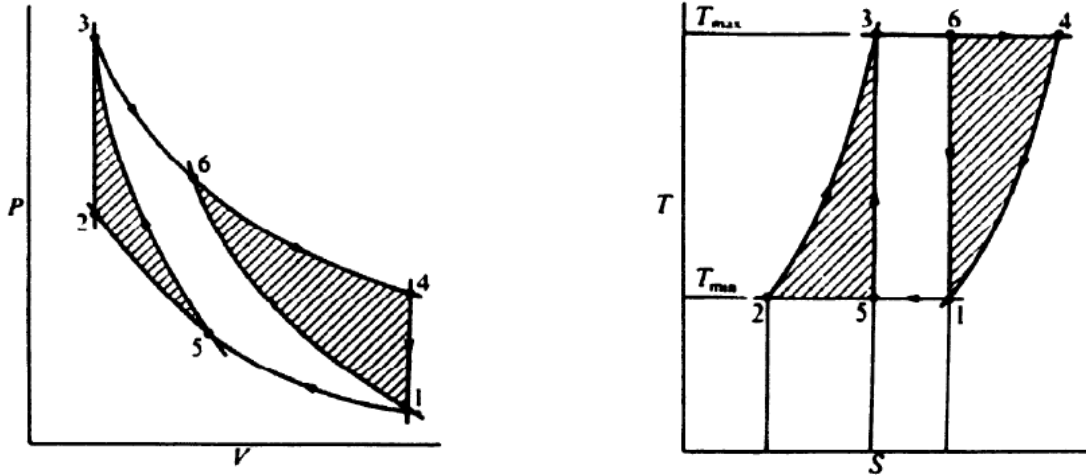


Figure 40. Thermodynamic Scheme of the Stirling Cycle

As the Otto and Diesel processes, the Stirling power cycle is based on the compression of cold gas and expansion of hot gas [55]. The work required for compression is less than the resulting work for the expansion and therefore, it is said that these cycles changes head to work. Having a step by step review of the motion is crucial to clarify the process. For this reason, *Figure 40* [55] illustrates the thermodynamic scheme of the cycle, *Figure 41* show the Pressure-Volume (P-V) and Temperature-Specific Entropy (T-s) diagram respectively of the Stirling Cycle and the Carnot Cycle.

The scheme (*Figure 40*) is built up of a cylinder that contains two opposed pistons, the one on the left is found in the expansion space and the second in the compression space, as well as a regenerator in the middle. The regenerator can be considered to be a “thermodynamic sponge” that alternatively release and absorbs heat [55]. It is actually a matrix of finely “divided metal in the form of wires or strips”. At the expansion space, the temperature is maintained at the highest value of  $T_{\max}$ , and at the compression space the temperature is maintained at the lowest value of  $T_{\min}$ . Thus there’s a temperature gradient from  $T_{\max}$  to  $T_{\min}$  between both limits of the regenerator and the heat is assumed to be transferred by conduction in the horizontal direction. For the ideal cycle analysis, it is assumed that the regenerator is 100% efficient, the pistons move without friction losses and the working fluid is enclosed between the pistons leakages free.

The cycle starts at point 1 of the diagrams (*Figure 2 and 3*), where the expansion



*Figure 41. (right) P-V diagram and (left) T-s diagram of the Stirling Cycle (1-2-3-4) and the Carnot Cycle (1-5-3-6)*

piston is just near the regenerator and the compression piston is at the outer dead point, forming the biggest volume in the cycle, at the lowest temperature  $T_{min}$  and pressure  $P_1=P_{min}$ . All the fluid is then in the compression space.

In the process 1-2, the compression piston moves towards the regenerator and the expansion space remains stationary. In fact, the working fluid is compressed in the compression space and thus the pressure increases to  $P_2$ . The temperature remains constant because the heat is transferred from the system to the surrounding ( $Q_C$  by the help of fins or passage of cold water), for this reason process 1-2 is considered to be isothermal. The volume decreased to the minimal value ( $V_{min}$ ).

Process 2-3 is characterized by a constant volume heating where the pistons move simultaneously to keep the volume constant. The heating is done by the regenerator whose goal is to increase the temperature of the gas moving through the porous matrix from the

compression to the expansion space from  $T_{\min}$  to the  $T_{\max}$ . The volume is kept the same as the expansion piston is slightly moving far from the Regenerator while the compression piston is getting the nearest possible to the inner dead point. The pressure in this case increases as the temperature increases  $P_3=P_{\max}$  and the volume remains the same.

From point 3 to 4, the expansion process occurs. The expansion piston continues to move away from the regenerator and the compression piston remains stationary at the inner point of the regenerator. In fact, the volume increases and the temperature remains constant as heat is added to the system ( $Q_E$  from the heater). As the process 2-3, this one is characterized by being an isothermal process and for these reasons, the pressure will decrease to reach the value of  $P_4$ .

Finally, the process 4-1 illustrates a return to the point 1 of the cycle via a constant volume process where the temperature of the gas decreases from  $T_{\max}$  to  $T_{\min}$ . Actually, the pistons move simultaneously and the gas is transferred from the expansion space to the compression space through the regenerator. In this case, the heat from the working fluid is transferred to the regenerator to reach a lower temperature value ( $T_{\min}$ ). The gas stored in the matrix will then be transferred to the gas in the process 2-3 of the next cycle.

In a nutshell, and as described by [55]:

- ✓ Process 1-2: isothermal compression; heat transfer from the working fluid at  $T_{\min}$  to the external heat sink
- ✓ Process 2-3: constant volume;  $T_{\min}$  to  $T_{\max}$  via the heat transfer to the working fluid from the regenerator matrix

- ✓ Process 3-4: isothermal expansion; heat transfer to the working fluid at  $T_{\max}$  from the external heat source
- ✓ Process 4-1: constant volume;  $T_{\max}$  to  $T_{\min}$  via the heat transfer from the working fluid to the regenerator matrix

In the *Figure 2 and 3*, the Stirling Engine is compared to the Carnot Cycle. The advantage of the Stirling Engine is the presence of constant volume processes instead of the isentropic processes in the Carnot Cycle (2-3 vs 5-3 and 4-1 vs 6-1). Due to this, the area of the P-V diagram is greater in the Stirling Engine and thus generate more work for the same values of pressure and temperature. Actually, referring back to the last two figures, hatched areas 5-2-3 and 1-6-4 illustrates the additional work obtained just by replacing isentropic processes with constant volume ones. However, the efficiency, which is nothing but the ratio of supplied heat which is converted to work, is the same in both cycles and this will be proven in the following section [55].

## B. Different Kinds of Stirling Engines

### 1. Alpha ( $\alpha$ ) Stirling Engine

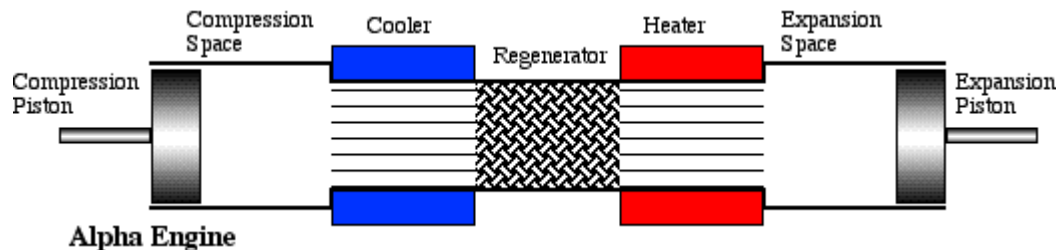


Figure 42. Alpha type Stirling Engine [51]

The  $\alpha$ -type Stirling Engine, as shown in the previous figure, has two sealed working pistons with one holding the name of the expansion piston, and the other, the compression

piston. The regenerator is a component usually made of a sheet of foil, steel wool or metallic sponge, that stores heat from one cycle, explained earlier, for it to be used in the next cycle. By doing so, the regenerator acts as a heat integrator within the engine, instead of wasting the heat to the atmosphere, by increasing the efficiency and the power output [56].

## 2. Beta ( $\beta$ ) Stirling Engine

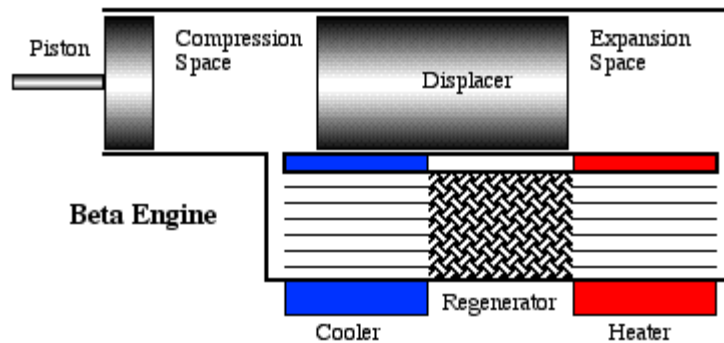


Figure 43. Beta Type Stirling Engine

The  $\beta$ -type Stirling Engine has gained popularity among the three types of Stirling Engines and the official patent from Robert Stirling shows a beta configuration. By contrast to the  $\alpha$ -type, the  $\beta$ -type contains a single working piston and a displacer in the same cylinder.

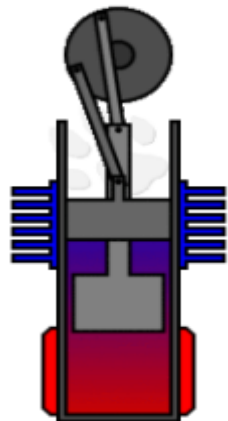


Figure 44. Beta Stirling Engine configuration showing the linkage between the power piston and the displacer

This last one's purpose in to displace the working gas at constant volume and “shuttle it



between the expansion and the compression spaces through the series arrangement cooler, regenerator and heater” [57].

As shown in the last figure, the linkage between the power piston and the displacer will drive them such that the gas will compress while it is in the cool space and expand when it is in the hot space.

### 3. Gamma ( $\gamma$ ) Stirling Engine

Having a very similar arrangement when compared to the  $\beta$ -type configuration however the displacer and the power piston are positioned in different cylinders with the displacer cylinder having the bigger diameter and the compression cylinder having the smaller diameter. The two cylinders are connected through the regenerator and the three compartment (heated, cooled and regenerator) are interconnected. The  $\gamma$ -type benefits from a “good self-pressurization and with a double acting piston arrangement it has theoretically the highest possible mechanical efficiency” [58, 59].

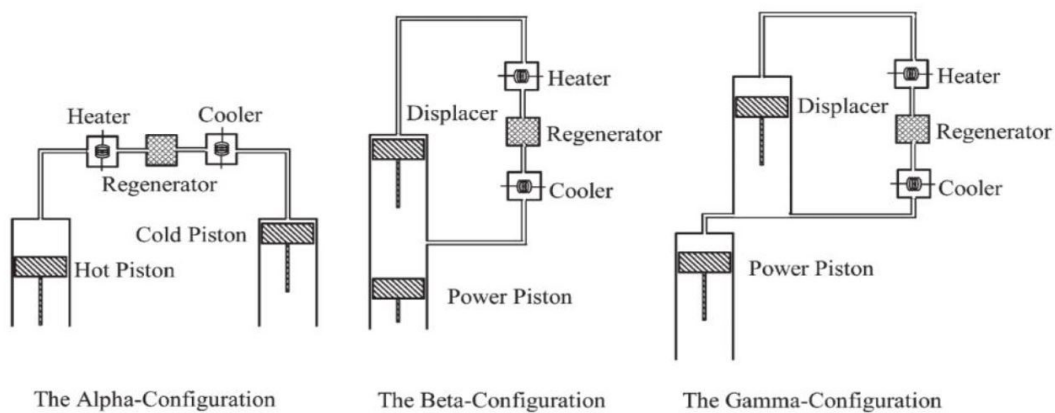


Figure 45. The three kinds of Stirling Engine

#### 4. Assessment of the three Stirling Engines

In order to assess the performance of those engines, a matrix is built and assigned weighing factors [60].

Table 33. Decision Matrix for the Three Types of Stirling Engines

Criterion	Weight (%)	Alpha	Beta	Gamma
Efficiency	20	4	5	3
Engine Size	6	2	4	2
Ideal Dead Space	8	3	4	3
Industrial Popularity	4	2	5	3
Maintenance	8	4	2	3
Ease of Construction	8	4	2	3
Material Cost	8	1	5	3
Noise Output	8	2	3	2
Power Density	16	5	3	2
Salability	14	2	5	3
<b>Raw Score</b>		29	38	27
<b>Weighted Score</b>		3.2	3.9	2.7
<b>Relative Rank</b>		2	1	3

In fact, the Beta Stirling Engine is found to be the best configuration. Actually, according to [27], an important thing to take into account when designing a Stirling Engine is keeping the dead volume at the minimum value. The dead space is defined as a volume that is kept constant at all the stages of the thermodynamic cycle. Unlike the swept volume by the pistons, the dead space is always kept un-swept by neither the power piston nor the displacer. This volume is most commonly found near the hot and cold sides, in the

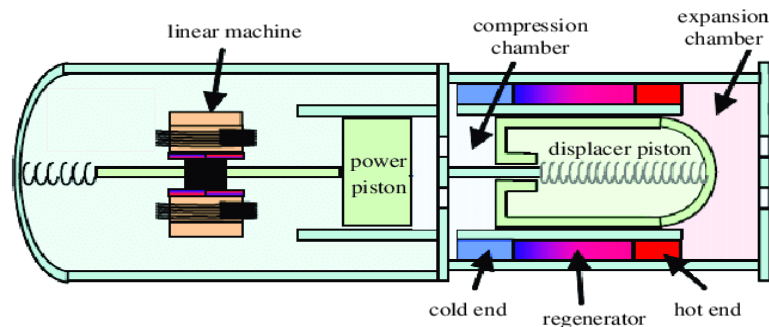


Figure 46. Free Piston Stirling Engine Parts [55]

regenerator as well as between the displacer and power piston in the gamma Stirling Engine. In the Beta Stirling Engine, the displacer and power piston barely touches each other during the cycle. Therefore, this dead volume is considered to be nil and that's why the Beta Engine is the most widely used Engine. In fact, it is the only engine that was evolved and transformed into a free piston Stirling Engine. The free piston Stirling Engine is the actually used engine in the industry.

The difference between the free piston Stirling Engine and the common beta Stirling Engine is the replacement of the flywheel by a membrane that acts as a mechanical spring, as seen in the picture below. In fact, electricity is generated by the use of a linear alternator rather than a rotary generator, or a dynamo. In fact, this resulted in a less complex mechanical configuration. Moreover, a connecting rod between the piston and the flywheel is not needed anymore, thus resulting in a better sealing and limited leakages [61].

The free piston Stirling Engine is a wide area of study that won't be elaborated in this work. The focus will remain on the beta and gamma Stirling Engines as they're the ones that are going to be tested in the lab.

### **C. Efficiency of the ideal Stirling Cycle**

If we consider an ideal regenerator, and we consider that the heat transferred in process 2-3 has the same value as in process 4-1, "then the only heat transfers between the engine and its surroundings are isothermal heat supply at  $T_{\max}$  and heat rejection at  $T_{\min}$ " [55]. Thus, only these values are important for the calculation of the efficiency. Moreover,

from the cycle definition, the working fluid at the end of the cycle has to have the same state as the beginning of the cycle. For this reason, the internal energy  $U$  has to be the same at both ends of the cycle. Now we can use the second law of thermodynamics and show that:

$$\int dQ + \int dW = \Delta U = 0$$

$$Q_{1-2} + Q_{3-4} = -W$$

Thus, having in mind the thermal efficiency of a thermodynamic Cycle, we can write:

$$\eta_{thermal} = \frac{|W|}{Q_{3-4}}$$

$$\eta_{thermal} = \frac{Q_{1-2} + Q_{3-4}}{Q_{3-4}} = 1 + \frac{Q_{1-2}}{Q_{3-4}}$$

Knowing that we are dealing with an isothermal compression and expansion, lets imagine we have a volume  $v(1) \text{ cm}^3$  of hydrogen at a pressure of  $p(1) \text{ MPa}$  and we compress it isothermally to  $v(2) \text{ cm}^3$ . The path taken by the compression can be plotted easily because  $P * V = n * R * T$  is a line as the number of moles is constant (because at this stage of the analysis we consider that all the molecules inside system are at one place together), such as R and T. Thus, if we continue with the numbers that we assumed:

$$P * V = p(1) * 10^6 \text{ Pa } (v(1) * 10^{-6} \text{ m}^3) = pv(1) \text{ Joules}$$

$$\text{where } P = \frac{pv(1)}{V}$$

The work increment is then:

$$dW = P(x) * d(V(x)) = \frac{pv(1)}{V(x)} d(V(x))$$

After integrating we get:

$$W = pv(1) \int_{V(1)}^{V(2)} \frac{d(Vx)}{V(x)} = pv(1) * [\ln V(x)]_{V(1)}^{V(2)} = pv(1) * \ln\left(\frac{V(2)}{V(1)}\right)$$

By the perfect gas law

$$P(x) * V(x) = pv(1) = m * R * T(x)$$

Thus, we can now write that the work produced by this compression is nothing but

$$W = m * R * T * \ln\left(\frac{V(2)}{V(1)}\right)$$

Please note that this value will end up being negative because the work is being supplied and the heat is being removed from the cycle.

Getting back to the system that we were describing, during the isothermal changes of state 1-2 and 3-4, the two equations obtained are as follow:

$$Q_{1-2} = m * R * T_1 * \ln\left(\frac{V_2}{V_1}\right)$$

$$Q_{3-4} = m * R * T_3 * \ln\left(\frac{V_4}{V_3}\right) = m * R * T_3 * \ln\left(\frac{V_1}{V_2}\right) = -m * R * T_3 * \ln\left(\frac{V_2}{V_1}\right)$$

The work done by the process is then:

$$W = Q_{1-2} + Q_{3-4} = -m * R * (T_3 - T_1) * \ln\left(\frac{V_1}{V_2}\right)$$

By using results in equations (10) and (11) in equation (4) we obtain the following:

$$\eta_{thermal} = \frac{Q_{1-2} + Q_{3-4}}{Q_{3-4}} = 1 + \frac{Q_{1-2}}{Q_{3-4}} = 1 + \frac{m * R * T_1 * \ln\left(\frac{V_2}{V_1}\right)}{-m * R * T_3 * \ln\left(\frac{V_2}{V_1}\right)} = 1 - \frac{T_1}{T_3}$$

Knowing that  $T_1=T_2=T_C$  represent the compression space temperature and  $T_3=T_4=T_E$  expansion space temperature, we can conclude that the ideal process efficiency is represented by

$$\eta_{th} = 1 - \frac{T_C}{T_E} = 1 - \frac{T_{min}}{T_{max}}$$

#### D. Heat and Work of the ideal Stirling Cycle

The work of the isothermal compression can be described as follows:

$$Q_{1-2} = m * R * T_1 * \ln\left(\frac{V_2}{V_1}\right)$$

The answer will be negative as the work is being supplied.

The work of the isothermal expansion can be described as follows:

$$Q_{3-4} = m * R * T_3 * \ln\left(\frac{V_4}{V_3}\right)$$

However, stages 2 to 3 and 4 to 1 describes how the heat of the working fluid reacts with the regenerator, considered here to be 100% efficient containing no dead volumes. The heat supplied to the gas by the regenerator is then

$$Q_{2-3} = m * C_v * (T_3 - T_2)$$

On the other hand, the heat supplied from the gas to the regenerator is

$$Q_{4-1} = m * C_v * (T_1 - T_4)$$

In perfect cases, the absolute value of these numbers will be the same.

## E. Losses in the Stirling Engine

### 1. Sinusoidal approximation, Crank Angle and Phase shift angle

In the process model of the Stirling Engine, three different kinds of spaces are found: expansion space, compression space and regenerator space. A graph that visualizes the change of expansion and compression space with respect to the phase shift angle is important to determine the phase shift angle of the system [55].

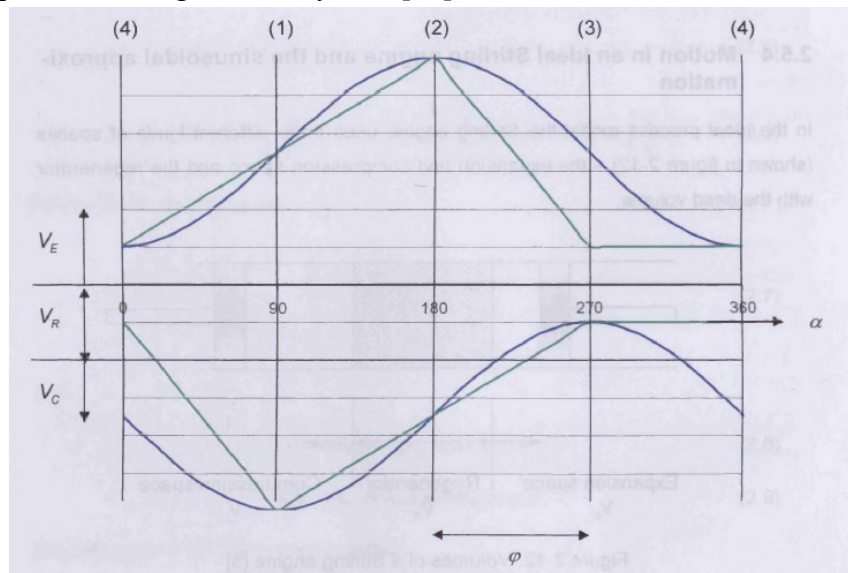


Figure 47. Motion in the Stirling Engine

The volume of the regenerator obviously stays the same throughout the process. The ideal Stirling process is characterized by a discontinuous motion on the graph. In real life it is impossible to maintain this discontinuous unless a very complex crank drive mechanism should be installed and this will lead to huge accelerations, high forces on the moving parts and eventually noise generation. For this reason, usual crank drives, similar to the ones used in Diesel engines are installed in Stirling Engines. This will yield to a continuous/sinusoidal motion that approximates the discontinuity in the ideal process. However, for this reason, the corners in the p-v diagram will be curved and this will decrease the work produced by the system as the area will become smaller [55].

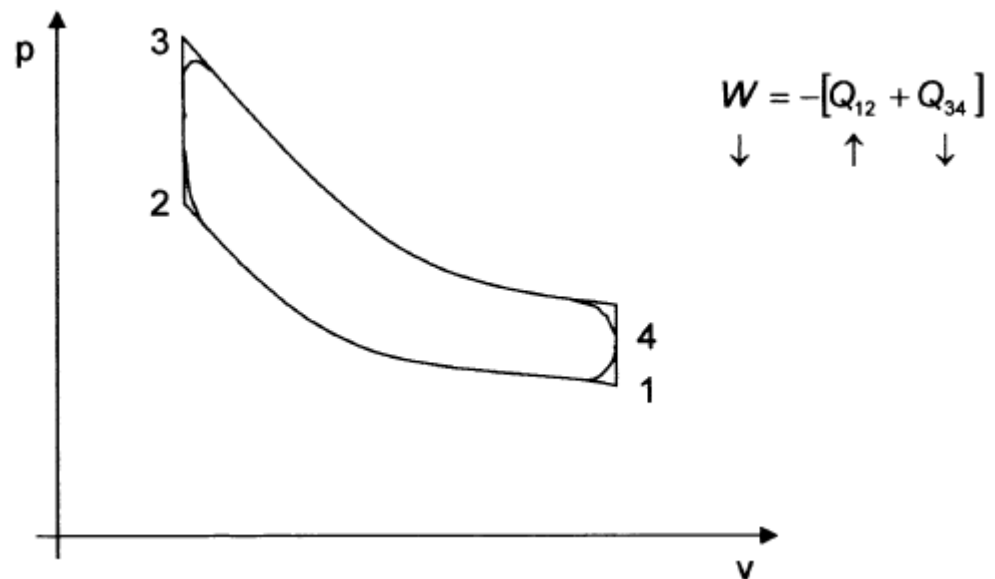


Figure 48. p-v diagram with continuous motion



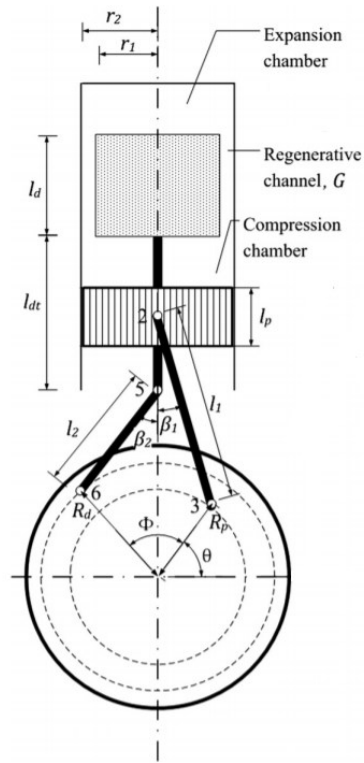


Figure 49. Angles and Dimensions in a Beta Stirling Engine

The crank angle ( $\alpha$ , illustrated by  $\theta$  in Figure 49) is “the angle of rotation of a crankshaft measured from the position in which the piston is at its highest point known as top dead center (TDC)”.

The phase shift angle ( $\phi$ ) by definition is the difference of the crank angles of both the power piston and the displacer piston. It is most commonly  $90^\circ$ .

## ***2.Effect of the Regenerator on the performance***

As stated by both sources [27, 55], “Stirling Engines require highly efficient regenerators”. The regenerator plays a role in the constant volume processes (2-3 and 1-4). In the cases where the regenerator is not present, when the gas flows from the cold to the hot

space and oppositely, the required heat for these changes in temperature will be higher. Thus the system will require higher demand for heat absorption and a higher demand for heat released to the surroundings. “This would result in huge heat fluxes without improving the machines performance” and the efficiency will decrease significantly. This principle is mathematically explained by Martini.

Let’s consider the efficiency of the regenerator to be “ $E$ ”. Thus for the transfer from the cold space to hot space  $E$  becomes:

$$E = \frac{T_L - T_C}{T_H - T_C}$$

where  $T_L$  is the temperature of the gas leaving the regenerator,  $T_C$  and  $T_H$  are respectively the temperature of the cooler and the heater.

Following the fact that the temperature that leaves the generator is different from the ideal temperatures of the heater and the cooler, the heat delivered from the regenerator is nothing but

$$Q_{2-3}' = m * Cv * (T_L - T_C)$$

and the heat from the gas heater is now

$$Q_{heater} = m * Cv * (T_H - T_L)$$

Therefore, by adding the equation (20) to the denominator of the thermal efficiency of the Stirling cycle, that means by taking into account the additional heat required to elevate the gas temperature to  $T_H$ , the thermal efficiency becomes:

$$\eta_{th} = \frac{m * R * T_H * \ln\left(\frac{V_1}{V_2}\right) - m * R * T_C * \ln\left(\frac{V_1}{V_2}\right)}{m * R * T_H * \ln\left(\frac{V_1}{V_2}\right) + m * C_v * (T_H - T_L)}$$

By dividing the numerator and denominator by  $m * R * \ln\left(\frac{V_1}{V_2}\right)$  we can reach the following form:

$$\eta_{th} = \frac{T_H - T_C}{T_H + \frac{C_v}{R} * \frac{(T_H - T_C)(1 - E)}{\ln\left(\frac{V_1}{V_2}\right)}}$$

Equation (22) gives the thermal efficiency of the system with respect to the regenerator efficiency. An interesting curve would be to draw the changes in thermal efficiency for different regenerator efficiency for a heater temperature of 900K and a cooler

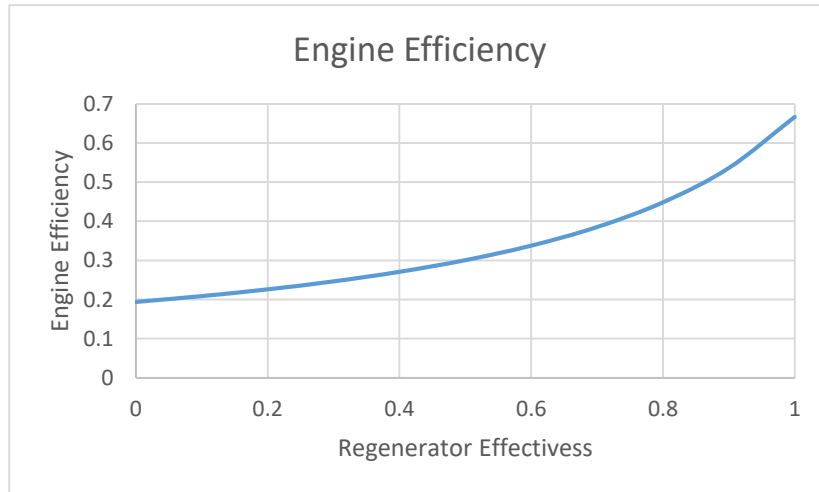


Figure 50. Effect of Regenerator Effectiveness on Efficiency

temperature of 300K with a volume ratio  $V_1$  to  $V_2$  equivalent to  $\frac{V_1}{V_2} = 2$  and hydrogen as working fluid.

Even when the regenerator is removed, the thermal efficiency is still reasonable however it reaches a maximum of 66.67% for a fully effective regenerator, which is nothing but the Carnot efficiency for the indicated temperatures.

$$\eta_{th} = 1 - \frac{T_C}{T_H} = 1 - \frac{300}{900} = 0.6667 = 66.67\%$$

In a nutshell, in real cases, the working gas reaches the cold space warmer and the hot space colder. Thus, the cooler has to absorb more energy while the heater has to add more energy as is needed in the ideal process.

### ***3. Remarks about the stored heat from the regenerator***

The following analysis will highlight the relation between the stored energy of the regenerator and the work done by the process.

As previously mentioned,

$$Q_{2-3} = -Q_{4-1} = m * C_v * (T_3 - T_1)$$

knowing that  $T_2 = T_1$

As previously mentioned, the work done by the process is:

$$W = Q_{1-2} + Q_{3-4} = -m * R * (T_3 - T_1) * \ln\left(\frac{V_1}{V_2}\right)$$

The ratio of volumes between step 1 and 2 can be expressed by

$$\varepsilon = \frac{V_1}{V_2}$$

Another way of writing the compression ratio can be expressed using the compression and expansion swept volumes ( $V_{SC}$  and  $V_{SE}$ ) as well as the dead volume of the engine ( $V_D$ ).

$$\varepsilon = \frac{V_1}{V_2} = \frac{V_{max}}{V_{min}} = \frac{V_{SE} + V_{SC} + V_D}{V_{SE} + V_D} = 1 + \frac{V_{SC}}{V_{SE} + V_D}$$

By substituting equation (25) and (11.1) into equation (24) we obtain a relation between the work done and the heat of the regenerator as proven below

$$W = -m * R * (T_3 - T_1) * \ln(\varepsilon) \text{ where } (T_3 - T_1) = \frac{W}{-m * R * \ln(\varepsilon)}$$

$$Q_{2-3} = m * Cv * (T_3 - T_1) = m * Cv * \frac{W}{-m * R * \ln(\varepsilon)}$$

By simplifying we get

$$Q_{2-3} = -Cv * \frac{W}{R * \ln(\varepsilon)} \text{ or } \frac{Q_{2-3}}{|W|} = \frac{Cv}{R * \ln(\varepsilon)}$$

where the ratio  $\frac{Cv}{R}$  can be referred by:

$$\frac{Cv}{R} = \frac{1}{\kappa - 1}$$

And finally,

$$\frac{Q_{2-3}}{|W|} = \frac{1}{(\kappa - 1) * \ln(\varepsilon)}$$

The last equation states that for a known work, “the energy which has to be stored in the regenerator rises with a decreasing compression ratio” [55]. Thus, for a higher heat storage capacity, there has to be a larger regenerator. However, a large regenerator is associated to a high dead volume and this a decrease in the performance of the machine.

Changing the fluids in this case affects the heat storage requirement. In fact,

$$\kappa_{air} = 1.402$$

$$\kappa_{He} = 1.630$$

$$\kappa_{H_2} = 1.410$$

and the following graph will be drawn to visualize the changes in the ratio of  $\frac{Q_{2-3}}{W}$

with the values of  $\varepsilon$  for different working fluid.

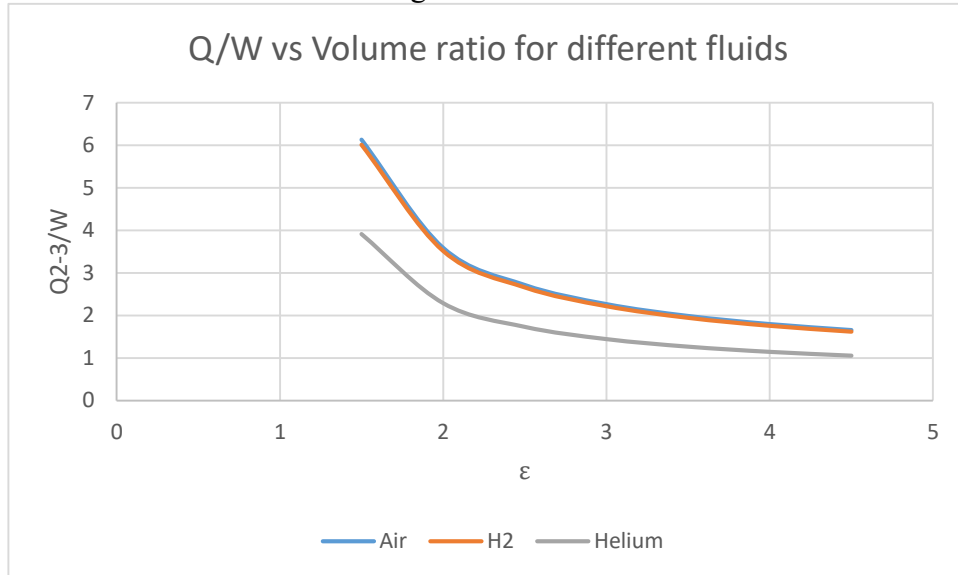


Figure 51. Regenerator heat and work produced for different working fluids

Thus for a machine with a compression ratio of 2 and air as a working fluid, the regenerator has to store 3.5 times more energy than the work produced. On the other hand, if helium is used as a working fluid, 2.3 times more energy has to be stored in the regenerator.

#### ***4. Remarks on the isothermal changes of state***

Let's take a reference speed of 1000 RPM for any Stirling Engine. This leads to the fact that each cycle is realized about 17 times per second, or a cycle each 60 milliseconds. Therefore, there's very little time for the heat transfer to happen. Thus, the ideal isothermal change of state rather functions as an adiabatic state of change, closer to the Carnot cycle. It can then be deduced that the area under the p-v diagram gets smaller which leads to the fact that the work produced is less than the ideal work and a higher work is needed for the compression.

To better simulate the isothermal change of state, a better thermal conductivity or lower speed (less than 200 RPM) of the engine should be realized. In fact, the adiabatic losses appear at machine speeds more than 200 RPM.

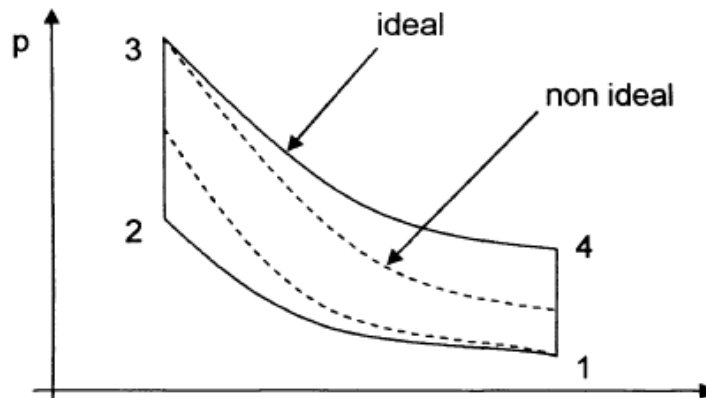
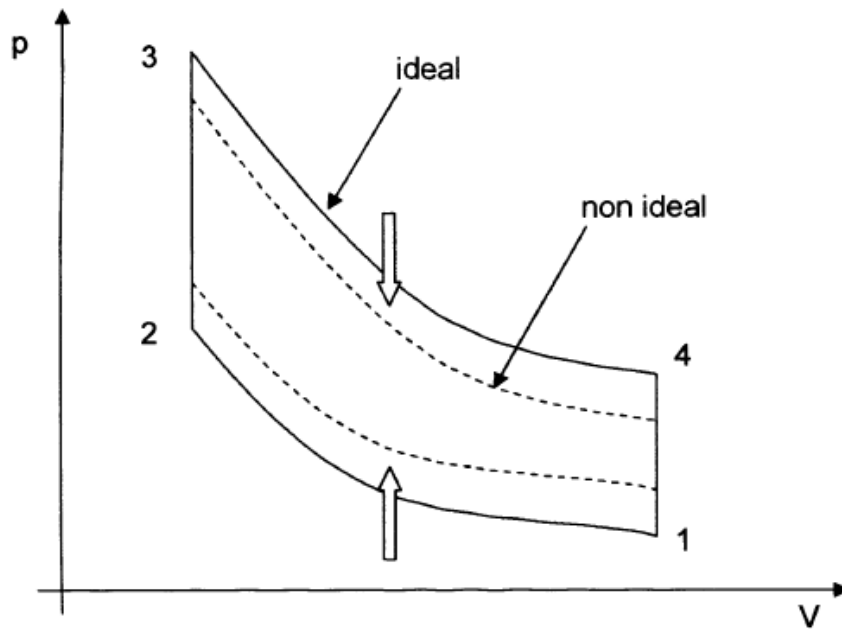


Figure 52. Effect of the imperfect isothermal processes

### ***5. Dead Volume losses in Power***

In ideal cases, the analysis considers that all the working fluid is present in the expansion and the compression space. However, in common real Stirling Engines the dead volume is considered to occupy 40 to 50% of the inner volume, especially in the parts of the heat exchangers (heater, regenerator and cooler). The problem with dead volumes is that they cause a reduction in the pressure as well as a decrease of the total efficiency [55].



*Figure 53. Dead Volume effect illustrated in the p-v diagram*

### ***6. Leakages and Pressure Losses in the Stirling Engine***

As it has been already mentioned, different gases will undergo the Stirling Cycle in order to create a back and forth movement of the piston. For this reason, sealing the engine's volume and eliminating any leak is important to reach and maintain the engine's nominal performance.



When it is easy to seal stable parts, totally sealing moving parts from their surroundings is problematic. “Especially in high loaded engines with helium or hydrogen as working fluid, leakages and pressure losses cannot be avoided” [55]. This will actually result in a reduction in efficiency. According to [55], the working piston parts has to be sealed well as most of the performance can be lost in this volume.

Sealing has always been a problem in old engines, until new engine where the generator is placed inside the crank case so that only electric cables have to be sealed.

### ***7.Mechanical Friction and Heat Losses inside the Stirling Engine***

Friction losses usually appear at all areas of contact including gear wheels, pistons as well as bearings. In the case of mechanical friction, mechanical energy is converted to useless heat.

Heat losses also play a major role as the cycle is based on a thermodynamic cycle. Those losses result from a conductive transfer from the engine’s working fluid to the outwards surroundings.

### 8. Real Stirling Engine process

Adding up the losses described in the earlier sections, as well as the heat losses through the material, the dissipations and leakages problems and the power dissipation by the mechanical friction, the power delivered by the engine will be much lower than the power estimated by the ideal case. This can be illustrated in the diagram below [55].

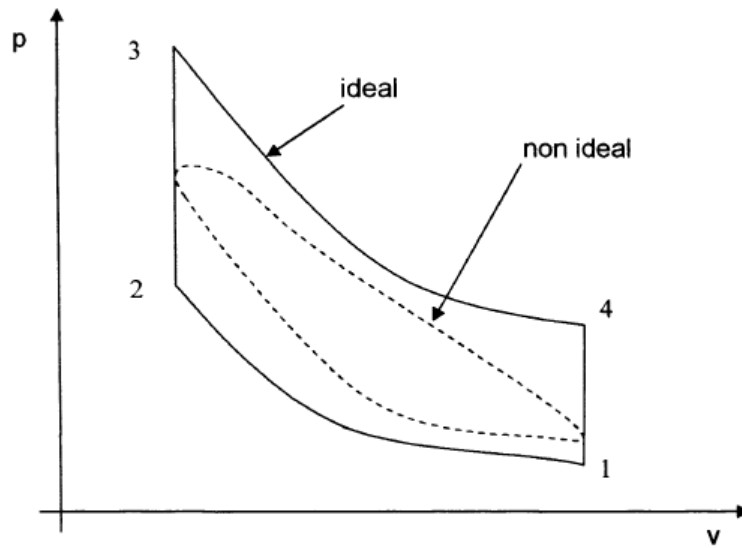


Figure 54. Realistic p-v diagram

### F. Volume Measurements

For Stirling Engines with Piston-displacer arrangements, the expansion volume is defined by the position of the displacer piston and the compression volume is defined by the position of both the displacer and working pistons. Thus, the expansion volume ( $V_E$ ) and the compression volumes ( $V_C$ ) are described as follows [27, 55, 62, 63], with a swept volume for the displacer piston ( $V_{SE}$ ), a displacer for the power piston ( $V_{SC}$ ), a phase angle ( $\varphi$ ) of  $90^\circ$  between the displacer piston and power piston as well as the crank angle ( $\alpha$ ).

$$V_E = \frac{V_{SE}}{2} [1 - \cos(\alpha)] + V_{DE}$$

$$V_{C(\gamma-SE)} = \frac{V_{SE}}{2} [1 + \cos(\alpha)] + \frac{V_{SC}}{2} [1 - \cos(\alpha - \varphi)] + V_{DC}$$

$$V_{C(\beta-SE)} = \frac{V_{SE}}{2} [1 + \cos(\alpha)] + \frac{V_{SC}}{2} [1 - \cos(\alpha - \varphi)] + V_{DC} - V_B$$

The total volume is obviously the sum of the previously mentioned volumes.

$$V_D = V_{DE} + V_{DC}$$

$$V_{Total} = V(\alpha) = V_{SE} + \frac{V_{SC}}{2} [1 - \cos(\alpha - \varphi)] + V_D$$

Where

$$V_{SE} = \frac{\pi}{4} * d_d^2 * h$$

$$V_{SC} = \frac{\pi}{4} * d_w^2 * h$$

The crank angles at the extreme volumes can be calculated to validate the value of the phase shift angle  $\varphi$ . By deriving the total volume, we get the following equation.

$$\frac{dV(\alpha)}{d\alpha} = \frac{V_{SC}}{2} [\sin(\alpha - \varphi)]$$

The previous equation reaches a value of zero,

$$0 = [\sin(\alpha - \varphi)]$$

for

$$\alpha = \varphi$$

$$\alpha = \pi + \varphi$$

“The crank angle  $\alpha$  reaches a value of zero when the displacer is at the upper dead point” and a positive number for the phase shift angle  $\varphi$  means that the working piston reaches its upper dead point after the displacer reaches it by  $90^\circ$  [55].

### **G. Ideal Cycle Analysis: Performance of both the Lab Scale Gamma Stirling Engine and Beta Stirling Engine**

A numerical analysis using the formulas above has been done on Microsoft Excel software for the Lab Scale Gamma Stirling Engine and the 10W Beta Stirling Engine. In fact, the gamma-Stirling Engine used was lab-scale prototype manufactured by a team of Mechanical Engineers under the supervision of Dr. Zeaiter some years ago. While the beta-Stirling Engine was a small demo-type engine manufactured by GreenPowerScience.

The input values to the Excel run were the length of the Stroke of the Power and Working Piston (that used to be equal) as well as the Displacer and Power piston diameter, and finally the temperature at both ends of the engine.

Table 34. Inputs to the Numerical Run

Measurement		Notation	$\gamma$ -SE	$\beta$ -SE
Length of the Stroke (cm)	Displacer	h	2.0	2.1
	Power Piston		1.5	1.3
Displacer Piston Diameter (cm)		$D_p$	1.7	1.9
Working Piston Diameter (cm)		$D_w$	1.2	1.98

The values obtained using the formulas from [27, 55] can be shown in the following sections.

### 1. Thermal Efficiency

As mentioned previously, the thermal efficiency can be calculated by only knowing the temperatures on the hot and cold side of the engine. In fact, the temperature of both the engines on the hot side was considered to be around 500 °C. Without the application of water, the temperature on the cold side of the engine is around 70 °C.

Table 35. Thermal Efficiency of the Stirling Cycle without water cooling

Measured Magnitude	Value	
$T_{max}$	500 °C	773 K
$T_{min}$	70 °C	343 K
<b>Thermal Efficiency</b>	55.6%	

Knowing that the efficiency of the auxiliaries in the system is constant, increasing the thermal efficiency is necessary to reach a higher power. In order to increase the

temperature difference, reaching lower temperatures on the cold side of the engine,  $T_{\min}$ , is needed as the hot side temperature is usually constant (butane burning) or even transient (solar thermal energy). Thus, a water cooling system will be elaborated in the following sections with a goal to reach a minimal cold side temperature. If we estimate that the cold side will reach a temperature near 15 °C, the thermal efficiency will be as follows.

*Table 36. Thermal Efficiency of the Stirling Cycle with water cooling*

<b>Measured Magnitude</b>	<b>Value</b>	
$T_{\max}$	500 °C	773 K
$T_{\min}$	15 °C	288 K
<b>Thermal Efficiency</b>	62.7%	

This leads to a thermal efficiency increase of 7.1%. For this reason, water cooling system is considered to be a crucial part for maximum energy generation.

## ***2. Volume Analysis: Results***

Using the values displaced in *Table 34*, as well as the equations gathered from [27, 55], the different swept volumes can be obtained. Concerning the hot dead volume, it was obtained by measuring the length of the volume of the inner space that the displacer is not filling inside the cylinder on the hot side of the engine. The same measurement is done for the cold dead volume. The engines used in those experiments do not include a regenerator.

a. Volume Study of the Gamma Stirling Engine

Table 37. Volume Analysis on the Gamma-Type SE

Measurement	Notation	$\beta$ -SE	
Swept Expansion Volume (cm <sup>3</sup> )	V <sub>SE</sub>	0.340	
Swept Compression Volume (w/r to displacer) (cm <sup>3</sup> )	V <sub>SC</sub>	0.329	
Swept Compression Volume (w/r to piston) (cm <sup>3</sup> )	V <sub>SCp</sub>	0.158	
		Crank Angle	
		(°)	
		0	0
Expansion Volume (cm <sup>3</sup> )	V <sub>E</sub>	90	0.170
		180	0.340
		270	0.170
		360	0
		0	0.426
Compression Volume (cm <sup>3</sup> )	V <sub>C</sub>	90	0.170
		180	0.085
		270	0.340
		360	0.426
		0	0.425
Total Volume (cm <sup>3</sup> )	V	90	0.340

		180	0.425
		270	0.510
		360	0.425
<b>Maximum Volume (cm<sup>3</sup>)</b>	$V_{\max}$		0.510
<b>Minimum Volume (cm<sup>3</sup>)</b>	$V_{\min}$		0.340

For this analysis, the dead volumes are not being taken into consideration for the lack of information available about the inner dimensions of the Gamma Stirling Engine. The following plot expresses the changes of the volumes in function of the crank angle of the Gamma Stirling Engine.

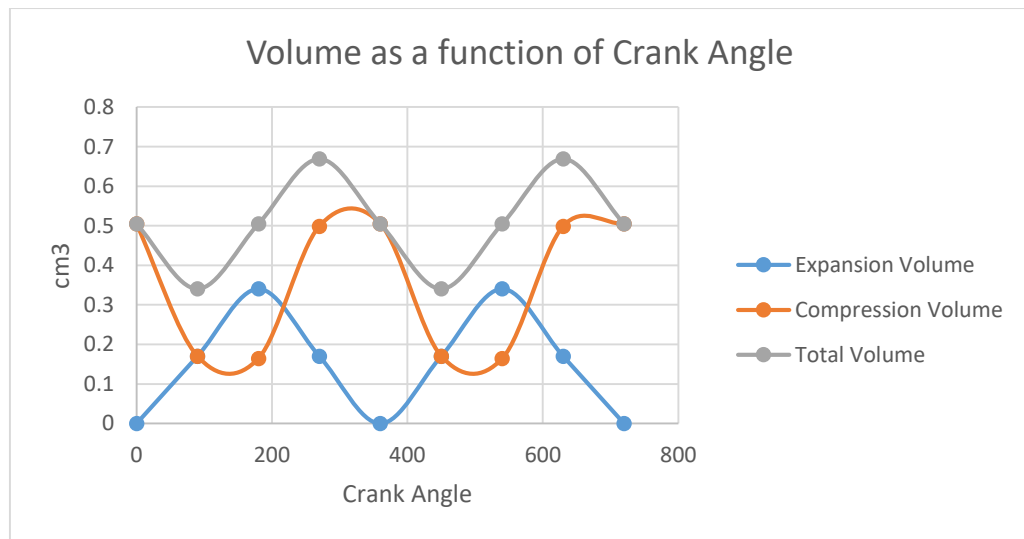


Figure 55. Expansion, Compression and total volume change with respect to crank angle in the Beta Stirling Engine



b. Volume Study of the Beta Stirling Engine

Table 38. Volume Analysis on the Beta-Type SE

Measurement	Notation	$\beta$ -SE	
Swept Expansion Volume (cm <sup>3</sup> )	V <sub>SE</sub>	5.95	
Swept Compression Volume (w/r to displacer) (cm <sup>3</sup> )	V <sub>SC</sub>	5.79	
Swept Compression Volume (w/r to piston) (cm <sup>3</sup> )	V <sub>SCP</sub>	3.74	
		Crank Angle	
		(°)	
		0	2.09
Expansion Volume (cm <sup>3</sup> )	V <sub>E</sub>	90	5.07
		180	8.04
		270	5.07
		360	2.09
		0	5.94
Compression Volume (cm <sup>3</sup> )	V <sub>C</sub>	90	1.18
		180	0.15
		270	4.91
		360	5.94
		0	8.03
Total Volume (cm <sup>3</sup> )	V	90	6.25

		180	8.20
		270	9.98
		360	8.03
<b>Maximum Volume (cm<sup>3</sup>)</b>	$V_{\max}$		9.98
<b>Minimum Volume (cm<sup>3</sup>)</b>	$V_{\min}$		6.25
<b>Hot Dead Volume (cm<sup>3</sup>)</b>	$V_{\text{HD}}$		2.10
<b>Cold Dead Volume (cm<sup>3</sup>)</b>	$V_{\text{CD}}$		6.54
<b>New Cold Dead Volume (cm<sup>3</sup>)</b>	$V_{\text{CD}}'$		4.84
<b>Overall Dead Volume (cm<sup>3</sup>)</b>	$V_{\text{D}}$		6.94
<b>Ratio of Dead Volume to Total Volume (%)</b>	$R_{\text{Dv}}$		42

In the cases of the Beta Stirling Engine, “the strokes of the displacer and the power piston should overlap so that they almost touch at one point in the cycle” [27]. The overlap volume should be subtracted from the cold volume which is the common volume for the two pistons. Therefore, the new cold dead volume will be then equivalent to [27]

$$V'_{\text{CD}} = V_{\text{CD}} - V_{\text{P}} \left( 1 - \frac{\sqrt{2}}{2} \right) = 4.845 \text{ cm}^3 \text{ instead of } V_{\text{CD}} = 6.541 \text{ cm}^3$$

Instead of following this method, Macháček [63] calculated the overlap volume which he called  $V_B$  in the following way.

$$V_B = \frac{V_{\text{SE}} + V_{\text{SC}}}{2} - \sqrt{\frac{V_{\text{SE}}^2 + V_{\text{SC}}^2}{4} - \frac{V_{\text{SE}} + V_{\text{SC}}}{2} * \cos\varphi} = 1.720 \text{ cm}^3$$

After subtracting this value from the cold dead volume originally calculating, the new cold dead volume will be equivalent to

$$V''_{CD} = V_{CD} - V_B = 4.821 \text{ cm}^3$$

which is very close to the value obtained using Martini's method, with less than 0.5% deviation.

$$V''_{CD} = 4.821 \text{ cm}^3 \approx V'_{CD} = 4.845 \text{ cm}^3$$

Which leads us to draw the volume change in the Beta Stirling Engine with respect

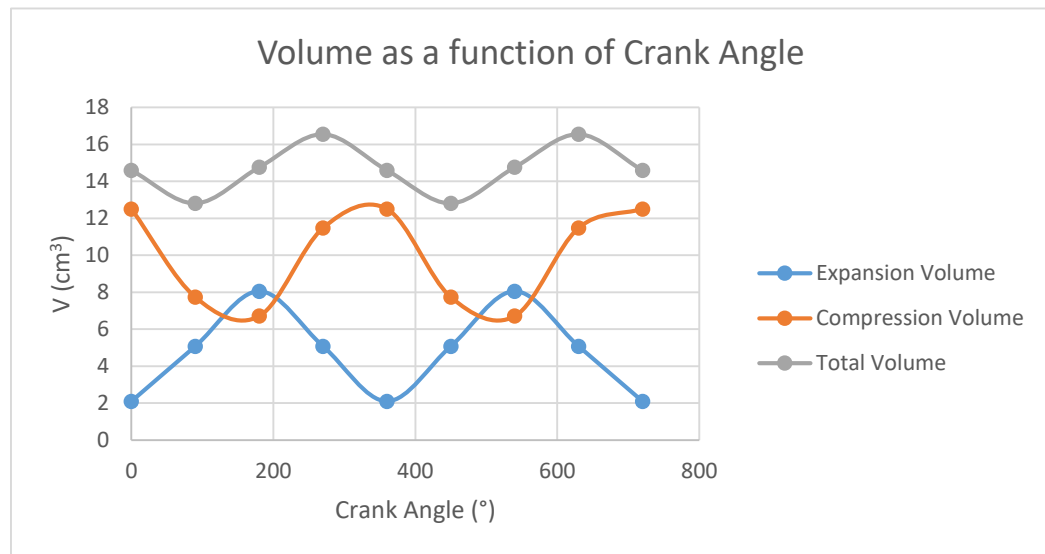


Figure 56. Expansion, Compression and total volume change with respect to crank angle in the Beta Stirling Engine

to the changes of the crank shaft angle.

The compression ratio can also be concluded using the previously mentioned calculation

$$\varepsilon_{\beta} = 1 + \frac{V_{SC}}{V_{SE} + V_D} = 1 + \frac{5.79}{5.95 + 6.94} = 1.45$$

### ***3.Heat and Work performance of the ideal Stirling Cycle in the given Engine***

To obtain the heat and work performance of the engine, the maximum and minimal volume as well as the temperature at the points 1 and 3 of the cycle

$$Q_{1-2} = m * R * T_1 * \ln\left(\frac{V_2}{V_1}\right)$$

$$Q_{3-4} = m * R * T_3 * \ln\left(\frac{V_4}{V_3}\right)$$

knowing that the ideal gas constant for air is known to be

$$R_{air} = 287.1 \frac{J}{kg.K}$$

The maximum and minimum volumes of the engines are

$$\text{Gamma SE: } V_1 = V_4 = V_{max} = 0.5101 \text{ cm}^3$$

$$\text{Gamma SE: } V_2 = V_3 = V_{min} = 0.3405 \text{ cm}^3$$

$$\text{Beta SE: } V_1 = V_4 = V_{max} = 16.55 \text{ cm}^3$$

$$\text{Beta SE: } V_2 = V_3 = V_{min} = 12.81 \text{ cm}^3$$

The mass of gas in the engine, initially at the atmospheric pressure, is calculated as follows.

$$m_{air} = \frac{p_{initial} * V_{max}}{R_a * T_{initial}}$$

For the Gamma SE:

$$m_{air} = \frac{101,325 \text{ Pa} * 0.5101 \text{ cm}^3 * \frac{1 \text{ m}^3}{1,000,000 \text{ cm}^3}}{287.1 \frac{\text{J}}{\text{kg} \cdot \text{K}} * 293 \text{ K}} = 6.1 * 10^{-7} \text{ kg} = 0.00061 \text{ g}$$

For the Beta SE:

$$m_{air} = \frac{101,325 \text{ Pa} * 16.55 \text{ cm}^3 * \frac{1 \text{ m}^3}{1,000,000 \text{ cm}^3}}{287.1 \frac{\text{J}}{\text{kg} \cdot \text{K}} * 293 \text{ K}} = 2 * 10^{-5} \text{ kg} = 0.02013 \text{ g}$$

Fitting those values in the equation obtained earlier, the work and heat transferred during the Stirling Process can be calculated as follows:

For the Gamma Stirling Engine (GSE):

$$Q_{1-2(GSE)} = -0.02184 \text{ J}$$

$$Q_{3-4(GSE)} = 0.05514 \text{ J}$$

Resulting in a work produced of:

$$W_{(GSE)} = 0.03330 \text{ J}$$

and a rotational speed of 1000 RPM, the power of the engine is;

$$P_{(GSE)} = 0.5551 \text{ W}$$

For the Beta Stirling Engine (BSE):

$$Q_{1-2(BSE)} = -0.5272 \text{ J}$$

$$Q_{3-4(BSE)} = 1.188 \text{ J}$$

Resulting in a work produced of:

$$W_{(BSE)} = 0.6607 J$$

and a rotational speed of 1000 RPM, the power of the engine is;

$$P_{(BSE)} = 11.01 W$$

#### ***4.p-v Diagram of the ideal process***

The minimum and maximum volumes, as well as the minimum and maximum temperatures of the ideal process have been calculated. Using the equation of state, considering the working fluid, air in this case, an ideal gas, the pressure at the 4 points of the processes can be determined as shown in the tables below:

*Table 39. Volume, Temperature and Pressure for different points in the ideal process for the GSE*

<b>V</b>	<b>T</b>	<b>P</b>
<b>cm3</b>	<b>K</b>	<b>atm</b>
<b>0.510116</b>	306.15	1.044881
<b>0.34047</b>	306.15	1.565513
<b>0.34047</b>	773.15	3.953541
<b>0.510116</b>	773.15	2.638737
<b>0.510116</b>	306.15	1.044881

*Table 40. Volume, Temperature and Pressure for different points in the ideal process for the BSE*

<b>V</b>	<b>T</b>	<b>P</b>
<b>cm3</b>	<b>K</b>	<b>atm</b>
<b>16.71199</b>	293.15	1.17116041
<b>12.8105</b>	293.15	1.527841791
<b>12.8105</b>	773.15	3.442374707
<b>16.71199</b>	773.15	2.638737201
<b>16.71199</b>	293.15	1.17116041

Finally, the p-v diagram can be built for the two engines.

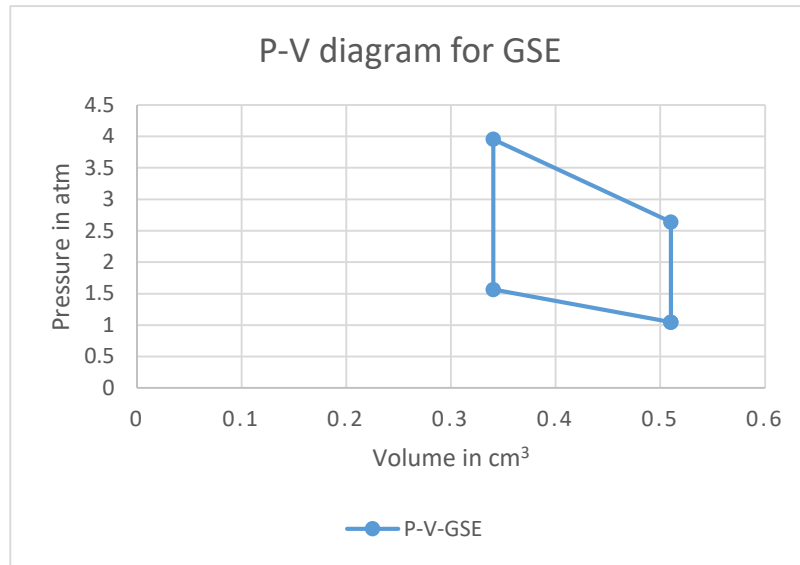


Figure 58. p-v diagram for the ideal process of the GSE

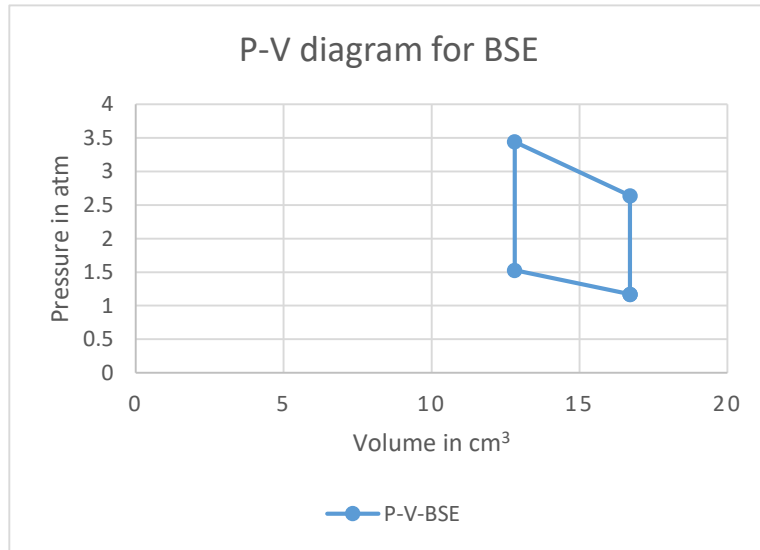


Figure 57. p-v diagram for the ideal process of the BSE

## H. 0<sup>th</sup> order analysis

### *1. Goal of the 0<sup>th</sup> order analysis*

Designed for a simple preliminary analysis of the Stirling Engine, this paper based method relates “the power output and efficiency of a machine to the heater and cooler temperature, the engine displacement and the speed” [55]. It basically assumes that a manufacturer team runs the engine and predicts the power and efficiency of the engine. Three methods are going to be executed for the GSE and the BSE: The Carlquist’s method, the Beale’s method and finally the West’s method [55].

### *2. Efficiency Prediction by the Carlquist’s Method*

It was previously demonstrated that the ideal efficiency of a Stirling Engine is the same as the thermal efficiency of a Carnot cycle. In fact, this method, presented initially in the Martini’s “Stirling Engine design manual Volume 2” [27], presents a way to find the maximum efficiency of a well optimized engine operating on hydrogen [55]. Although the engines we have uses atmospheric air as a working fluid, this method will still be used to have an idea of the efficiency drop. In fact, the overall effective efficiency of a Stirling Engine by Carlquist is nothing but:

$$\eta_{eff} = \left(1 - \frac{T_C}{T_E}\right) * C * \eta_H * \eta_M * f_A$$

where  $C$  is the Carnot efficiency ratio usually from 0.65 to 0.75,  $\eta_H$  is the heater efficiency, which is nothing but the ratio of the energy flow to the heater to the fuel energy



flow, this range between 0.85 and 0.90,  $\eta_M$  is the mechanical efficiency commonly between 0.85 and 0.90 and finally  $f_A$  the auxiliary ratio at a maximum efficiency point of 0.95 [55]. By taking an average of these 4 factors, the effective efficiency of the engine can be described by the following equation.

$$\eta_{eff} = \left(1 - \frac{T_C}{T_E}\right) * 0.512$$

### ***3.Power Estimation by Beale’s Method***

According to [55], Graham Walker said that : “William Beale, of Sunpower, Inc. in Athens, Ohio, observed several years ago that the power output of many Stirling Engines conformed approximately to the simple equation”:

$$P = Be * p_m * f * V_0$$

Where  $Be$  is the Beale number,  $P$  is the engine’s power in W,  $p_m$  is the mean cycle pressure in bar,  $f$  is the rotational speed of the engine in Hz and finally  $V_0$  is the displacement of the power piston in  $\text{cm}^3$ .

The equation can be written in this form:

$$Be = \frac{P}{p_m * f * V_0}$$

Leading to a dimensionless group that is actually called the Beal number. The difference between this method and the Carlquist’s method is that this one applies for all kinds of engine including free piston engines and the ones with a crank mechanism, like the

ones we are operating in the Lab. Recent works suggest that the Beale number varies with the heater temperature as shown on the full line in the graph below [55]. In fact, a “large number of engines will be found to lie within the bounds of the confidence limits” illustrated as broken lines in the figure below. Actually, well designed engine will be concentrated on the upper bound while not well designed engines will be located at the lower bound. Moreover, when the hot part of the engine is made of conventional stainless steel, the Beale number will fall somewhere near the A-A line. On the other hand, “high alloy steels for the hot parts will permit the elevation of heater temperature to the limit of B-B” [55].

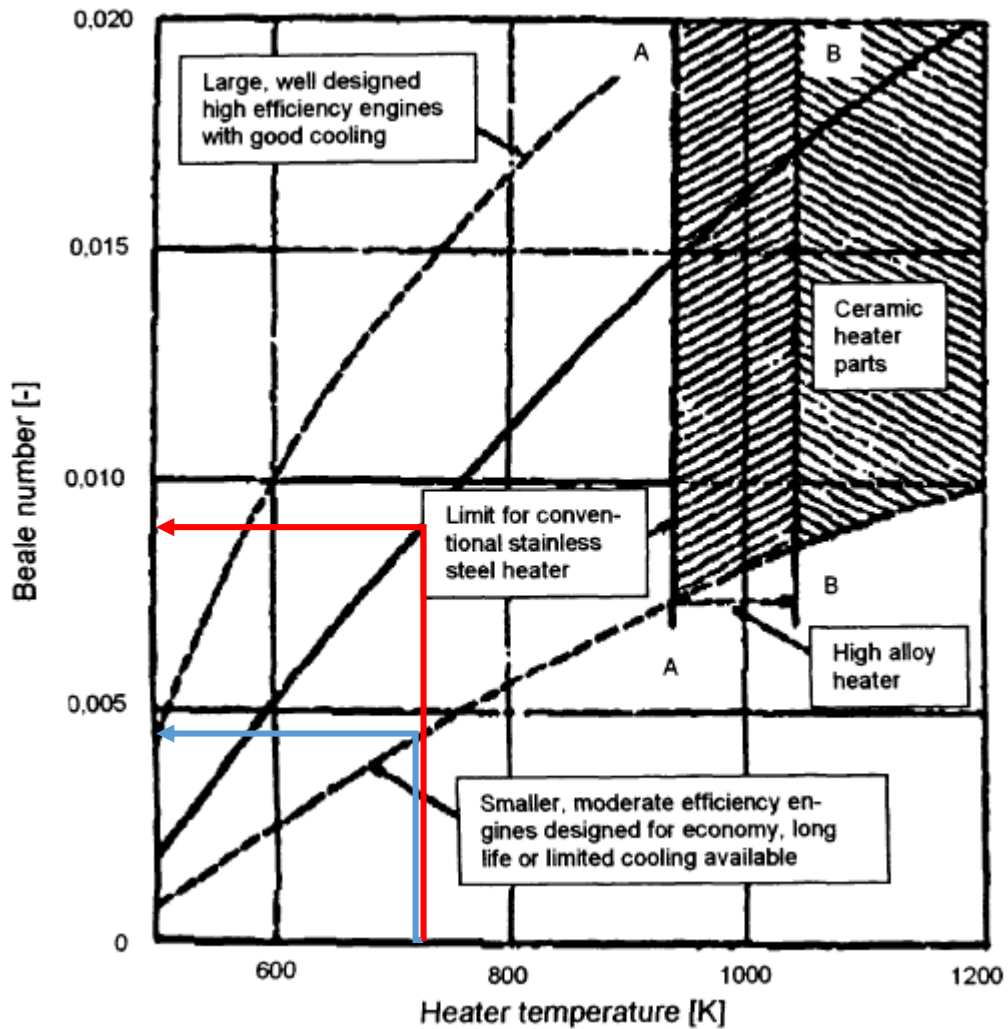


Figure 59. Beale Number variation in function of the hot side temperature (from Wagner)

#### 4. Power Estimation by West's Method

West estimated that the power of an Engine is characterized by the following formula.

$$P = F * n * p_m * V_0 * \frac{T_E - T_C}{T_E + T_C}$$

where  $F$  is the West factor,  $n$  is the rotational speed of the engine in Hz,  $p_m$  is the average cycle pressure in Pa,  $V_0$  is power piston's displacement in  $m^3$  and finally  $T_E$  and  $T_C$  are the expansion and compression space temperature respectively.

Of course the Beale and West factors cannot be used in designing a new machine but they give an overview of the performance of the engine, what we actually need for the Engines we are operating in the Lab.

Table 41. 0<sup>th</sup> order analysis of the GSE

Method Used		Value	Unit
<b>Carlquist</b>	$\eta_{\text{eff Car}}$	31%	
	Power by Car	0.17	W
<b>Beale</b>	Power by Be		
	Be	0.0045	
	Mean Pressure	2.30	atm
	RPM	1000	
	Speed of engine per s	16.66666667	Hz
	Swept Volume Compression	0.329	$cm^3$
	Power by Be	0.0567	W
<b>West</b>	Power by We		
	West Factor	0.35	
	$T_E$	773.15	
	$T_C$	306.15	
	Power by We	0.193	W

In fact, knowing that the heater temperature of the GSE used was around 773.15 K, that water cooling was applied and that the design is not optimally made, the Beale number used was 0.004.

However, since the BSE was designed in a better way by adding a combustion chamber and a water cooling chamber, the Beale factor chosen is 0.009.

Table 42. 0<sup>th</sup> order analysis of the BSE

Method Used		Value	Unit
<b>Carlquist</b>	$\eta_{\text{eff}}$ Car	28%	
	Power by Car	3.14	W
<b>Beale</b>	Power by Be		
	Be	0.009	
	Mean Pressure	2.195028527	atm
	RPM	1000	
	Speed of engine per s	16.66666667	Hz
	Swept Volume Compression	5.790448098	cm <sup>3</sup>
	Power by Be	1.91	W
	Power by We		
<b>West</b>	West Factor	0.35	
	T <sub>E</sub>	773.15	
	T <sub>C</sub>	293.15	
	Power by We	2.893831763	W

### ***5. Conclusion of the 0<sup>th</sup> order analysis***

The idea behind performing a preliminary analysis is to predict the ideal performance of the Engine in hand. It is then followed by a 0<sup>th</sup> order analysis that is done to predict the real efficiency and power output of the Stirling Engine. In fact, a summary of the results is found in the table below.

*Table 43. Comparison of ideal process values and 0<sup>th</sup> order analysis values*

	<b>GSE</b>	<b>BSE</b>
<b>Nominal Value</b>	-	10
<b>Ideal Process</b>	0.56	11.01
<b>Carlquist</b>	0.17	3.14
<b>Beale</b>	0.0567	1.91
<b>West</b>	0.19	2.89

## CHAPTER VII

### TESTING OF A LAB SCALE GAMMA STIRLING ENGINE

In this chapter, the electrical performance of the gamma-Stirling Engine, discussed above, is going to be tested. The electrical power will then be compared to the results obtained with the 0<sup>th</sup> order analysis.

#### **A. Equipment**

The set of equipment needed for the following experiments is as follows:

- 1W DC motor (dynamo) with Gears for a 1 to 4 gear ratio
- Breadboard, Electric Cables and two multi-meters (one to measure the voltage and the second to measure the current)
- A burette and its stand continuously filled with cold water
- Resistors of 150 Ohm
- A load resistor for a bigger load (Resistance values from 1-47 Ohm)

The electric circuit can be modeled as shown in the figure below.

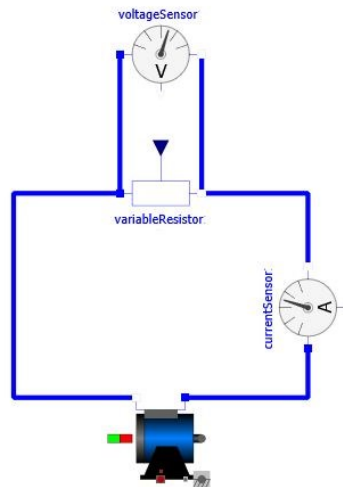


Figure 60. Electrical Circuit of the generator (coupled with the Stirling Engine) in series with the load resistor and Ampere-meter as well as in parallel with the voltmeter (drawn on openModelica)

### B. First Approach using different resistance values and Power Expected from the Generator at different RPMs

A first approach was to couple a resistance of 150 Ohm with the generator as shown in the following figure, and then to add two 150 Ohm resistances in series to model a 300 Ohm resistance. The power obtained with respect to the field resistance and the RPM of the Stirling Engine is expressed as follows.

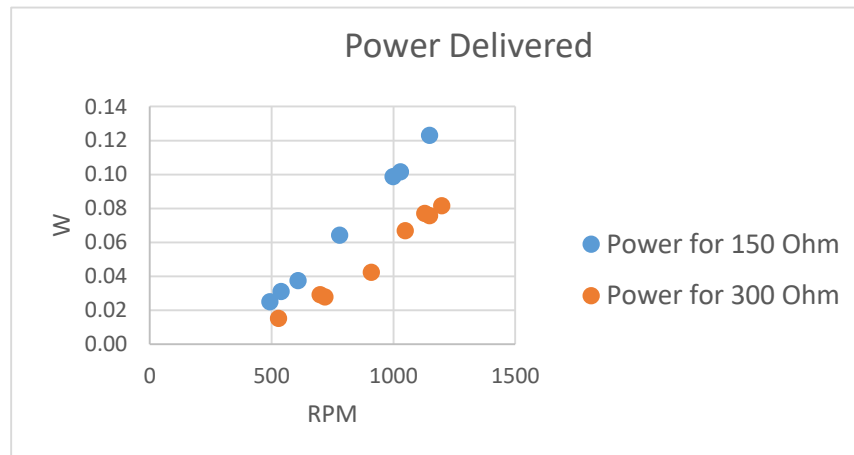


Figure 61. Electrical Power Delivered by the Engine when coupled to different resistance values



The power obtained at a lower resistance for the same RPM is higher than the one obtained at 300 Ohm. In order to understand more the results graphs were drawn showing

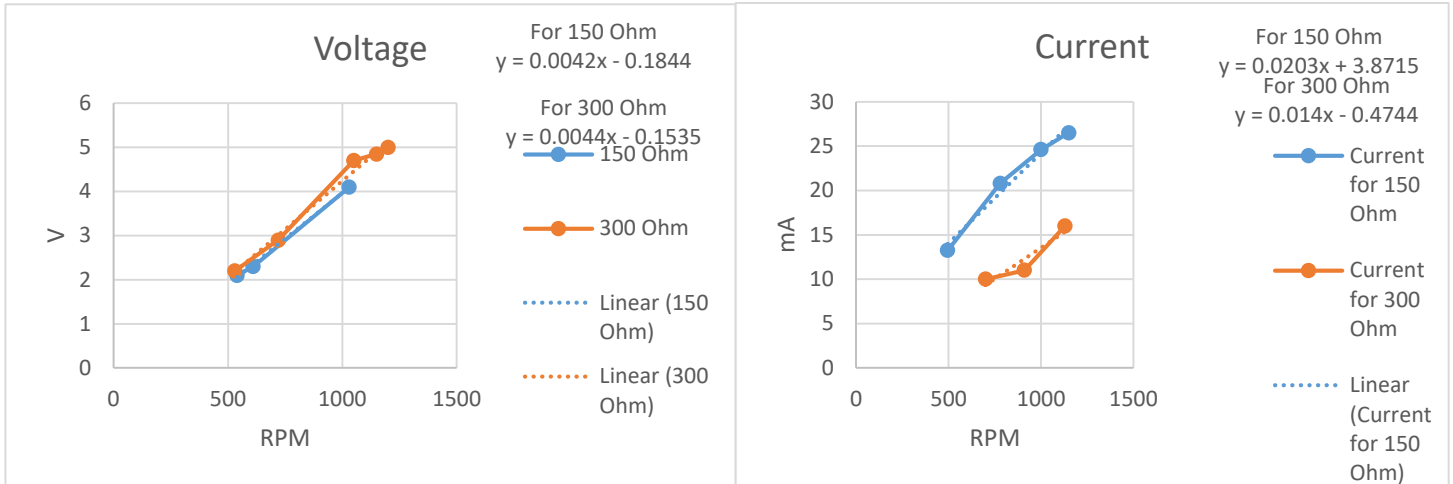


Figure 62. Voltage and Current changes with respect to the field resistance and the RPM

the variation of the current and the voltage with the RPM at different resistances and the following was obtained.

As observed in the graphs, for lower resistances more current is extracted from the engine for the same voltage at each RPM. Thus for lower resistances the load assigned to the generator will increase and the Stirling Engine will be required to deliver more power to the system. A linear function describing the change in voltage with respect to RPM can be written for this specific generator.

$$Voltage = 0.0043 * RPM + 0.017$$

In fact, the voltage delivered is only a function of rotational speed and will remain the same for different resistance values. Using this formula, as well as Ohm's law and the data obtained from the previous resistances, a graph for the power of the generator at different resistances can be drawn and the result is presented as follows.

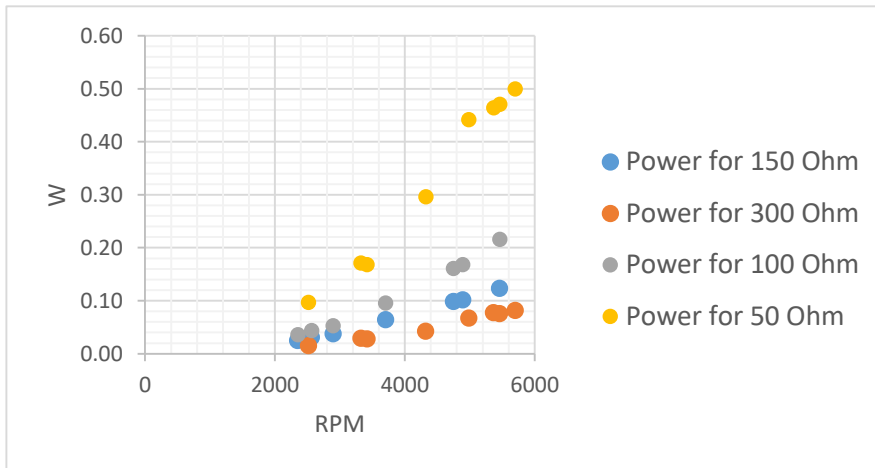


Figure 63. Power of the generator as a function of Rotational Speed for different resistance values

This last figure actually proves what has been explained earlier. The voltage is a function of rotational speed. Thus, for the same RPM value and a smaller resistor, the current must increase to keep the same voltage. Therefore, the power delivered by the generator will increase for smaller resistors. This conclusion is backed by two basic formulas, the power formula and the Ohm's law.

$$\text{Ohm's law: } R = \frac{V}{I} \text{ or } V = R * I$$

$$\text{Power formula: } P = V * I = R^2 * I$$

where R is the field resistance, V is the voltage, I is the current and finally P is the power expressed in W.

In order to find the optimal power of the Stirling Engine, more electrical load should be added to the field, thus lower electrical resistance values.

### C. Second Approach: Finding the Engine's optimal power

Starting with the fixed 150 Ohm, each run was done using a different circuit configuration to model different loads on the engine.

1. Two 150 Ohm resistance in series to model the 300 Ohm load
2. One 150 Ohm resistance coupled with the engine
3. Two 150 Ohm resistances in parallel to model 75 Ohm load resistance by respecting the following principle:

$$\frac{1}{R_{Total}} = \frac{1}{R_1} + \frac{1}{R_2} + \frac{1}{R_3} \dots$$

$$\frac{1}{R_{Total}} = \frac{1}{150 \text{ Ohm}} + \frac{1}{150 \text{ Ohm}}$$

$$R_{Total} = \frac{150 \text{ Ohm}}{2} = 75 \text{ Ohm}$$

4. Three 150 Ohm resistances in parallel to model a 50 Ohm load resistance
5. Four 150 Ohm resistances to model a 37.5 Ohm load resistance

In order to reach lower resistances values, a Load Resistor was borrowed from the Electrical Engineering Department at AUB with values varying from 1 to 47 Ohm.

#### ***1. Increasing the load***

As much as it might seem counter intuitive, decreasing the field resistance is equivalent to increasing the load on the engine.

Mechanically speaking, a physical load is proportional to the mechanical resistance on an engine. However, in an electrical circuit with a generator as a power source, the bigger the field resistance is, the lower the load on that engine is. Thus, higher load demands are obtained at lower field resistances.

In fact, when a load is added to an electrical system, it is added in parallel to the power source. Thus, the voltage at the nodes of the system will be the same and the current will increase, demanding more power from the engine. The overall resistance in this case will decrease because of the inverse relationship of the total resistance value in parallel. A lower resistance value will require a higher current to pass into the system, and thus a higher load will be demanded.

$$\frac{1}{R_{Total}} = \frac{1}{R_1} + \frac{1}{R_2} + \frac{1}{R_3} \dots$$

## 2. First run: Varying the field resistance value and the heat input to the engine

As described earlier, the setup is made as follows.

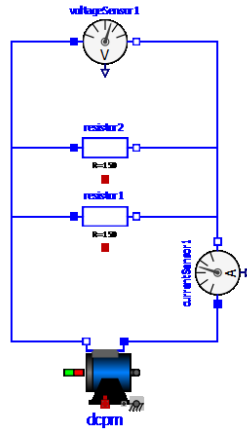


Figure 64. Set up for two 150 Ohm resistances in parallel, equivalent to a 75 Ohm load

The results can be shown in the table and figures below. It should be noted that to model the effect of temperature difference on the power output, a first run is made on minimum heat input, and a second run is made using a higher heat flow on the heat side of the engine, thus creating a higher temperature difference.

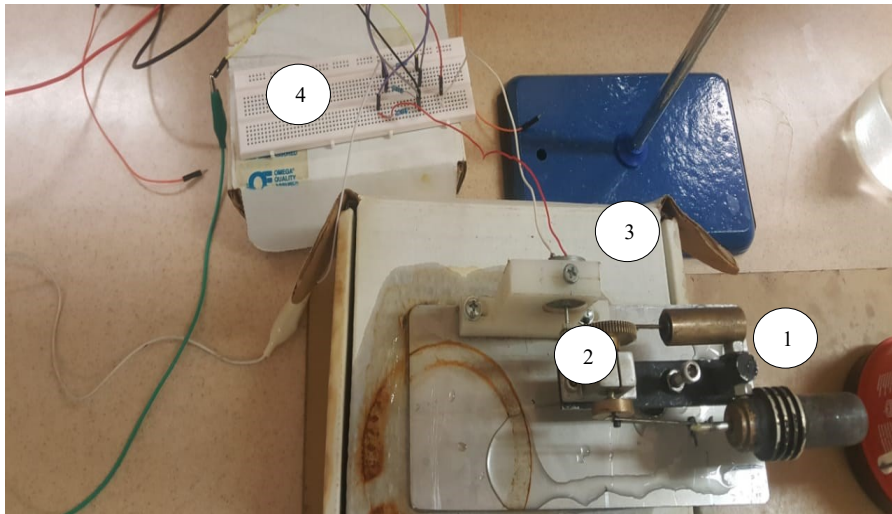


Figure 65. Set up for three 150 Ohm resistances in parallel to model the 75 Ohm load: 1 – gamma-Stirling Engine 2 – Gear Ratio of 1 to 4 3 – Dynamo 4 – Breadboard with three 150 Ohm resistors in parallel connected to a voltmeter and an amperemeter.

Table 44. Experimental Results at resistances from 300 to 37.5 Ohm.

Resistance	Voltage	Current	Current	Speed of Engine	Speed of Dynamo (1:4)	Power	Heat Power
Ohm	V	mA	A	RPM	RPM	W	Input
300	1.4	5	0.005	360	1,710	0.007	Min
300	2.8	9	0.009	700	3,325	0.0252	Max
150	1.85	12.5	0.0125	475	2,256	0.0231	Min
150	2.6	18	0.018	670	3,183	0.0468	Max
75	1.7	23	0.023	470	2,233	0.0391	Min
75	2	27	0.027	570	2,708	0.054	Max
50	1.25	25	0.025	400	1,900	0.03125	Min
50	1.74	35	0.035	520	2,470	0.0609	Max
37.5	1.03	28	0.028	330	1,568	0.0288	Min
37.5	1.4	38	0.038	490	2,328	0.0532	Max

The data shown in the table above are plotted as follows.

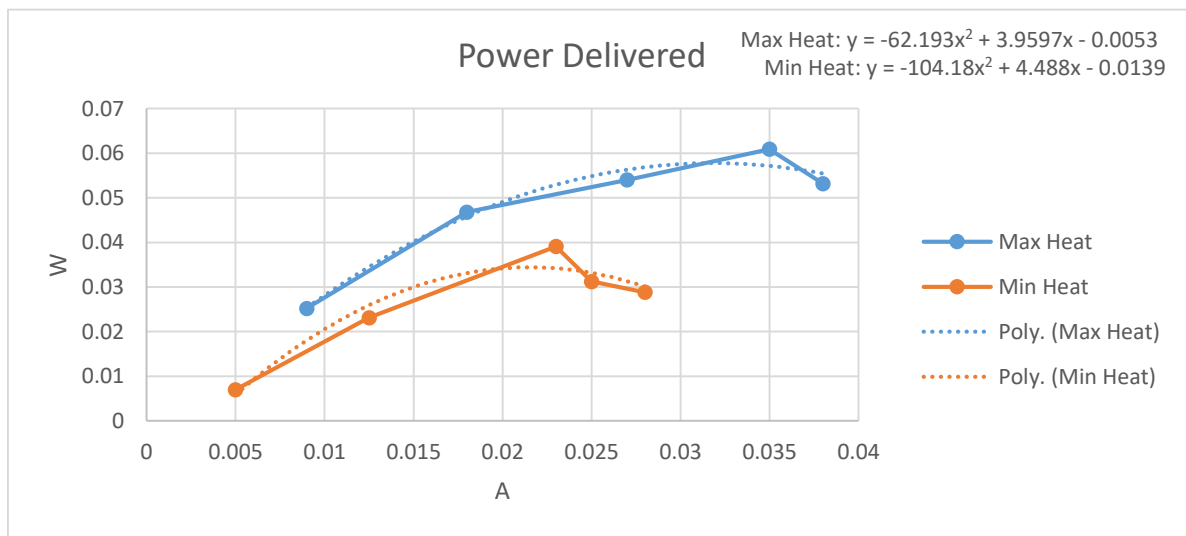


Figure 66. Figure showing the Power of the engine for different loads in Amps

In fact, the heat input to the engine is affecting the result, which proves what has been analyzed in the ideal cycle analysis. The bigger the heat flow is, the bigger the power

delivered will be. Actually, results show that the optimal power of the engine is 0.0609 W. In order not to fall into a local optimum, the following section examines the power output of the engine at even higher loads.

The figure below shows the variation of RPM with respect to the current. In fact, as the current increases, as the load on the engine increases. When the electrical load on the engine increases, a bigger mechanical load is applied on the engine and this causes a reduction in the rotational speed values.

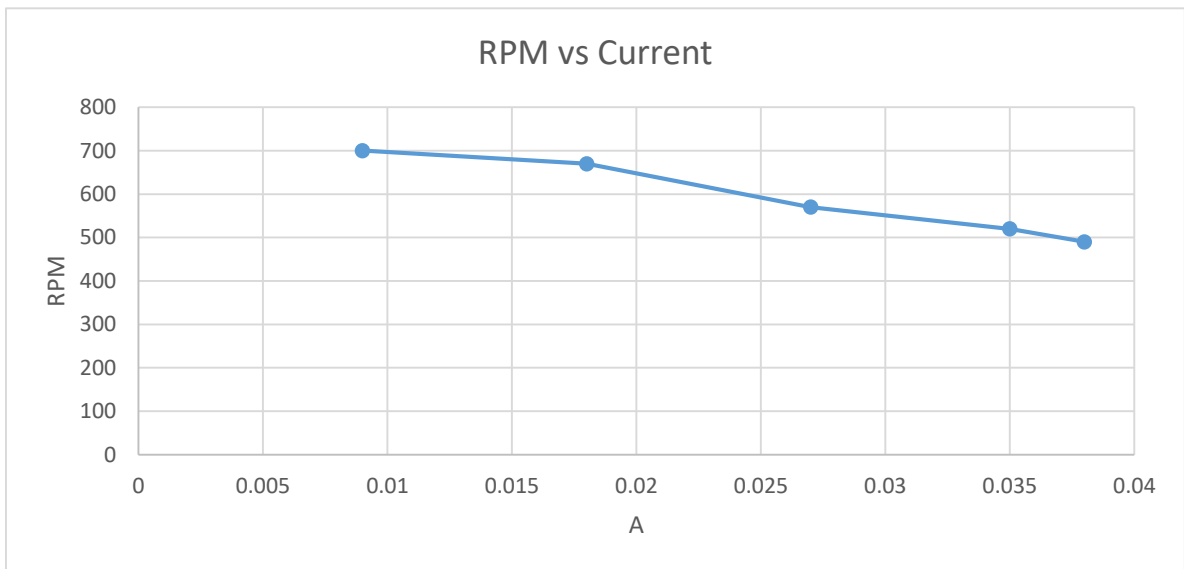


Figure 67. RPM vs Load in Amps

### ***3.Second run: Higher loads***

While maintaining the heat input to the system at its maximum, another run is done with lower resistances and the values are obtained as follows.

Table 45. Experimental results at resistance values from 43.2 to 3.6 Ohm

Resistance	Voltage	Current	Current	Speed of Engine	Speed of Dynamo (1:4)	Power
Ohm	V	mA	A	RPM	RPM	W
43.2	1.6	35	0.035	515	2,446.25	0.056
38.6	1.6	38	0.038	515	2,446.25	0.0608
34.2	1.4	40	0.04	505	2,398.75	0.056
25	1.32	49	0.049	490	2,327.50	0.06468
16.55	1	50	0.05	425	2,018.75	0.05
7.65	0.55	55	0.055	330	1,567.50	0.03025
3.6	0.3	60	0.06	280	1,330.00	0.018

It seems like the maximum power obtained earlier was a local optimum. In fact, the maximum power obtained is 0.065 W at 25 Ohm as it can be visualized in the figure below.

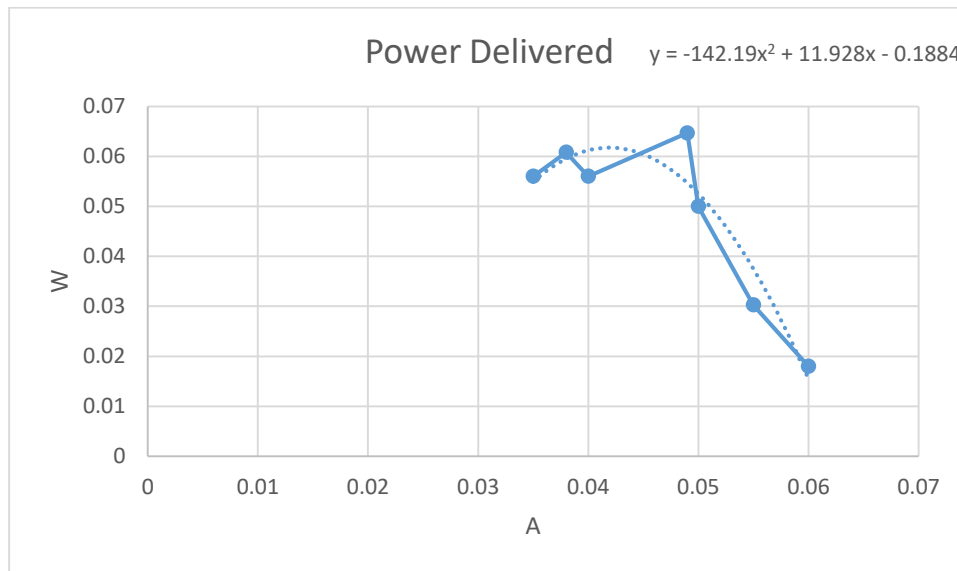


Figure 68. Variation in the power delivered by the engine with respect to low resistance values

As the resistance lowered, the load on the engine increased leading to a decrease in the voltage and a decrease in the RPM values.



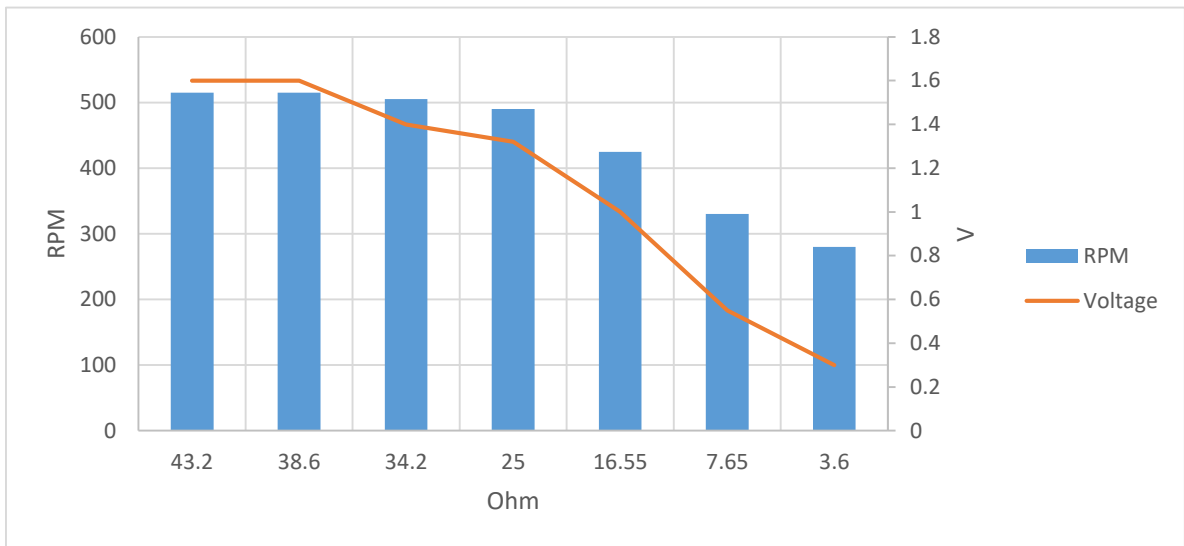


Figure 70. Variation of the RPM and the voltage with the decrease in the field resistance

The next figure shows the variation of the power along with the change in the field resistance.

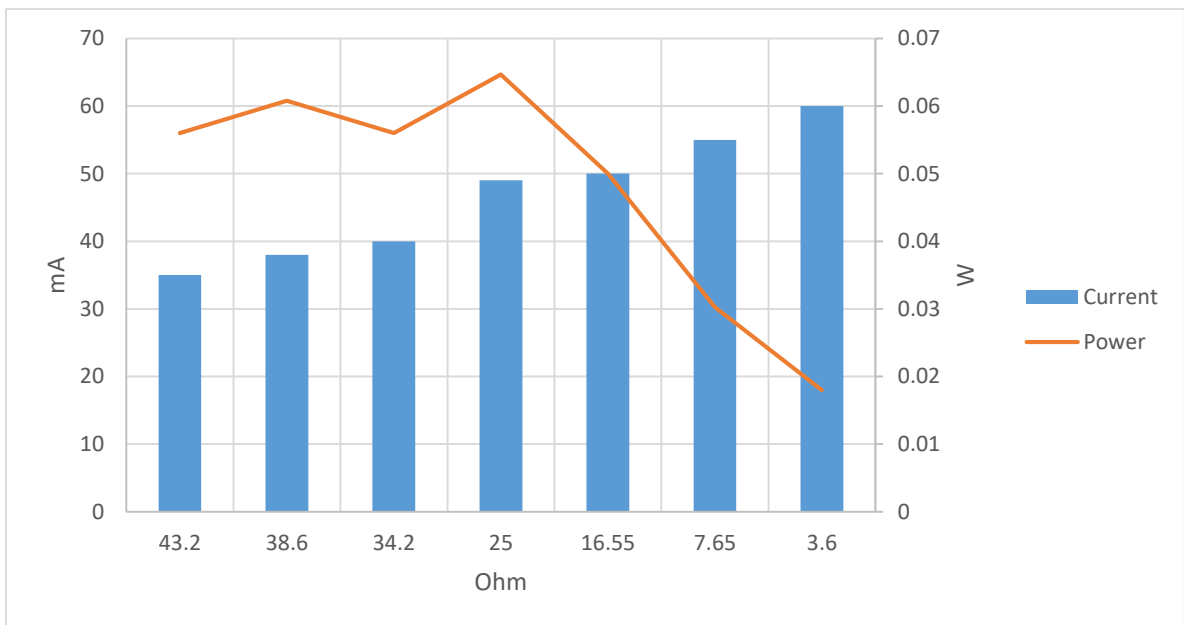


Figure 69. Effect of the variation in the field resistance on the current and the power of the engine

#### D. Third approach: Combining the results and calculation of power dissipated by the dynamo

By combining the results from the values obtained at 300 Ohm till 3.7 Ohm, the graph obtained looks as follows.

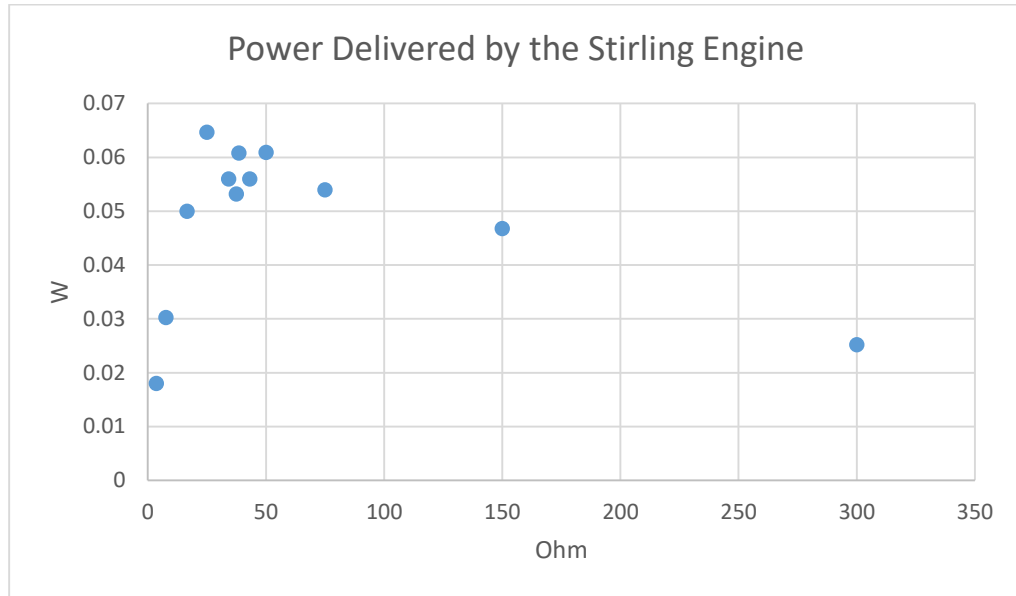


Figure 71. Power Delivered by the Stirling Engine for different resistance values

Thus, the nominal power of this lab scale gamma-Stirling Engine is 0.065 W.

On the other hand, the inner resistance of the dynamo can be modeled by a resistance in series with the dynamo. Therefore, finding the value of the internal resistance can be done by studying the variations of the voltage and the current in function of the changes in the field resistance. The plot will look like a linear curve characterized by the following equation

$$\text{voltage} = a * \text{current} + b$$

where  $a$ , the slope of the line, is the inner resistance and  $b$ , the intercept with the y axis, is the Electromotive Force (EMF) of the generator, also known as the open circuit voltage.

The V-I curve obtained for resistance values that range from 300 to 3.6 Ohm looks as follows.

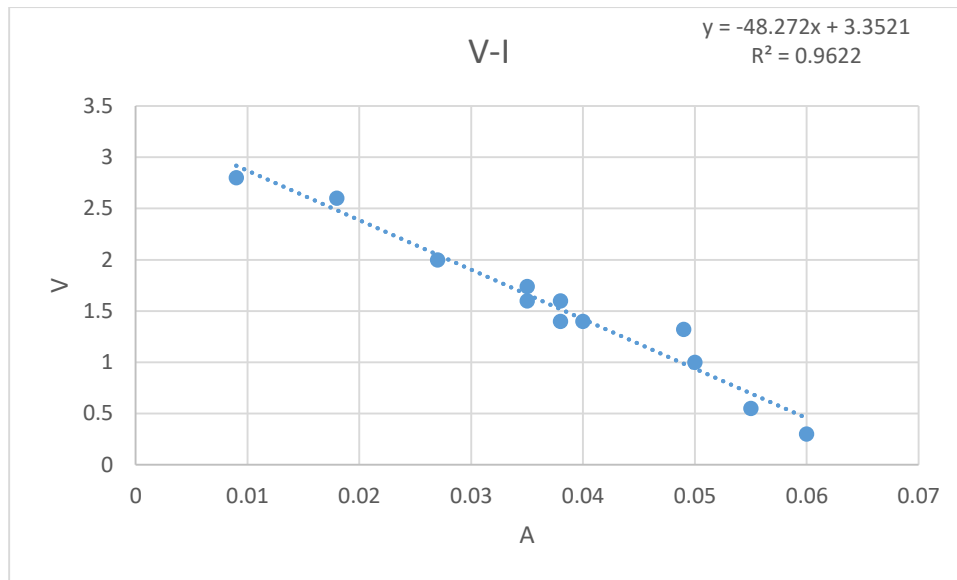


Figure 72. V-I line

The inner resistance is then 48.272 Ohm and the circuit voltage is then 3.352 V. The power dissipated can then be obtained by the following equation

$$P = I^2 * r$$

where  $r$  is the internal resistance of the dynamo.

The power dissipated is plotted with the power of the Engine below.

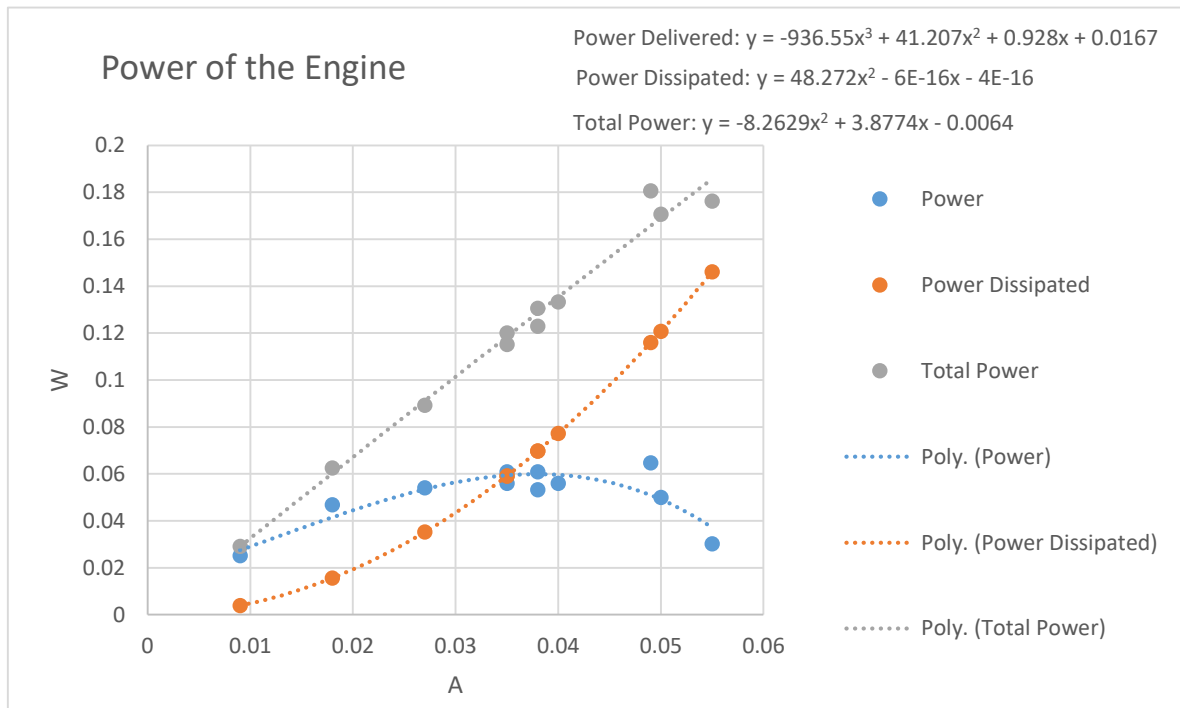


Figure 73. Power Delivered, Power Dissipated and total power

Thus by adding the power obtained to the dissipated power, the total electrical power of the engine is modeled by the grey curve in the figure above. Thus, the nominal electrical power of the engine is considered to be 0.181 W.

### E. Conclusion and outcomes of these experiments

Table 46. 0th Order results compared to the experimental result

	0 <sup>th</sup> Order	Experimental
Ideal Process	0.56	
Carlquist	0.17	
Beale	0.0567	
West	0.19	
		0.181

Actually, the result obtained are close to the 0<sup>th</sup> order analysis results. It can be seen that 0.181 is exactly within the bounds of Carlquist and West values. However, it is far above the value obtained using Beale's method. This can be due to the fact that the Beale factor chosen was slightly underrated. Knowing that this Stirling Engine is a lab scale design, the cooling system implemented was enough and the efficiency in heat deliverability was sufficient.

The Beale factor obtained knowing that the power obtained is 0.181W is as follows:

$$Be = \frac{P}{p_m * f * V_0} = 0.014$$

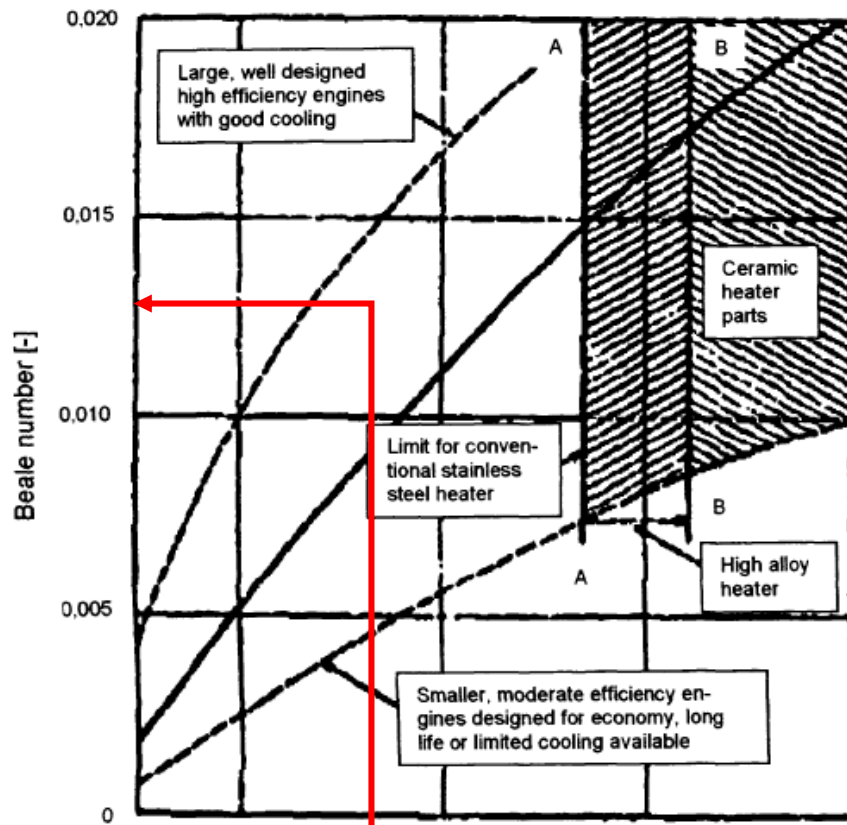


Figure 74. Beale factor for the gamma-Stirling Engine

In fact, there isn't much work to do with the gamma-Stirling Engine concerning increasing the efficiency of cooling and heating.

However, the first results obtained illustrating the power of the engine, showed values around 0.1W while the final experiments displayed values of around 0.065 W. The same goes for the rotational speed of the engine that wasn't able to reach values above 670 RPM. Many reasons stand behind this drop in power output:

- The piston expansion inside the engine led to an increase in the friction and thus a decrease in speed and power. The gamma-Stirling Engine used was a lab scale engine not designed for huge heat flows
- The friction losses from the displacer rod, the power rod, as well as the connection between the flywheel and the smaller gear of the dynamo. In fact, the power delivered was very dependent on the torque with which the screws were connected
- The inner resistance of the dynamo plays a role in decreasing the power as seen previously. The inner resistance of a dynamo increases with time.
- Air leakage through the metal of the displacer cylinder was checked using soapy water but no leakages were detected. However, huge leakages are found between the rod connecting the flywheel to the displacer and power piston.

## CHAPTER VIII

### TESTING OF A LAB SCALE BETA STIRLING ENGINE

The beta-Stirling Engine, bought from GreenPowerScience is illustrated in the following image.



*Figure 75. Beta-Stirling Engine from GreenPowerScience with adaptor and gear addition*

#### **A. Modifications and Addition to the engine**

The first modification made to the engine is the addition of an aluminum adaptor installed on the axle of the flywheel. Its function is to act as link between the gear and the engine. The gear is chosen to be compatible with a smaller one of 1-7 ratio.

The second modification made to the engine is its implementation in a metal casing as shown in the figure below.

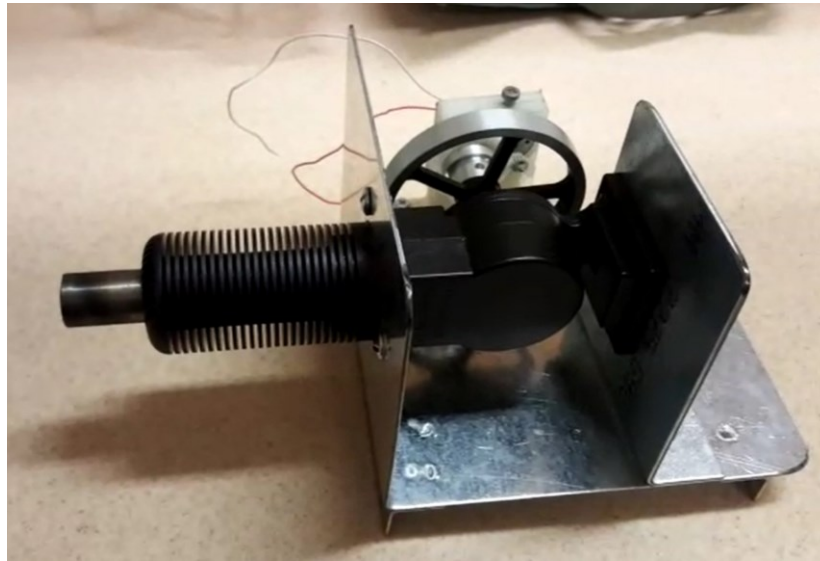


Figure 76. Stirling Engine Casing

## B. Addition of a Combustion Chamber

A first experiment is then made by applying a direct flame on the hot side of the engine. However, after 5min of running, the hot cylinder of the engine undergone a small deformation. In fact, a hot zone appeared on the expansion cylinder and led to an unequal distribution of heat. Moreover, applying a direct flame without any insulated casing around the flame caused heat losses and inefficient energy transfer.

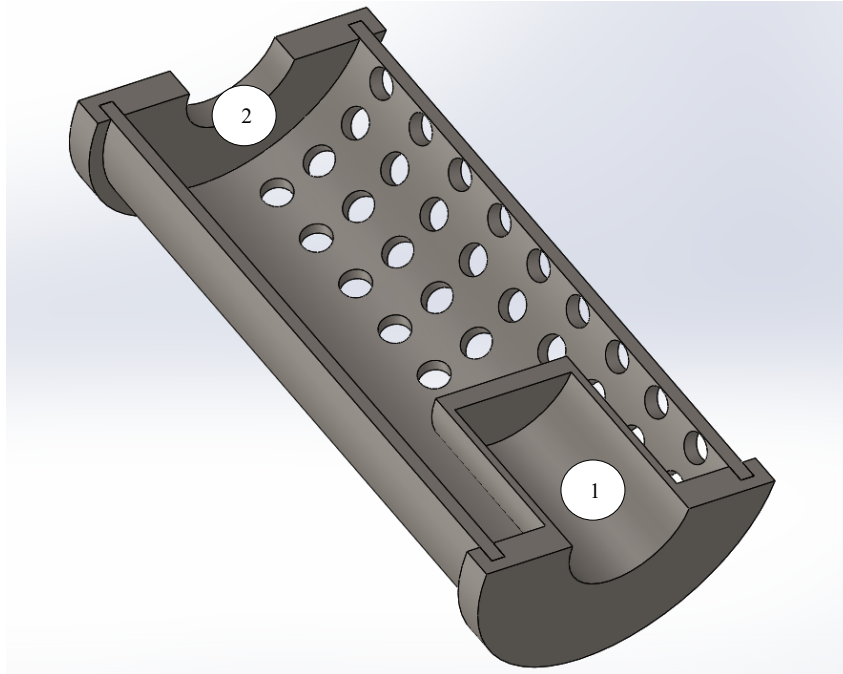


Figure 77. Hot zone on the Expansions Cylinder



Therefore, a combustion chamber was made and attached on the hot side of the engine.

The hot combustion chamber is made out of stainless steel 316L. A 3D image of the combustion chamber can be visualized via SolidWorks in the figure below.



*Figure 78. Cross section view of the Combustion chamber 1 - hot zone of the engine 2 - Flame side*

A cover (figure 78 1-) protects the hot cylinder of the engine to be deformed by the direct flame application and ensure a better heat distribution. Circular cuts were made on the lower part of the heat chamber to keep the air flowing. The image below shows manufactured combustion chamber.

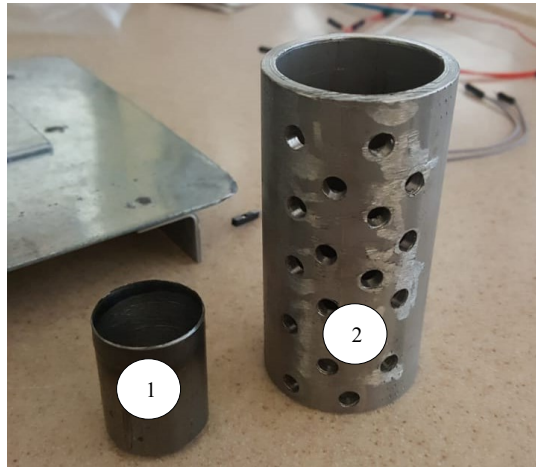


Figure 79. Combustion chamber parts 1 – cover for the hot zone 2 – chamber casing

### C. The implementation of a cooling system

After running the first experiments, it was realized that the “warm-up” time was around 20 min and with the dynamo connected to a circuit, generating a resistance on the generator, the system didn’t even start. In fact, the fins of the engine received a huge amount of heat coming out from the combustion chamber. For this reason, a water cooling system was envisaged to be the solution.

The ideal cycle analysis proved that the heat that should be rejected from the engine both from the cold side and from the regenerator, has a value around 110W. The assumptions present in Appendix D showed that the pipe should have a diameter of 3/8 inch. Moreover, the heat transfer area in the radiator should have a value of 824 cm<sup>2</sup>.

The pipes were bought and the closest radiator to the one we need found in the market is one with a heat transfer area of 821 cm<sup>2</sup>. The cooling system was then implemented with the Stirling Engine and the final setup is showed in the figure below.

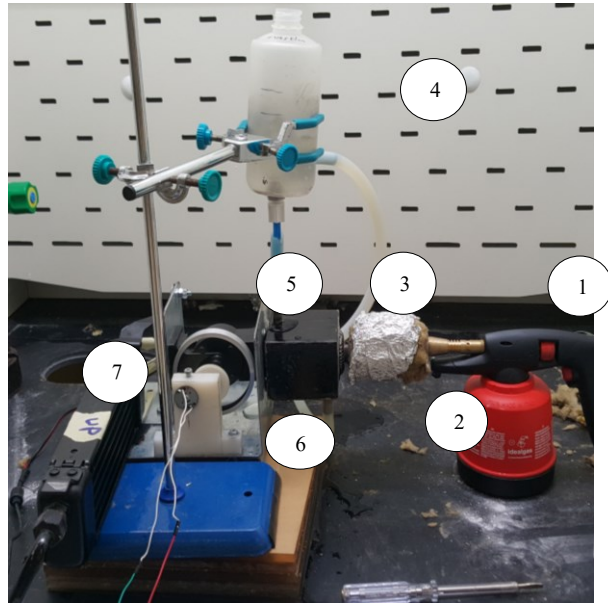


Figure 80. Final setup 1 - Flame Torch 2 - combustion chamber with mineral wool insulation 3 - water jacket 4 - overflow tank 5 - Stirling Engine's flywheel 6 - Dynamo 7 - Radiator

Actually, adding this water cooling system showed huge advantages and a better performance. The new warmup time was measure to be around 3 min. In fact, the engine started smoothly and showed a value of 0.250 W at a field resistance of 150 Ohm. However, the radiator's temperature increased with time and the performance of the engine deceased slightly. The solution was then to install a ventilation system just behind the radiator. Fans were bought, installed and the final system is shown in the figure below.

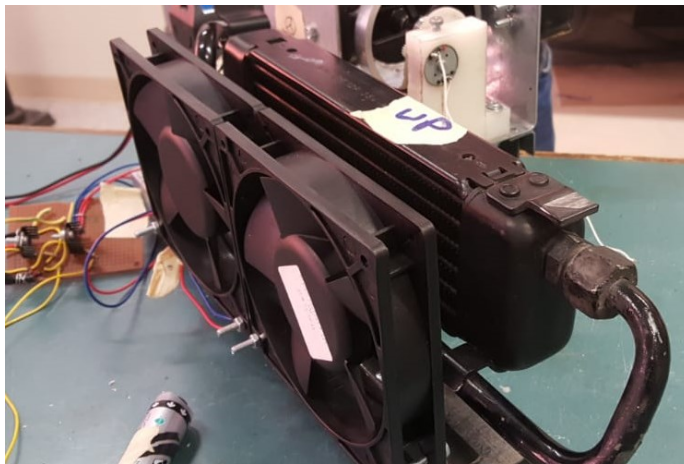


Figure 81. Fans attached behind the radiator

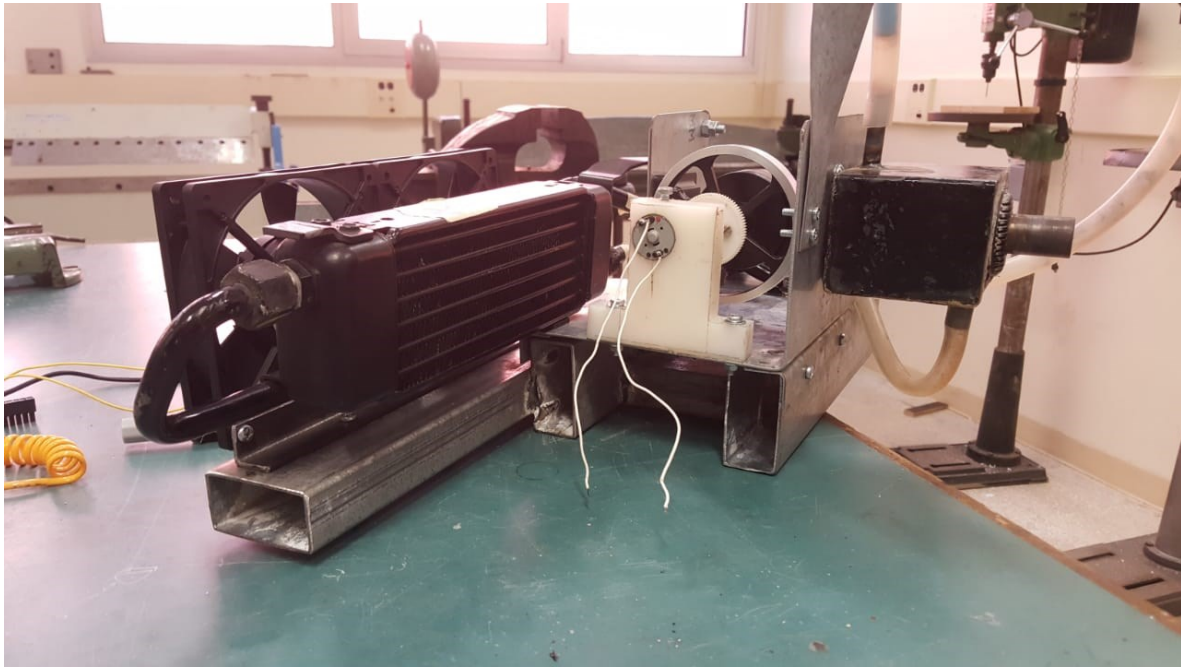


Figure 82. Overall Stirling Engine System

## D. Results

The water pump responsible of circulating water in the cooling system and the fans were controlled using LabView V14. The experiment is done with different field resistors just as done with the previous gamma-Stirling Engine, and the results are shown in the table and graph below. The results show a nominal electrical power of 0.54W.

Table 47. Results obtained from the beta-Stirling Engine

Field Resistance	Voltage	Current	Current	Speed	Power	Internal Resistance	Dissipated Power	Overall Power
Ohm	V	mA	A	RPM	W	Ohm	W	W
450	7.18	15.8	0.0158	910	0.113444	106.23	0.026519	0.139963257
300	6.5	21.2	0.0212	860	0.1378		0.047744	0.185544011
150	5.2	36.24	0.03624	706	0.188448		0.139516	0.327963853
75	3.5	47.4	0.0474	560	0.1659		0.238673	0.404573315
37.5	2.9	58.9	0.0589	512	0.17081		0.368534	0.539344178
18.75	2.23	60.3	0.0603	436	0.134469		0.386262	0.520730841

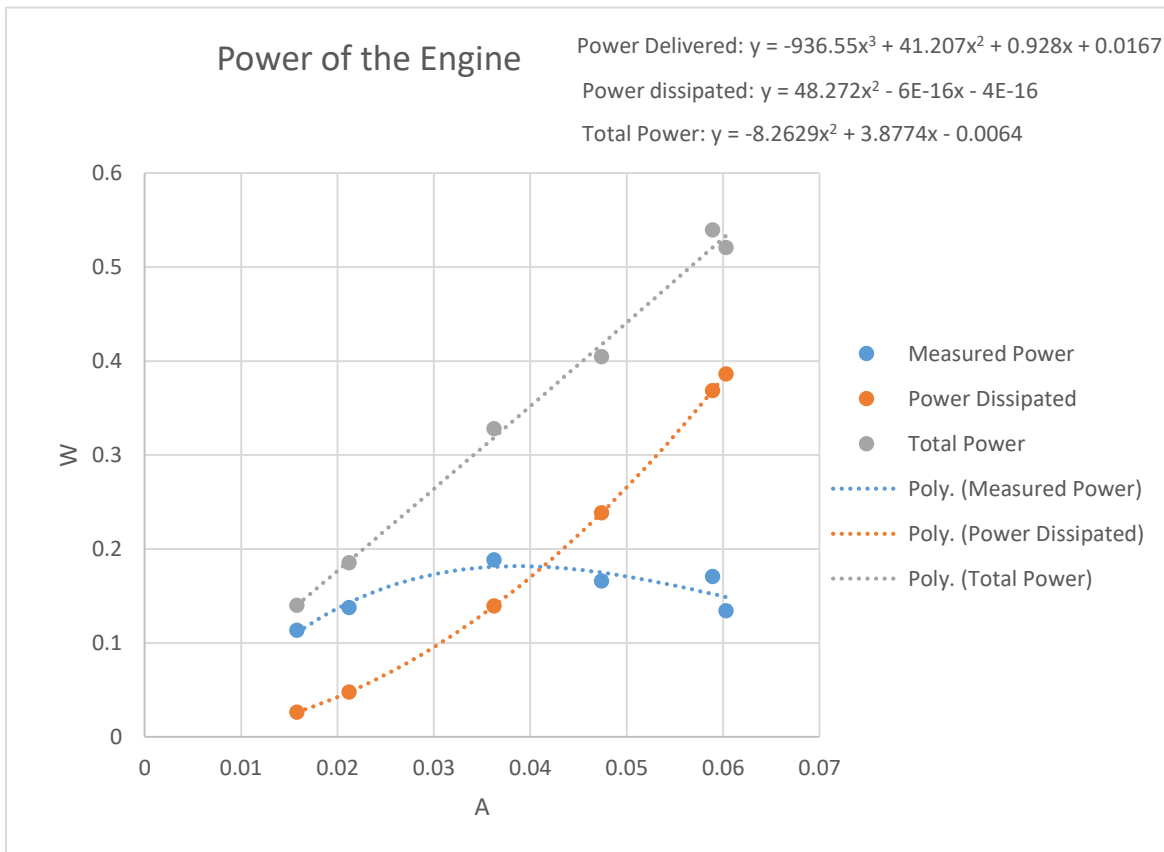


Figure 83. Power of the gamma-Stirling Engine

### E. Future Works with the beta-Stirling Engine

	BSE (W)	Experimental (W)
<b>Nominal Value</b>	10	
<b>Ideal Process</b>	11.01	
<b>Carlquist</b>	3.14	0.589
<b>Beale</b>	1.91	
<b>West</b>	2.89	

In fact, the power obtained in the experimental setup is much lower than the 0<sup>th</sup> order analysis results. The Beale factor is a bit overrated during the analysis and its actual value is shown as follows.

$$Be = \frac{P}{p_m * f * V_0} = 0.00291$$

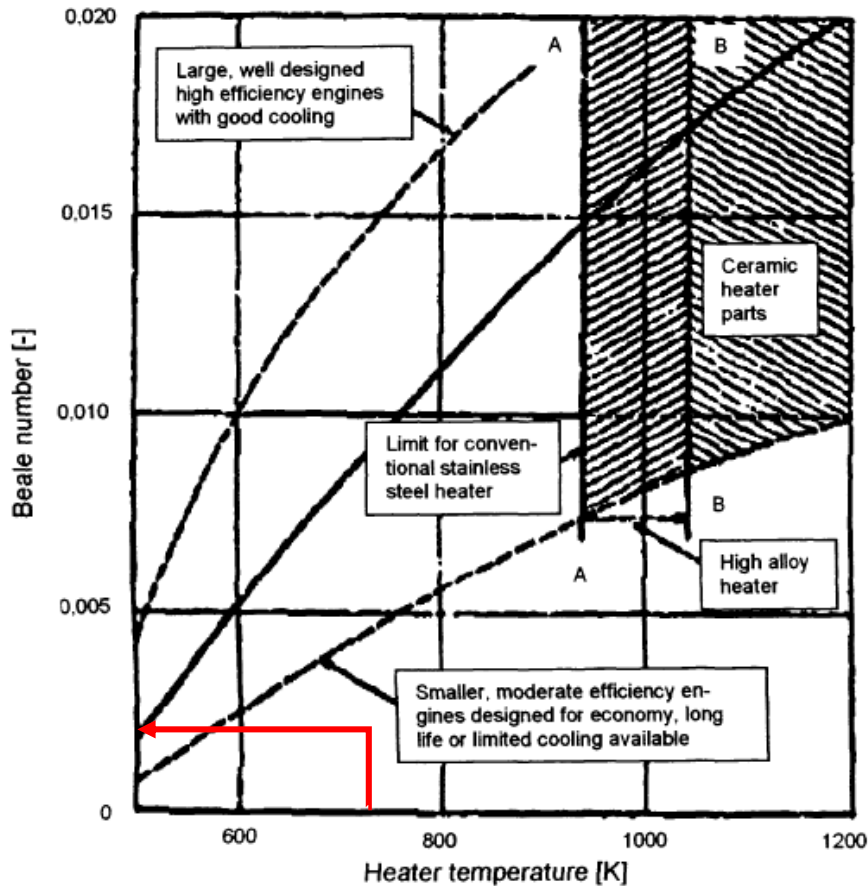


Figure 84. Beale factor for the beta-Stirling Engine

Actually, this shows that a lot of works needs to be done to obtain higher values with the beta Stirling Engine. This is much lower than the Beale factor obtained with the gamma Stirling Engine and this illustrated the difficulties that appeared when operating on a bigger scale engine.

During the experiments done for the beta-Stirling Engine, different problems were faced and solved such as the addition of a heat chamber and the implementation of a water cooling system. However, many other things need to be improved.

## ***1.Dynamo and Gears***

The gears were acting as an obstacle to a smooth operation. In fact, besides being at the origin of mechanical losses, they were at the origin of a back force on the flywheel of the engine. The problem was with aligning and centering the gears together. Actually, when the gears are too close to each other, they might alter the speed and power of the Stirling Engine and therefore giving inconclusive and smaller results. Even when aligning was applied before starting the experiment, the vibrations during running time modified randomly the alignment of the gears and thus altered the output.

In order to bypass the gears problem and reduce the mechanical friction losses, the idea of directly coupling a dynamo to the axe of the flywheel is envisaged. In fact, the DC motor used in this case is designed to deliver 1W at 7,000 RPM, and for this reason gear ratios were used. Actually, high speed DC motors designed to operate at 1,000 RPM+ doesn't need any gear ratio design because the Stirling Engine itself runs at a rotational speed of 1,500 RPM.

## ***2.Combustion chamber***

It has been realized that a huge amount of heat is being dissipated by the circular cuts on the lower side of the chamber. At the flame side, enough air is being accompanied by the flame. It turned out that closing those circular cuts won't affect the flame power and will help in insulating the system to keep the temperature as high as possible.

### ***3. Battery Storage***

After fixing the gear's issue, Li-ion battery storage will be tested. In order to achieve this, a buck converter is bought and ready to be used. The buck converter available acts as a voltage regulator by stabilizing any voltage value between 4 and 35V to 5V. In fact, battery bank usually charges at 5V.

### ***4. Solar Applications***

A group of mechanical engineering students, under the supervision of Dr. Zeaiter, designed a solar Fresnel Lens that tracks the sun and focus its thermal energy on its focal point. The system runs by using an initial open loop control and a closed loop control for fine tuning.

The Fresnel Lens was renewed, the code was debugged and it is now working perfectly. The next step would be to implement the beta Stirling Engine prototype with the lens, in a way that the hot side of the engine falls directly on the focal point. When this is done, experiments using solar energy will be achieved.



## CHAPTER IX

### CONCLUSION

Lebanon is actually facing an energy crisis. As a matter of fact, the electrical power supply is fronting a huge deficit with respect to the growing demand of energy. In response to this, diesel generators were spread in the country leading to an elevated average cost of energy of 20.25 ¢/kWh. In order to solve the problem, this thesis proposed the implementation of a Microgrid system for one household designed to combine a 3kW Hybrid Stirling Engine, a 4kW PV plant, a 5kWh li-ion Battery Storage. By using both solar thermal energy and natural gas simultaneously, this decentralized energy system showed a good performance characterized by a continuous energy generation. The cost of energy was estimated to be 16.3¢/kWh. Knowing that the capital cost of the Stirling Engine in the market is variable, a sensitivity study is made and showed that for the worst case scenario with a capital cost of 6,000 USD/kW, the NPC of the system over 25 years will remain less than any Diesel/PV/Batteries configuration.

Gaining momentum from these economic results, a lab scale gamma-Stirling Engine and a lab-scale beta-Stirling Engine were studied and tested. Results showed that there's a huge deficit between thermodynamic ideal power and the actual electrical power obtained. Suggestions were given to increase the electrical power delivered by the system.

## REFERENCES

- [1] Union of Concerned Scientists. *A short History of Energy*. Available: [https://www.ucsusa.org/clean\\_energy/our-energy-choices/a-short-history-of-energy.html#.W6QVG2gzZPZ](https://www.ucsusa.org/clean_energy/our-energy-choices/a-short-history-of-energy.html#.W6QVG2gzZPZ)
- [2] Pye J. *Problems with fossil fuels*. Available: <http://joanpyeproject.org/news/problems-with-fossil-fuels/>
- [3] (2019). *Oil (WTI)*. Available: <https://markets.businessinsider.com/commodities/oil-price?type=wti>
- [4] F. Mumtaz and I. S. Bayram, "Planning, Operation, and Protection of Microgrids: An Overview," *Energy Procedia*, vol. 107, pp. 94-100, 2017.
- [5] R. Khamis, "Analysis: Electricity in Lebanon, understanding the real problem," in *AN-NAHAR*, ed: Annahar, 2018.
- [6] E. Bouri and J. El Assad, "The Lebanese Electricity Woes: An Estimation of the Economical Costs of Power Interruptions," *Energies*, vol. 9, no. 8, p. 583, 2016.
- [7] O. Ibrahim, F. Fardoun, R. Younes, and H. Louahlia-Gualous, "Energy status in Lebanon and electricity generation reform plan based on cost and pollution optimization," *Renewable and Sustainable Energy Reviews*, vol. 20, pp. 255-278, 2013.
- [8] (2019). *Understanding My Bill*. Available: <http://www.edl.gov.lb/page.php?pid=39&lang=en#1>
- [9] (2019). *Diesel Generator Pricing*. Available: <https://energyandwater.gov.lb/ar/prices?type=2>
- [10] (2019). *About Microgrids*. Available: <https://building-microgrid.lbl.gov/about-microgrids>
- [11] M. Serrano, S. I. Pu, Ed. *Concentrating solar thermal technologies*. 2017.
- [12] NASA. *Aerosol Optical Depth*. Available: [earthobservatory.nasa.gov/GlobalMaps/view.php?d1=MODAL2\\_M\\_AER\\_OD](http://earthobservatory.nasa.gov/GlobalMaps/view.php?d1=MODAL2_M_AER_OD)
- [13] UNDP. (2014). *Solar Photovoltaic Electricity for your house*. Available: [www.lb.undp.org/content/lebanon/en/home/library/environment\\_energy/solar-photovoltaic.html](http://www.lb.undp.org/content/lebanon/en/home/library/environment_energy/solar-photovoltaic.html)
- [14] Lebanese Center for Energy Conservation (LCEC), "The National Renewable Energy Action Plan for the Republic of Lebanon 2016-2020," 2016. Available: [www.lcec.org.lb](http://www.lcec.org.lb)
- [15] "The Duck Curve - California Energy Grid," ed: INTEGRAL Group, 2017.
- [16] F. Choueiri and P. Karawani, "Oil & Gas Sector: A New Economic Pillar For Lebanon," *Credit Libanais SAL2015*, Available: <https://www.creditlibanais.com.lb/Content/Uploads/LastEconomicAndCapitalResearch/150131113245106.pdf>
- [17] IRENA, "Renewable Power Generation Costs in 2017," 2018.
- [18] C. Turchi, M. Mehos, C. Ho, and G. Kolb, "Current and Future Costs for Parabolic Trough and Power Tower Systems in the US Market," 2010. Available: <https://www.nrel.gov/docs/fy11osti/49303.pdf>

- [19] IRENA, "The Power To Change: Solar And Wind Cost Reduction Potential To 2025," International Renewable Energy Agency 2016, Available: [www.irena.org/publications](http://www.irena.org/publications)
- [20] Ripasso Energy AB, "Annual Report 2016," 2016, Available: [ripassoenergy.com/wp-content/uploads/Arsredovisning\\_2016\\_Ripasso\\_Energy\\_eng.pdf](http://ripassoenergy.com/wp-content/uploads/Arsredovisning_2016_Ripasso_Energy_eng.pdf).
- [21] T. Boukelia and M. Mecibah, "4E comparative study of parabolic trough power plant using molten salt as HTF with and without integrated TES and FBS," presented at the Second International Conference on Applied Energetic and Pollution, 2014.
- [22] S. Ong, C. Campbell, P. Denholm, R. Margolis, and G. Heath, "Land-Use Requirements for Solar Power Plants in the United States," NREL 2013, Available: [www.nrel.gov](http://www.nrel.gov)
- [23] "Development of Local Supply Chain: The Missing Link for Concentrated Solar Power Projects in India," ESMAP, Available: [http://www.indiaenvironmentportal.org.in/files/file/ESMAP%20WB\\_Development%20of%20Local%20CSP%20Supply%20Chain%20in%20India.pdf](http://www.indiaenvironmentportal.org.in/files/file/ESMAP%20WB_Development%20of%20Local%20CSP%20Supply%20Chain%20in%20India.pdf)
- [24] Jadhao, Siddhant, and M. Y.V., "Literature Review on Development of Stirling Engine."
- [25] U. R. Singh and A. Kumar, "Review on solar Stirling engine: Development and performance," *Thermal Science and Engineering Progress*, vol. 8, pp. 244-256, 2018.
- [26] J. Coventry and C. Andraka, "Dish Systems for CSP," Sandia National Laboratories 2017.
- [27] W. R. Martini, *Stirling Engine Design Manual*, Second Edition ed. NASA, Lewis Research Center and U.S. Department of Energy, 1983.
- [28] C. Monné, Y. Bravo, F. Moreno, and M. Muñoz, "Analysis of a solar dish–Stirling system with hybridization and thermal storage," *International Journal of Energy and Environmental Engineering*, vol. 5, no. 2-3, 2014.
- [29] J. Barbee. (2015). *Could this be the world's most efficient solar electricity system?* Available: <https://www.theguardian.com/environment/2015/may/13/could-this-be-the-worlds-most-efficient-solar-electricity-system>
- [30] Y. Bravo, C. Monné, N. Bernal, M. Carvalho, F. Moreno, and M. Muñoz, "Hybridization of Solar Dish-Stirling Technology: analysis and design," *Environ. Prog. Sustain. Energy*, vol. 33, no. 4, pp. 1459-1466, 2014.
- [31] D. Laing, H. Thaler, L. Lundstrom, W. Reinalter, T. Keck, and O. Brost, "Development of Advanced Hybrid Heat Pipe Receivers in Dish/Stirling Systems for Decentralised Power Production," The European Commission in the framework of the Non Nuclear Energy Programme Joule III 1999, Available: [https://www.cordis.europa.eu/result/rcn/25291\\_en.html](https://www.cordis.europa.eu/result/rcn/25291_en.html)
- [32] S. Writers. (2018). *United Sun Systems and DoE launch new super cheap solar battery system.* Available: [http://www.solardaily.com/reports/United\\_Sun\\_Systems\\_and\\_DoE\\_launch\\_new\\_super\\_cheap\\_solar\\_battery\\_system\\_999.html](http://www.solardaily.com/reports/United_Sun_Systems_and_DoE_launch_new_super_cheap_solar_battery_system_999.html)
- [33] "BIOSTIRLING-4SKA : A cost effective and efficient approach for a new generation of solar dish-Stirling plants based on storage and hybridization: An Energy demo project for Large Scale Infrastructures," 2017, Available: <https://arxiv.org/ftp/arxiv/papers/1712/1712.03029.pdf>

- [34] IRENA, "Electricity storage and renewables: Costs and markets to 2030," 2017, Available: [irena.org/publications/2017/Oct/Electricity-storage-and-renewables-costs-and-markets](http://irena.org/publications/2017/Oct/Electricity-storage-and-renewables-costs-and-markets).
- [35] SAM, "System Advisor Model (SAM)," S. A. M. (SAM), Ed., ed, 2017.
- [36] P. R. Fraser, "Stirling Dish System Performance Prediction Model," Master of Science, Mechanical Engineering, University of Wisconsin-Madison, 2008.
- [37] S. Sinha and S. S. Chandel, "Review of software tools for hybrid renewable energy systems," *Renewable and Sustainable Energy Reviews*, vol. 32, pp. 192-205, 2014.
- [38] HOMER, "HOMER Pro version 3.7 User Manual," 2016, Available: [www.homerenergy.com/pdf/HOMERHelpManual.pdf](http://www.homerenergy.com/pdf/HOMERHelpManual.pdf)
- [39] T. Li, X. Song, X. Gui, D. Tang, Z. Li, and W. Cao, "Development and test of combustion chamber for Stirling engine heated by natural gas," *Journal of Thermal Science*, vol. 23, no. 2, pp. 196-201, 2014.
- [40] "High Tech Solar Trackers: MS-2E Tracker," Meca Solar2017, Available: <https://mecasolar.com/project/2-axis-tracker-2/>
- [41] P. Konstantin and M. Konstantin, *Power and Energy Systems Engineering Economics: Best Practice Manual*. Springer International Publishing AG, 2018.
- [42] K. Bataineh and Y. Taamneh, "Performance analysis of stand-alone solar dish Stirling system for electricity generation," *International Journal of Heat and Technology*, vol. 35, no. 3, pp. 498-508, 2017.
- [43] C. Andraka, "Cost/Performance Tradeoffs For Reflectors Used In Solar Concentrating Dish Systems," 2008.
- [44] D. Thimsen, "Stirling Engine Assessment," Electric Power Research Institute, Inc.2006, Available: [www.engr.colostate.edu/~marchese/mech337-10/epri.pdf](http://www.engr.colostate.edu/~marchese/mech337-10/epri.pdf)
- [45] H. Ritchie and M. Roser. (2019). *Fossil Fuels*. Available: <https://ourworldindata.org/fossil-fuels>
- [46] *How Long Do Solar Panels Last?* Available: <https://www.igs.com/energy-resource-center/energy-101/how-long-do-solar-panels-last>
- [47] M. Haber, N. El Sett, and Y. Bou Nassif, "Theoretical Analysis and Modeling the aging of the Li-ion battery combined with a PV-on grid system," American University of Beirut (AUB)2018.
- [48] K. Givaki, M. Parker, and P. Jamieson, "Estimation of the power electronic converter lifetime in fully rated converter wind turbine for onshore and offshore wind farms," IEEE Xplore Digital Library 2014, Available: <https://ieeexplore.ieee.org/document/6836866>
- [49] M. Solano-Peralta, M. Morner-Girona, W. van Sark, and X. Vallve, "'Tropicalisation' of Feed-in Tariffs: A custom-made support scheme for hybrid PV/diesel systems in isolated regions," *Renewable and Sustainable Energy Reviews*, 2009.
- [50] (2019). *Fuel Prices*. Available: <https://www.iptgroup.com.lb/ipt/en/our-stations/fuel-prices>
- [51] G. M. Masters, *Renewable and Efficient Electric Power Systems*. Stanford University: John Wiley & Sons, Inc., Hoboken, New Jersey., 2004.

- [52] (2018). *Renewable energy sources*. Available: <https://www.eea.europa.eu/airs/2018/resource-efficiency-and-low-carbon-economy/renewable-energy-sources>
- [53] "Energy Efficiency and Energy Savings," The Economist Intelligence Unit 2012, Available: [http://www.bpie.eu/uploads/lib/document/attachment/16/EIU\\_CaseStudy\\_Report\\_2012.pdf](http://www.bpie.eu/uploads/lib/document/attachment/16/EIU_CaseStudy_Report_2012.pdf)
- [54] R. Chedid, "Economics: Cost of PV Project," ed. American University of Beirut (AUB), 2018.
- [55] A. Wagner, "Calculations and experiments on gamma-type Stirling Engines," Doctor of Philosophy School of Engineering, University of Wales, Cardiff, 2008.
- [56] E. Rogdakis, G. Antonakos, and I. P. Koronaki, "Influence of a Regenerator on Stirling Engine Performance," *Journal of Energy Engineering*, vol. 142, no. 2, p. E4016002, 2016.
- [57] I. Urieli. *Alpha Stirling Engines* Available: <https://www.ohio.edu/mechanical/stirling/engines/engines.html>
- [58] B. Kongtragool and S. Wongwises, "A review of solar-powered Stirling engines and low temperature differential Stirling engines," *Renewable and Sustainable Energy Reviews*, vol. 7, pp. 131-154, 2003.
- [59] T. Gelu, "Analysis of Stirling engine and comparison with other technologies using low temperature heat sources," Energy Engineering and Management, TECNICO LISBOA, 2014.
- [60] M. Yunus, M. S. Alsoufi, and A. Kumar, ;, "Design, Manufacture and Measurements of Beta-Type Stirling Engine with Rhombic Drive Mechanism," *Modern Mechanical Engineering*, 2016.
- [61] J. Zheng, J. Chen, P. Zheng, H. Wu, and C. Tong, "Research on Control Strategy of Free-Piston Stirling Power Generating System," *Energies*, vol. 10, no. 10, p. 1609, 2017.
- [62] K. Hirata. *SCHMIDT THEORY FOR STIRLING ENGINES*. Available: <http://www.bekkoame.ne.jp/~khirata>
- [63] J. MACHÁCEK, "Analysis Of Stirling Engine Characteristics By Schmidt's Theory."

## APPENDIX A

---

<b>Economics</b>		
<b>Currency</b>		<b>USD</b>
<b>Nominal Discount Rate</b>		<b>8.00%</b>
<b>Expected inflation rate</b>		<b>2.00%</b>
<b>Real Discount Rate</b>		<b>5.88%</b>
<b>Project Duration</b>		<b>25 years</b>
<b>Fixed Capital Cost</b>	<b>\$</b>	<b>-</b>
<b>System Fixed O&amp;M</b>	<b>\$</b>	<b>-</b>
<b>Capacity Shortage Penalty</b>	<b>\$</b>	<b>-</b>

---

<b>Constraints</b>		
<b>Max Annual Shortage</b>		<b>0%</b>
<b>Min Renewable Fraction</b>		<b>0%</b>
<b>Operating Reserve</b>		
<b>As a % of Load</b>		
<b>Load in current time step</b>		<b>10%</b>
<b>Annual peak load</b>		<b>0%</b>
<b>As a % of renewable output</b>		
<b>Solar Power Output</b>		<b>25%</b>
<b>Wind Power Output</b>		<b>50%</b>
<b>Capacity Shortage</b>		<b>0%</b>

---

<b>Emissions</b>		
<b>(No penalties in Lebanon)</b>		

---

<b>Optimization</b>		
<b>Minutes per time step</b>		<b>60</b>
<b>Time Steps per Year</b>		<b>8,760</b>
<b>Allow Systems With Multiple Generators</b>		<b>Checked</b>
<b>Maximum Simulations per optimization</b>		<b>10,000</b>
<b>Focus Factor</b>		<b>1</b>

---

<b>Optimize category winners</b>	<b>Checked</b>
<b>Run Base Case</b>	<b>Unchecked</b>

### **Solar Powered Stirling Engine**

Description	
<b>Power Output (kW)</b>	<b>From SAM</b>
<b>Nominal Capacity (kW)</b>	<b>1</b>
<b>Capital (\$)</b>	<b>\$ 2,500.00</b>
<b>Replacement (\$)</b>	<b>\$ 2,500.00</b>
<b>O&amp;M (\$/yr)</b>	<b>\$ 17.52.00</b>
<b>time (years)</b>	<b>10.00</b>
<b>Optimization</b>	<b>HOMER</b>
<b>Required Operating Reserve</b>	<b>0%</b>
<b>Electrical Bus</b>	<b>AC</b>
<b>Lower Bound</b>	<b>Variable</b>
<b>Upper Bound</b>	<b>Variable</b>

### **Natural Gas Powered Stirling Engine**

Description	
<b>Power Output (kW)</b>	<b>Variable</b>
<b>Quantity</b>	<b>Variable</b>
<b>Capital (\$)</b>	<b>\$ -</b>
<b>Replacement (\$)</b>	<b>\$ -</b>
<b>O&amp;M (\$/hr)</b>	<b>\$ 0.02</b>
<b>time (hours)</b>	<b>40,000.00</b>
<b>Electrical Bus</b>	<b>AC</b>
<b>Required Operating Reserve</b>	<b>0%</b>
<b>Minimum Load Ratio (%)</b>	<b>40%</b>
<b>Fuel (Natural Gas)</b>	
<b>Price (\$/m3)</b>	<b>0.202</b>
<b>Lower Heating Value (MJ/kg)</b>	<b>45</b>
<b>Density (kg/m3)</b>	<b>0.79</b>
<b>Carbon Content (%)</b>	<b>67%</b>
<b>Sulfur Content (%)</b>	<b>0%</b>
<b>Fuel Curve</b>	
<b>Output (kW)</b>	<b>Consumption (m3/hr)</b>

3.73	1.493
4.84	1.586
5.99	1.87
<b>CO2 (g/m3 of fuel)</b>	<b>6.42</b>
<b>Particulate Matter (g/m3)</b>	<b>0.181</b>
<b>NOx (g/m3 of fuel)</b>	<b>13.47</b>
<b>Fuel (Diesel)</b>	
<b>Price (\$/L)</b>	<b>1</b>
<b>Lower Heating Value (MJ/kg)</b>	<b>43.2</b>
<b>Density (kg/m3)</b>	<b>820</b>
<b>Carbon Content (%)</b>	<b>88%</b>
<b>Sulfur Content (%)</b>	<b>0.4%</b>
<b>Fuel Curve</b>	
<b>Output (kW)</b>	<b>Consumption (L/hr)</b>
1	0.55
2	0.8
3	1.05
<b>CO (g/L of fuel)</b>	<b>16.5</b>
<b>Unburned Hydrocarbon (g/L of fuel)</b>	<b>0.72</b>
<b>Particulate Matter (g/L of fuel)</b>	<b>0.1</b>
<b>Fuel Sulfur to PM (%)</b>	<b>2.2</b>
<b>NOx (g/L of fuel)</b>	<b>15.5</b>
<b>Load</b>	
<b>Residential</b>	<b>59.25kWh/d</b>
<b>Average (kW)</b>	<b>2.47</b>
<b>Peak (kW)</b>	<b>4.32</b>
<b>Day to Day variability (%) *</b>	<b>2.08%</b>
<b>Time step (%) **</b>	<b>4.02%</b>
<b>Peak Month</b>	<b>January</b>
<b>Batteries</b>	
<b>Nominal Voltage (V)</b>	<b>600 or 6</b>
<b>Nominal Capacity (kWh)</b>	<b>100 or 1</b>
<b>Nominal Capacity (Ah)</b>	<b>167</b>
<b>Roundtrip efficiency (%)</b>	<b>90</b>
<b>Maximum Charge Current (A)</b>	<b>167</b>
<b>Maximum Discharge Current (A)</b>	<b>500</b>
<b>Unit Price (\$) for 100 kWh</b>	<b>\$ 70,000.00</b>



<b>Unit Price (\$) for 1 kWh</b>	<b>\$</b>	<b>600.00</b>
<b>Replacement for 100 kWh (\$)</b>	<b>\$</b>	<b>70,000.00</b>
<b>Replacement for 1 kWh (\$)</b>	<b>\$</b>	<b>600.00</b>
<b>O&amp;M for 100 kWh (%/year)</b>	<b>\$</b>	<b>1,000.00</b>
<b>O&amp;M for 1 kWh (%/year)</b>	<b>\$</b>	<b>10.00</b>
<b>Lifetime (year)</b>		<b>15</b>
<b>Throughput (kWh)</b>		<b>300,000</b>
<b>Initial State of Charge (%)</b>		<b>100%</b>
<b>Minimum State of Charge (%)</b>		<b>20%</b>
<b>Lower Bound</b>		<b>0</b>
<b>Upper Bound</b>		<b>1000</b>

### **Converter**

<b>Capacity (kW)</b>		<b>1</b>
<b>Capital (\$)</b>		<b>300</b>
<b>Replacement (\$)</b>		<b>300</b>
<b>O&amp;M (\$/year)</b>		<b>0</b>
<b>Inverter (DC to AC)</b>		
<b>Lifetime (years)</b>		<b>15</b>
<b>Efficiency (%)</b>		<b>95%</b>
<b>Rectifier (AC to DC)</b>		
<b>Relative Capacity (%)</b>		<b>100%</b>
<b>Efficiency (%)</b>		<b>90%</b>
<b>Lower Bound</b>		<b>0</b>
<b>Upper Bound</b>		<b>1000</b>

\* HOMER changes each day's load profile by a random amount,  $\pm 2\%$

\*\* This variability changes the shape of the load profile without affecting its size, by 4%.

## APPENDIX B – 2500 USD/KW

		HSE (kW)	PV (kW)	PV Area (m2)	Li-ion Batteries (Units 1kWh)	Converter (kW)	Initial Cost (USD)	NPC (USD)	Annualized NPC (USD)	O&M (USD/year) Including Fuel Cost	COE (USD/kWh)	Renewable Factor (%)
<b>Optimal SE 0kW PV</b>	Optimal 1	5	0	0	0	0	12500	47410	3667	2700	0.170	25
	Optimal 2	3	0	0	9	2.19	13557	48553	3755	2706	0.174	24
<b>Optimal PV</b>	Input	0	Optimizer	-	-	-	-	-	0	0	-	-
	Optimal	0	72.2	481	60	5.32	109783	184582	14275	5785	0.660	100
	Input	0,1	Optimizer	-	-	-	-	-	0	0	-	-
	Optimal	1	42.5	283	57	9.72	76149	139073	10755	4866	0.497	77
	Input	0,2	Optimizer	-	-	-	-	-	0	0	-	-
	Optimal	2	22.8	152	22	5.46	42670	85378	6603	3303	0.305	53
	Input	3	Optimizer	-	-	-	-	-	0	0	-	-
	Optimal	3	4.1	27	5	1.32	14996	45784	3541	2381	0.164	32
		3	5.6	37	4	1.33	15901	45946	3553	2324	0.164	33
		-	-	-	-	-	-	-	-	-	-	-
<b>1kW PV PV Area of 32m2</b>	Input	1	0,1	-	-	-	-	-	0	0	-	-
	Optimal	-	-	-	-	-	-	-	-	-	-	-
	Input	2	0,1	-	-	-	-	-	0	0	-	-
	Optimal	-	-	-	-	-	-	-	-	-	-	-
	Input	3,4	0,1	-	-	-	-	-	0	0	-	-
	Optimal	3	1	7	9	1.76	14429	49107	3798	2682	0.176	26
	Optimal 2	4	1	7	2	0.779	12434	44860	3469	2508	0.160	26
<b>2kW PV PV Area of 64m2</b>	Input	0,1	0,2	-	-	-	-	-	0	0	-	-
	Optimal	-	-	-	-	-	-	-	-	-	-	-
	Input	0,2	0,2	-	-	-	-	-	0	0	-	-
	Optimal	2	2	13	533	7.77	329131	840023	64965	39511	3.000	38
	Input	3,4	0,2	-	-	-	-	-	0	0	-	-
	Optimal 1	3	2	13	9	1.76	15427	49882	3858	2665	0.178	29
Optimal 2	4	2	13	2	0.846	13454	45803	3542	2502	0.164	28	

<b>3kW PV PV Area of 96m2</b>	Input	0,1	0,3	-	-				0	0		
	Optimal	1	1	7	-		-	-	-	-	-	-
	Input	0,2	0,3	-	-				0	0		
	Optimal	2	3	20	359	2.92	224275	574729	44448	27103	2.060	40
	Input	3,4	0,3	-	-				0	0		
	Optimal	3	3	20	9	1.76	16427	50753	3925	2655	0.182	31
<b>4kW PV PV Area of 133m2</b>	Optimal 2	4	3	20	3	1.42	15227	48281	3734	2556	0.173	30
	Input	0,1	0,4	-	-				0	0		
	Optimal	-	-	-	-	-	-	-	-	-	-	-
	Input	0,2	0,4	-	-				0	0		
	Optimal	2	4	27	275	5.76	175272	448877	34715	21160	1.610	42
	Input	3,4	0,4	-	-				0	0		
	Optimal	3	4	27	5	1.52	14956	45637	3529	2373	0.163	32
	Optimal 2	4	4	27	2	1.29	15586	47830	3699	2494	0.171	31

## APPENDIX B – 4000 USD/KW

		HSE (kW)	PV (kW)	PV Area (m2)	Li-ion Batteries (Units 1kWh)	Converter (kW)	Initial Cost (USD)	NPC (USD)	Annualized Cost (USD)	O&M (USD/year Including Fuel Cost)	COE (USD/kWh)	Renewable Factor (%)
<b>Optimal SE 0kW PV</b>	Optimal 1	5	0	0	0	0	20000	60638	4690	3143	0.217	25
	Optimal 2	3	0	0	9	2.1	18031	56461	4367	2972	0.202	24
	Input	0	Optimizer	-	-	-	-	-	0	0	-	-
<b>Optimal PV</b>	Optimal	0	72.2	481	60	5.32	109783	184582	14275	5785	0.660	100
	Input	0,1	Optimizer	-	-	-	-	-	0	0	-	-
	Optimal	1	45	283	44	10.1	78381	140321	10852	4790	0.502	77
	Input	0,2	Optimizer	-	-	-	-	-	0	0	-	-
	Optimal	2	22.8	152	22	5.46	45670	90669	7012	3480	0.324	53
	Input	3	Optimizer	-	-	-	-	-	0	0	-	-
	Optimal	3	3.4	27	9	3.67	21903	59607	4610	2916	0.213	31
		3	2.65	37	10	3.78	21783	60554	4683	2998	0.217	30
		3	1.35	-	14	3.74	22870	65582	5072	3303	0.235	27
		Input	1	0,1	-	-	-	-	-	0	0	-
<b>1kW PV PV Area of 32m2</b>	Optimal	-	-	-	-	-	-	-	0	0	-	-
	Input	2	0,1	-	-	-	-	-	0	0	-	-
	Optimal	-	-	-	-	-	-	-	-	-	-	#VALUE!
	Input	3,4	0,1	-	-	-	-	-	0	0	-	-
	Optimal	3	1	7	12	2	20799	61684	4770	3162	0.221	26
	Optimal 2	4	1	7	2	0.779	18434	54274	4197	2772	0.194	26
<b>2kW PV PV Area of 64m2</b>	Input	0,1	0,2	-	-	-	-	-	0	0	-	-
	Optimal	-	-	-	-	-	-	-	#VALUE!	#VALUE!	-	-
	Input	0,2	0,2	-	-	-	-	-	0	0	-	-
	Optimal	2	2	13	534	8.27	332882	847006	65505	39761	3.030	38
	Input	3,4	0,2	-	-	-	-	-	0	0	-	-

	Optimal 1	3	2	13	9	1.76	19927	57818	4471	2930	0.207	29
	Optimal 2	4	2	13	2	0.846	19454	56385	4361	2856	0.202	28
<b>3kW PV PV Area of 96m2</b>	Input	0,1	0,3	-	-				0	0		
	Optimal	1	1	7	-		-	-	-	-	-	-
	Input	0,2	0,3	-	-				0	0		
	Optimal	2	3	20	353	10.7	226000	573549	44357	26878	2.050	40
	Input	3,4	0,3	-	-				0	0		
	Optimal	3	3	20	9	1.76	20927	58690	4539	2920	0.210	31
	Optimal 2	4	3	20	3	1.42	21227	58863	4552	2911	0.211	30
<b>4kW PV PV Area of 133m2</b>	Input	0,1	0,4	-	-				0	0		
	Optimal	-	-	-	-		-	-	-	-	-	-
	Input	0,2	0,4	-	-				0	0		
	Optimal	2	4	27	275	5.76	178727	454168	35124	21302	1.620	42
	Input	3,4	0,4	-	-				0	0		
	Optimal	3	4	27	6	1.53	20060	55092	4261	2709	0.197	32
	Optimal 2	4	4	27	2	1.29	21586	58412	4517	2848	0.209	31

## APPENDIX B – 5000 USD/KW

		HSE (kW)	PV (kW)	PV Area (m2)	Li-ion Batteries (Units 1kWh)	Converter (kW)	Initial Cost (USD)	NPC (USD)	Annualized Cost (USD)	O&M (USD/year) Including Fuel Cost	COE (USD/kWh)	Renewable Factor (%)	
<b>Optimal SE 0kW PV</b>	Optimal 1	5	0	0	0	0	25000	69456	5372	3438	0.248	25	
	Optimal 2	3	0	0	9	2.19	21057	61781	4778	3149	0.221	24	
	Input	0	Optimizer	-	-	-	-	-	0	0	-	-	
<b>Optimal PV</b>	Optimal	0	72.2	481	60	5.32	109783	184582	14275	5785	0.660	100	
	Input	0,1	Optimizer	-	-	-	-	-	0	0	-	-	
	Optimal	1	50.5	283	37	6.06	79539	137072	10601	4449	0.490	77	
	Input	0,2	Optimizer	-	-	-	-	-	0	0	-	-	
	Optimal	2	21.4	152	22	4.29	45932	92100	7123	3570	0.329	53	
	Input	3	Optimizer	-	-	-	-	-	0	0	-	-	
	Optimal	3	4.1	27	5	1.32	22496	59012	4564	2824	0.211	32	
	Optimal	3	5.6	37	4	1.33	23401	59173	4576	2766	0.212	33	
	Input	-	-	-	-	-	-	-	-	-	-	-	-
	Input	1	0,1	-	-	-	-	-	0	0	-	-	
<b>1kW PV PV Area of 32m2</b>	Optimal	-	-	-	-	-	-	-	0	0	-	-	
	Input	2	0,1	-	-	-	-	-	0	0	-	-	
	Optimal	-	-	-	-	-	-	-	-	-	-	#VALUE!	
	Input	3,4	0,1	-	-	-	-	-	0	0	-	-	
	Optimal	3	1	7	9	1.76	21929	62335	4821	3125	0.223	26	
	Optimal 2	4	1	7	2	0.779	22434	62496	4833	3098	0.224	26	
<b>2kW PV PV Area of 64m2</b>	Input	0,1	0,2	-	-	-	-	-	0	0	-	-	
	Optimal	-	-	-	-	-	-	-	#VALUE!	#VALUE!	-	-	
	Input	0,2	0,2	-	-	-	-	-	0	0	-	-	
	Optimal	-	-	13	-	-	-	-	-	-	-	-	
	Input	3,4	0,2	-	-	-	-	-	0	0	-	-	
Optimal 1	3	2	13	9	1.76	22927	63109	4881	3108	0.226	29		
Optimal 2	4	2	13	2	0.846	23454	63439	4906	3092	0.227	28		

3kW PV	Input	0,1	0,3	-	-				0	0		
	Optimal	1	1	7	-				-	-	-	-
Area of 96m2	Input	0,2	0,3	-	-				0	0		
	Optimal	-	-	20	-	-	-	-	-	-	-	-
4kW PV	Input	3,4	0,3	-					0	0		
	Optimal	3	3	20	9	1.76	23927	63981	4948	3098	0.229	31
	Optimal 2	4	3	20	3	1.42	25227	65917	5098	3147	0.236	30
Area of 133m2	Input	0,1	0,4	-	-				0	0		
	Optimal	-	-	-	-	-	-	-	-	-	-	-
Area of 133m2	Input	0,2	0,4	-	-				0	0		
	Optimal	-	-	27	-	-	-	-	-	-	-	-
	Input	3,4	0,4	-					0	0		
	Optimal	3	4	27	5	1.52	22456	58865	4552	2816	0.211	32
	Optimal 2	4	4	27	2	1.29	25586	65466	5063	3084	0.234	31

## APPENDIX B – 6000 USD/KW

		HSE (kW)	PV (kW)	PV Area (m2)	Li-ion Batteries (Units 1kWh)	Converter (kW)	Initial Cost (USD)	NPC (USD)	Annualized Cost (USD)	O&M (USD/year) Including Fuel Cost	COE (USD/kWh)	Renewable Factor (%)
<b>Optimal SE 0kW PV</b>	Optimal 1	5	0	0	0	0	30000	78274	6053	3733	0.280	25
	Optimal 2	3	0	0	9	2.19	24057	67072	5187	3327	0.240	24
<b>Optimal PV</b>	Input	0	Optimizer	-	-	-	-	-	0	0	-	-
	Optimal	0	72.2	481	60	5.32	109783	184582	14275	5785	0.660	100
	Input	0,1	Optimizer	-	-	-	-	-	0	0	-	-
	Optimal	1	50.5	283	37	6.06	80539	138836	10737	4509	0.497	77
	Input	0,2	Optimizer	-	-	-	-	-	0	0	-	-
	Optimal	2	21.4	152	22	4.29	47932	95627	7396	3689	0.342	53
	Input	3	Optimizer	-	-	-	-	-	0	0	-	-
	Optimal	3	4.1	27	5	1.32	25496	64303	4973	3001	0.230	32
	Optimal	3	5.6	37	4	1.33	26401	64464	4985	2944	0.231	33
	Input	-	-	-	-	-	-	-	-	-	-	-
<b>1kW PV PV</b>	Input	1	0,1	-	-	-	-	-	0	0	-	-
	Optimal	-	-	-	-	-	-	-	-	-	-	-
<b>Area of 32m2</b>	Input	2	0,1	-	-	-	-	-	0	0	-	-
	Optimal	-	-	-	-	-	-	-	-	-	-	-
	Input	3,4	0,1	-	-	-	-	-	0	0	-	-
	Optimal	3	1	7	9	1.76	24929	67626	5230	3302	0.242	26
<b>2kW PV PV</b>	Optimal 2	4	1	7	2	0.779	26434	69551	5379	3335	0.249	26
	Input	0,1	0,2	-	-	-	-	-	0	0	-	-
	Optimal	-	-	-	-	-	-	-	0	0	-	-
	Input	0,2	0,2	-	-	-	-	-	0	0	-	-
<b>Area of 64m2</b>	Optimal	-	-	13	-	-	-	-	-	-	-	-
	Input	3,4	0,2	-	-	-	-	-	0	0	-	-
	Optimal 1	3	2	13	9	1.76	25927	68400	5290	3285	0.245	29
	Optimal 2	4	2	13	2	0.846	27454	70494	5452	3329	0.252	28
Input	0,1	0,3	-	-	-	-	-	0	0	-	-	



<b>3kW PV</b>	Optimal	1	1	7	-	-	-	-	-	-	-	-
	Input	0,2	0,3	-	-	-	-	-	0	0	-	-
<b>Area of 96m2</b>	Optimal	-	-	20	-	-	-	-	-	-	-	-
	Input	3,4	0,3	-	-	-	-	-	0	0	-	-
	Optimal	3	3	20	9	1.76	26927	69272	5357	3275	0.248	31
	Optimal 2	4	3	20	3	1.42	29227	72972	5643	3383	0.264	30
<b>4kW PV</b>	Input	0,1	0,4	-	-	-	-	-	0	0	-	-
	Optimal	-	-	-	-	-	-	-	-	-	-	-
<b>Area of 133m2</b>	Input	0,2	0,4	-	-	-	-	-	0	0	-	-
	Optimal	-	-	27	-	-	-	-	-	-	-	-
	Input	3,4	0,4	-	-	-	-	-	0	0	-	-
	Optimal	3	4	27	5	1.52	25456	64156	4962	2993	0.229	32
	Optimal 2	4	4	27	2	1.29	29586	72521	5609	3320	0.259	31

## APPENDIX C

<b>Diesel Engine (kW)</b>	<b>PV (kW)</b>	<b>PV Area (m2)</b>	<b>1kWh Li-ion</b>	<b>Initial Cost (USD)</b>	<b>Annualized Initial Cost (USD)</b>	<b>NPC (USD)</b>	<b>Annualized NPC</b>	<b>O&amp;M</b>	<b>COE (USD)</b>	<b>Renewable Factor (%)</b>
4.8	9.6	320	3	14,838.00	1,147.53	79,855.00	6,175.74	5,028.22	0.286	39
4.8	12.1	403.3	0	15,488.00	1,197.80	84,310.00	6,520.28	5,322.49	0.302	35
4.8	0	0	0	2,400.00	185.61	97,394.00	7,532.16	7,346.55	0.348	0

## APPENDIX D

<b>Q of the engine</b>	110	W
<b>T<sub>in water</sub></b>	20	C
<b>T<sub>out water</sub></b>	30	
<b>C<sub>p</sub></b>	4184	J/kgK
<b>Water Mass Flow Rate</b>	0.002629063	kg/s
<b>Water Volumetric Flow rate</b>	2.63433E-06	m <sup>3</sup> /s
<b>Water Velocity</b>	0.15	m/s
<b>Tube diameter</b>	0.472880133	cm
	0.186173281	inch
<b>Ambient air</b>	17	C
<b>LMTD</b>	15.70	C
<b>Correction Factor Ft</b>	0.85	Assumed
<b>Overall Heat Transfer Coefficient U</b>	100	W/m <sup>2</sup> K
<b>HT A</b>	0.082412	m <sup>2</sup>
	824.12	cm <sup>2</sup>